CHAPTER SIX

Beams

The response of composite beams to loading is more complex than that of isotropic beams, and the analyses of composite beams must take these complexities into account. This requires analyses that are, by necessity, more involved than for isotropic beams but which, nonetheless, result in expressions readily amenable to numerical computations.

In this chapter we treat rectangular solid cross sections as well as thin-walled beams that undergo small deformations and in which the material behaves in a linearly elastic manner. We neglect shear deformations and adopt the Bernoulli–Navier hypothesis, according to which the originally plane cross sections of a beam undergoing bending remain plane and perpendicular to the axis of the beam.

Axial, transverse, and torque loads may be applied to the beam (Fig. 6.1), resulting in the following *internal forces*: normal force $\widehat{N}$; bending moments $\widehat{M}_y$, $\widehat{M}_z$; torque $\widehat{T}$; and the transverse shear forces $\widehat{V}_z$, $\widehat{V}_y$ (Fig. 6.2).

6.1 Governing Equations

The response of a beam to the applied forces is described by the strain–displacement, force–strain, and equilibrium equations. These equations are given in this section for conditions in which there is no restrained warping. The effect of restrained warping is discussed in Sections 6.5.5, 6.5.6, and 6.6.4.

Here, as well as in the following analyses, we employ an x–y–z coordinate system with the origin at the centroid. The centroid is defined such that an axial load acting at the centroid does not change the curvature of the axis passing through the centroid. As a consequence of this definition, a bending moment acting on the beam does not introduce an axial strain along this axis. Unlike for isotropic beams, for composite beams the centroid does not necessarily coincide with the center of gravity of the cross section.

There are four independent displacements (Fig. 6.3): the axial displacement u, the transverse displacements v and w in the y and z directions, respectively, and the twist of the cross section ψ. The corresponding axial strain ϵ_x^{o}, curvatures $1/\rho_y$

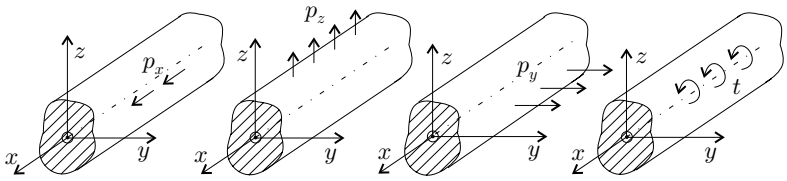

Figure 6.1: Axial, transverse, and torque loads acting on a section of a beam.

and $1/\rho_z$ in the x–z and x–y planes,[1] and the rate of twist ϑ are defined through the strain–displacement relationships

$$\epsilon_x^{\mathrm{o}} = \frac{\partial u}{\partial x} \qquad \frac{1}{\rho_z} = -\frac{\partial^2 v}{\partial x^2} \qquad \frac{1}{\rho_y} = -\frac{\partial^2 w}{\partial x^2} \qquad \vartheta = \frac{\partial \psi}{\partial x}. \tag{6.1}$$

The generalized force–strain relationship is defined as

$$\begin{Bmatrix} \widehat{N} \\ \widehat{M}_y \\ \widehat{M}_z \\ \widehat{T} \end{Bmatrix} = \begin{bmatrix} P_{11} & P_{12} & P_{13} & P_{14} \\ P_{12} & P_{22} & P_{23} & P_{24} \\ P_{13} & P_{23} & P_{33} & P_{34} \\ P_{14} & P_{24} & P_{34} & P_{44} \end{bmatrix} \begin{Bmatrix} \epsilon_x^{\mathrm{o}} \\ \frac{1}{\rho_y} \\ \frac{1}{\rho_z} \\ \vartheta \end{Bmatrix}, \tag{6.2}$$

where P_{ij} are the elements of the stiffness matrix.

The equilibrium equations for a straight beam subjected to the loads shown in Figure 6.1 are[2]

$$\begin{aligned} \frac{\partial \widehat{N}}{\partial x} &= -p_x & \frac{\partial \widehat{T}}{\partial x} &= -t \\ \frac{\partial \widehat{V}_y}{\partial x} &= -p_y & \frac{\partial \widehat{V}_z}{\partial x} &= -p_z \\ \frac{\partial \widehat{M}_y}{\partial x} &= \widehat{V}_z & \frac{\partial \widehat{M}_z}{\partial x} &= \widehat{V}_y. \end{aligned} \tag{6.3}$$

The preceding three sets of equations, (together with the appropriate boundary conditions) completely describe the displacements of, and the forces in, a composite beam.

The internal forces $\widehat{N}$, $\widehat{M}_y$, $\widehat{M}_z$, $\widehat{V}_y$, $\widehat{V}_z$, and $\widehat{T}$ are determined by the simultaneous solution of Eqs. (6.1)–(6.3) together with the appropriate boundary conditions given below. When a beam is statically determinate, the internal forces can be obtained from the equilibrium equations. When a composite beam is statically indeterminate, the internal forces can be obtained with the use of replacement stiffnesses in the relevant isotropic beam expressions provided that either the beam is orthotropic or the cross section is symmetrical and the load is applied in the plane of symmetry. The concepts of orthotropic beam and replacement stiffnesses are discussed in Section 6.1.2.

[1] T. H. G. Megson, *Aircraft Structures for Engineering Students*. 3rd edition. Halsted Press, John Wiley & Sons, New York, 1999, p. 284.

[2] B. K. Donaldson, *Analysis of Aircraft Structures. An Introduction*. McGraw-Hill, New York, 1993, pp. 277–278.

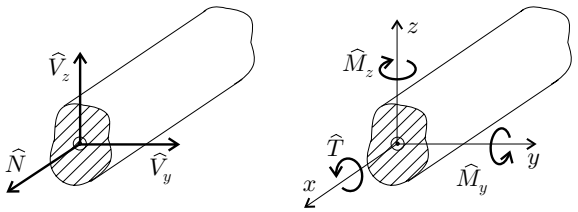

Figure 6.2: The normal force $\widehat{N}$; the bending moments $\widehat{M}_y$, $\widehat{M}_z$; the torque $\widehat{T}$; and the transverse shear forces $\widehat{V}_y$, $\widehat{V}_z$ inside a beam.

6.1.1 Boundary Conditions

At a built-in end, the in-plane displacements and the slopes are zero. At a simply supported end, the in-plane displacements and the moments are zero. At a free end, the moments and the transverse shear forces are zero.

When the end of the beam is restrained axially, the axial displacement is zero. When the end is not restrained axially, the axial force is zero.

When the end may rotate, the torque is zero. When the end is rotationally restrained, the twist is zero.

The preceding boundary conditions are summarized in Table 6.1.

6.1.2 Stiffness Matrix

The stiffness matrix depends on the geometry of the cross section and on the type of material used in the construction of the beam. The geometry (i.e., the shape) of the cross section changes when the beam is loaded. We neglect the effects of this change in shape on the stiffness and evaluate the stiffness matrix for the cross section of the unloaded beam.

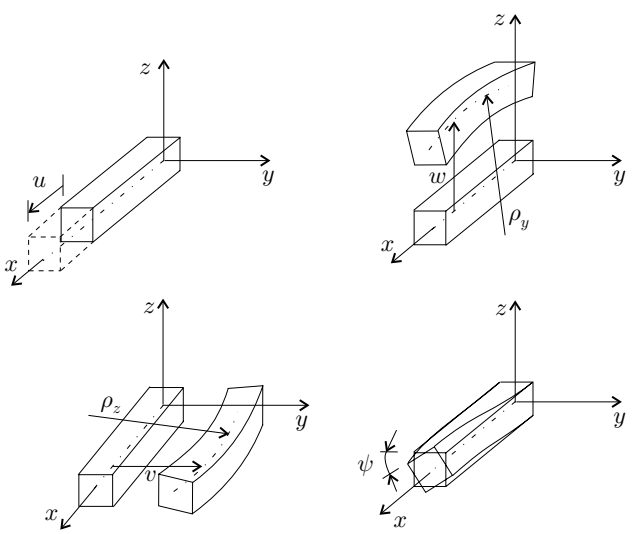

Figure 6.3: Displacements of a beam.

Table 6.1. Boundary conditions for beams.

	x–z plane		*x–y* plane	
Built-in	$w = 0$	$\frac{\partial w}{\partial x} = 0$	$v = 0$	$\frac{\partial v}{\partial x} = 0$
Simply supported	$w = 0$	$\widehat{M}_y = 0$	$v = 0$	$\widehat{M}_z = 0$
Free	$\widehat{V}_z = 0$	$\widehat{M}_y = 0$	$\widehat{V}_y = 0$	$\widehat{M}_z = 0$
Axially restrained		$u = 0$		
unrestrained		$\widehat{N} = 0$		
Rotationally restrained		$\psi = 0$		
unrestrained		$\widehat{T} = 0$		

For a beam made of an isotropic material ("isotropic beam") the force–strain relationships are[3]

$$\begin{Bmatrix} \widehat{N} \\ \widehat{M}_y \\ \widehat{M}_z \\ \widehat{T} \end{Bmatrix} = \begin{bmatrix} (EA) & 0 & 0 & 0 \\ 0 & (EI_{yy}) & (EI_{yz}) & 0 \\ 0 & (EI_{yz}) & (EI_{zz}) & 0 \\ 0 & 0 & 0 & (GI_{\mathrm{t}}) \end{bmatrix} \begin{Bmatrix} \epsilon_x^{\mathrm{o}} \\ \frac{1}{\rho_y} \\ \frac{1}{\rho_z} \\ \vartheta \end{Bmatrix} \qquad \text{isotropic.} \tag{6.4}$$

The terms in parentheses are the tensile EA, bending EI_{yy}, EI_{zz}, $EI_{yz}\,(= EI_{zy})$, and torsional GI_{t} stiffnesses.

We observe that for an isotropic beam there is no coupling between tension (or compression), bending, and torsion. On the other hand, for a beam made of composite materials, in general, none of the elements of the stiffness matrix is zero, and there is coupling between tension, bending, and torsion. Accordingly, tension may cause bending and torsion, torsion may cause tension and bending, and bending may cause tension and torsion (see Eq. 6.2). The displacements resulting from these couplings are often unexpected and are most of the time undesirable. Fortunately for the designer, some of the couplings and the corresponding displacements are not present when either the beam's cross section is symmetrical or when the beam is orthotropic.

Symmetrical cross-section beams. First, we consider an isotropic beam whose cross section is symmetrical about the z-axis. An axial load $\widehat{N}$ and a bending moment $\widehat{M}_y$ (acting in the x–z symmetry plane) are applied to the beam. For this beam the force–strain relationships (Eq. 6.4) reduce to

$$\begin{Bmatrix} \widehat{N} \\ \widehat{M}_y \end{Bmatrix} = \begin{bmatrix} (EA) & 0 \\ 0 & (EI_{yy}) \end{bmatrix} \begin{Bmatrix} \epsilon_x^{\mathrm{o}} \\ \frac{1}{\rho_y} \end{Bmatrix} \qquad \begin{array}{l} \text{isotropic} \\ \text{symmetrical cross section.} \end{array} \tag{6.5}$$

Next, we consider a composite beam whose cross section is symmetrical about the z-axis (Fig. 6.4). As a result of the symmetry, an axial load $\widehat{N}$ acting at the centroid does not introduce either bending or twisting of the beam, whereas a

[3] T. H. G. Megson, *Aircraft Structures for Engineering Students*. 3rd edition. Halsted Press, John Wiley & Sons, New York, 1999, pp. 56 and 285.

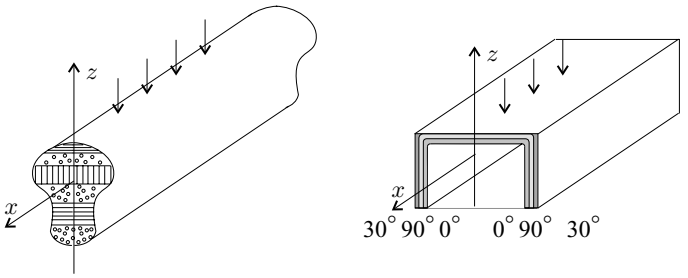

Figure 6.4: Illustrations of composite beams with symmetrical cross sections subjected to a transverse load in the x–z symmetry plane.

moment $\widehat{M}_y$ acting in the x–z symmetry plane introduces only bending in this plane. We designate the elements of the stiffness matrix by $\widehat{EA}$ and $\widehat{EI}_{yy}$ and write the stress–strain relationships as

$$\begin{Bmatrix} \widehat{N} \\ \widehat{M}_y \end{Bmatrix} = \begin{bmatrix} \widehat{EA} & 0 \\ 0 & \widehat{EI}_{yy} \end{bmatrix} \begin{Bmatrix} \epsilon_x^{\mathrm{o}} \\ \frac{1}{\rho_y} \end{Bmatrix} \qquad \begin{matrix} \text{composite} \\ \text{symmetrical cross section.} \end{matrix} \tag{6.6}$$

Orthotropic beams. A beam is orthotropic when its wall is made of an orthotropic laminate and one of the orthotropy axes is aligned with the axis of the beam. A laminate is orthotropic when every layer is made of either an isotropic material or a fiber-reinforced composite (page 75). In the latter case, a layer may consist of plies made either of woven fabric or of unidirectional fibers (Fig. 6.5). Woven fabric plies must be arranged such that one of the ply symmetry axes is aligned with the longitudinal x-axis of the beam. Unidirectional plies must be

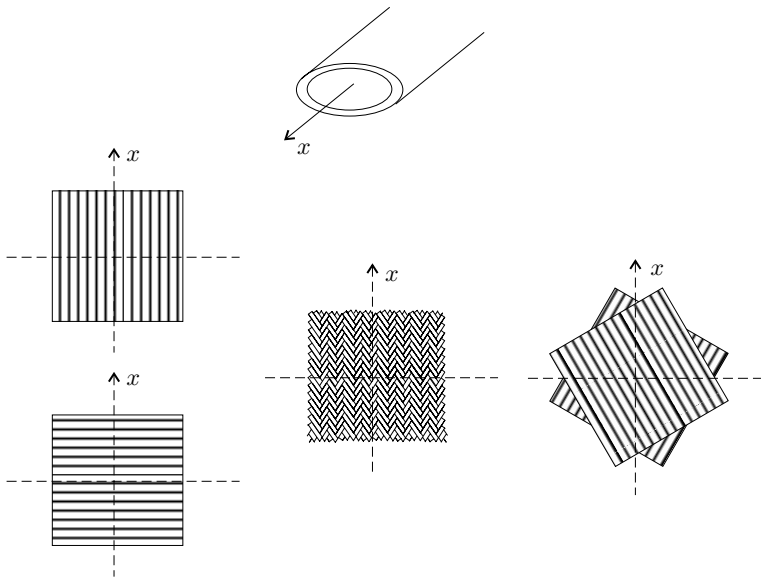

Figure 6.5: Layups that result in no coupling between tension, bending, and torsion. Unidirectional ply (left); woven fabric (middle); two-ply layer (right). For each configuration, one of the symmetry axes must be parallel to the beam's longitudinal x-axis.

mounted so that all the fibers are either parallel or perpendicular to the longitudinal x-axis or one of the symmetry axes of two adjacent unidirectional plies (treated as a single layer) must be parallel to the beam's longitudinal axis.

It is shown subsequently (Section 6.3.3) that for an orthotropic beam $P_{12} = P_{13} = P_{14} = P_{24} = P_{34} = 0$, and the force–strain relationship is

$$\begin{Bmatrix} \widehat{N} \\ \widehat{M}_y \\ \widehat{M}_z \\ \widehat{T} \end{Bmatrix} = \underbrace{\begin{bmatrix} P_{11} & 0 & 0 & 0 \\ 0 & P_{22} & P_{23} & 0 \\ 0 & P_{23} & P_{33} & 0 \\ 0 & 0 & 0 & P_{44} \end{bmatrix}}_{[P]} \begin{Bmatrix} \epsilon_x^{\mathrm{o}} \\ \frac{1}{\rho_y} \\ \frac{1}{\rho_z} \\ \vartheta \end{Bmatrix} \qquad \text{orthotropic.} \tag{6.7}$$

From the preceding equation we see that there is no tension–bending–torsion coupling in an orthotropic beam.

We designate the elements of the stiffness matrix by $\widehat{EA}$, $\widehat{EI}$, $\widehat{GI}_{\mathrm{t}}$ and write

$$[P] = \begin{bmatrix} \widehat{EA} & 0 & 0 & 0 \\ 0 & \widehat{EI}_{yy} & \widehat{EI}_{yz} & 0 \\ 0 & \widehat{EI}_{yz} & \widehat{EI}_{zz} & 0 \\ 0 & 0 & 0 & \widehat{GI}_{\mathrm{t}} \end{bmatrix} \qquad \text{orthotropic.} \tag{6.8}$$

Principal direction. For isotropic beams, there is a coordinate system y'–z' (Fig. 6.6) in which the moment of inertia $I_{y'z'}$ is zero ($I_{y'z'} = 0$). The angle between the y'-axis of this coordinate system and the y-axis is[4]

$$\tan\, 2\varphi = -\frac{2I_{yz}}{I_{yy} - I_{zz}} = -\frac{2EI_{yz}}{EI_{yy} - EI_{zz}}. \tag{6.9}$$

The relationships between the moments of inertia in the y–z and y'–z' coordinate systems are

$$I_{y'y'} = \frac{I_{yy} + I_{zz}}{2} + \sqrt{\left(\frac{I_{yy} - I_{zz}}{2}\right)^2 + I_{yz}^2} \tag{6.10}$$

$$I_{z'z'} = \frac{I_{yy} + I_{zz}}{2} - \sqrt{\left(\frac{I_{yy} - I_{zz}}{2}\right)^2 + I_{yz}^2} \tag{6.11}$$

$$I_{y'z'} = 0. \tag{6.12}$$

The directions y' and z' are called principal directions.

As in Eq. (6.9), for an orthotropic beam we write the angle between y' and y as

$$\tan\, 2\varphi = -\frac{2\widehat{EI}_{yz}}{\widehat{EI}_{yy} - \widehat{EI}_{zz}}. \tag{6.13}$$

[4] E. P. Popov, *Engineering Mechanics of Solids*. Prentice-Hall, Englewood Cliffs, New Jersey, 1990, p. 342.

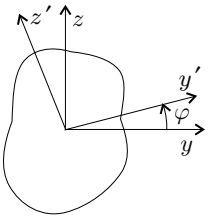

Figure 6.6: The y', z' coordinate system in which $I_{y'z'}$ is zero.

By referring to Eqs. (6.10)–(6.12), we express the bending stiffnesses in the y'–z' coordinate system in the forms

$$\widehat{EI}_{y'y'} = \frac{\widehat{EI}_{yy} + \widehat{EI}_{zz}}{2} + \sqrt{\left(\frac{\widehat{EI}_{yy} - \widehat{EI}_{zz}}{2}\right)^2 + \widehat{EI}_{yz}^2} \tag{6.14}$$

$$\widehat{EI}_{z'z'} = \frac{\widehat{EI}_{yy} + \widehat{EI}_{zz}}{2} - \sqrt{\left(\frac{\widehat{EI}_{yy} - \widehat{EI}_{zz}}{2}\right)^2 + \widehat{EI}_{yz}^2} \tag{6.15}$$

$$\widehat{EI}_{y'z'} = 0. \tag{6.16}$$

6.1.3 Compliance Matrix

With respect to the x–y–z coordinate system attached to the centroid, the strain–force relationships are defined as

$$\begin{Bmatrix} \epsilon_x^{\mathrm{o}} \\ \frac{1}{\rho_y} \\ \frac{1}{\rho_z} \\ \vartheta \end{Bmatrix} = \begin{bmatrix} W_{11} & 0 & 0 & W_{14} \\ 0 & W_{22} & W_{23} & W_{24} \\ 0 & W_{23} & W_{33} & W_{34} \\ W_{14} & W_{24} & W_{34} & W_{44} \end{bmatrix} \begin{Bmatrix} \widehat{N} \\ \widehat{M}_y \\ \widehat{M}_z \\ \widehat{T} \end{Bmatrix}. \tag{6.17}$$

The W_{21} and W_{31} terms are zero because an axial force applied at the centroid does not cause bending, whereas W_{12} and W_{13} are zero because the compliance matrix is symmetrical. The compliance matrix $[W]$ is the inverse of the stiffness matrix

$$\begin{bmatrix} W_{11} & 0 & 0 & W_{14} \\ 0 & W_{22} & W_{23} & W_{24} \\ 0 & W_{23} & W_{33} & W_{34} \\ W_{14} & W_{24} & W_{34} & W_{44} \end{bmatrix} = \begin{bmatrix} P_{11} & P_{12} & P_{13} & P_{14} \\ P_{12} & P_{22} & P_{23} & P_{24} \\ P_{13} & P_{23} & P_{33} & P_{34} \\ P_{14} & P_{24} & P_{34} & P_{44} \end{bmatrix}^{-1}. \tag{6.18}$$

We obtain the compliance matrix of an orthotropic beam by substituting the elements of the matrix $[P]$ given in Eq. (6.8) into this expression. The

result is

$$[W] = \begin{bmatrix} \frac{1}{\widehat{EA}} & 0 & 0 & 0 \\ 0 & \frac{\widehat{EI}_{zz}}{\widehat{EI}_{yy}\widehat{EI}_{zz} - (\widehat{EI}_{yz})^2} & \frac{-\widehat{EI}_{yz}}{\widehat{EI}_{yy}\widehat{EI}_{zz} - (\widehat{EI}_{yz})^2} & 0 \\ 0 & \frac{-\widehat{EI}_{yz}}{\widehat{EI}_{yy}\widehat{EI}_{zz} - (\widehat{EI}_{yz})^2} & \frac{\widehat{EI}_{yy}}{\widehat{EI}_{yy}\widehat{EI}_{zz} - (\widehat{EI}_{yz})^2} & 0 \\ 0 & 0 & 0 & \frac{1}{\widehat{GI}_t} \end{bmatrix} \quad \text{orthotropic.} \tag{6.19}$$

6.1.4 Replacement Stiffnesses

The parameters $\widehat{EA}$, $\widehat{EI}$, $\widehat{GI}_t$ are referred to as replacement stiffnesses. By comparing Eq. (6.5) with Eq. (6.6) and Eqs. (6.4) with Eqs. (6.7) and (6.8), we note the similarity in the force–strain relationships of isotropic and composite beams. Therefore, the strains (and consequently the displacements) of an orthotropic beam and of a composite beam with symmetrical cross section can be obtained by replacing EA, EI, GI_t by $\widehat{EA}$, $\widehat{EI}$, $\widehat{GI}_t$ in the corresponding isotropic beam solution. For an orthotropic beam, the necessary substitutions are

Isotropic beam		Orthotropic beam
EA	$\Longrightarrow$	$\widehat{EA}$
$EI_{yy}, EI_{zz}, EI_{yz}$	$\Longrightarrow$	$\widehat{EI}_{yy}, \widehat{EI}_{zz}, \widehat{EI}_{yz}$
GI_t	$\Longrightarrow$	$\widehat{GI}_t$

For a composite beam with symmetrical cross section and loaded in the symmetry plane the following substitutions apply:

Isotropic beam symmetrical cross section		Composite beam symmetrical cross section
EA, EI_{yy}	$\Longrightarrow$	$\widehat{EA}, \widehat{EI}_{yy}$

As the preceding discussion indicates, the displacements of orthotropic beams and of composite beams with symmetrical cross section are similar to the displacements of isotropic beams. However, the stresses are markedly different in isotropic and in composite beams. In an isotropic beam subjected to an axial load and pure bending, there is only axial stress. In a composite beam subjected to an axial load and pure bending, in addition to the axial stress, there are also transverse normal and shear stresses. Furthermore, in an isotropic beam subjected to pure torque, there is only shear stress, whereas in a composite beam there are also axial and transverse normal stresses.

In this chapter the stresses are calculated by the laminate plate theory, which does not take into account the interlaminar stresses near free edges (page 166).

6.2 Rectangular, Solid Beams Subjected to Axial Load and Bending

We consider rectangular laminated beams having solid cross sections with an axial force $\widehat{N}$ acting at the centroid and a pure bending moment $\widehat{M}_y$ acting in the

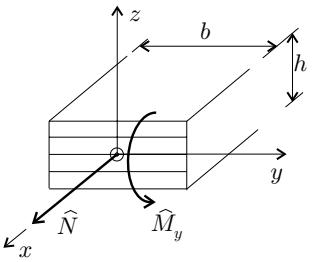

Figure 6.7: Rectangular laminated beam.

x–z plane (Fig. 6.7). In this section, we develop expressions for calculating the displacements and the stresses.

We treat the beam as a narrow plate and build the analysis on the results of laminate plate theory presented in Chapter 3. By convention, for plates along an edge parallel to the y-axis, the in-plane force per unit length is N_x, and the moment per unit length is M_x (Fig. 6.8). For beams, the total force $\widehat{N}$ along an edge parallel to y and the total moment in the x–z plane $\widehat{M}_y$ are specified. The total axial force in the beam $\widehat{N}$ corresponds to bN_x in the plate, and the total moment in the beam $\widehat{M}_y$ corresponds to bM_x in the plate (where b is the width). Thus, we can apply the laminate plate theory expressions to beams by making the following substitutions:

$$N_x = \frac{\widehat{N}}{b} \qquad M_x = \frac{\widehat{M}_y}{b}. \tag{6.20}$$

6.2.1 Displacements – Symmetrical Layup

The layup of the beam is symmetrical. As noted in the preceding section, we analyze this beam by the laminate plate theory, according to which the midplane strain and curvature of the plate are (Eqs. 3.31 and 3.32)

$$\epsilon_x^{\circ} = a_{11} N_x \qquad \kappa_x = d_{11} M_x \qquad \text{plate.} \tag{6.21}$$

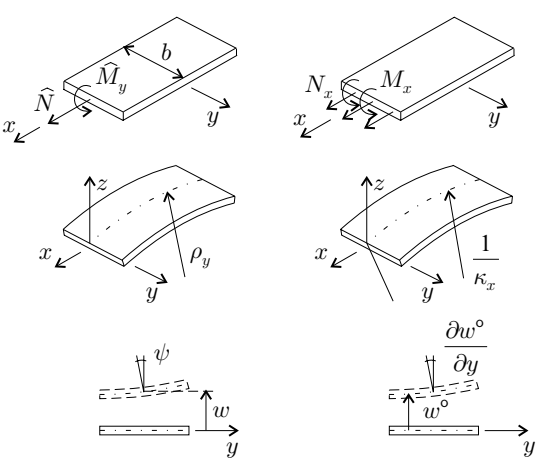

Figure 6.8: Internal forces and curvatures in a beam and in the corresponding plate.

where a_{11} and d_{11} are the elements of the compliance matrices (Eqs. 3.29 and 3.30). We observe that the curvature of the plate in the x–z plane κ_x corresponds to the curvature of the beam $1/\rho_y$ (Fig. 6.8). If we replace κ_x with $1/\rho_y$, for a beam Eqs. (6.20) and (6.21) yield

$$\epsilon_x^{\mathrm{o}} = \underbrace{\left(\frac{a_{11}}{b}\right)}_{W_{11}} \widehat{N} \qquad \frac{1}{\rho_y} = \underbrace{\left(\frac{d_{11}}{b}\right)}_{W_{22}} \widehat{M}_y \qquad \begin{matrix}\text{composite}\\ \text{beam.}\end{matrix} \tag{6.22}$$

By comparing this equation with Eq. (6.17), we see that the terms in parentheses are the W_{11} and W_{22} elements of the compliance matrix.

For a beam made of an isotropic material, the strain and curvature are (Eq. 6.5)

$$\epsilon_x^{\mathrm{o}} = \frac{1}{EA}\widehat{N} \qquad \frac{1}{\rho_y} = \frac{1}{EI}\widehat{M}_y \qquad \begin{matrix}\text{isotropic}\\ \text{beam.}\end{matrix} \tag{6.23}$$

It follows from Eqs. (6.22) and (6.23) that the axial strain and the curvature of the axis (and consequently the displacements u and w) of a composite beam (symmetrical layup) can be calculated by replacing EA and EI by $\frac{b}{a_{11}}$ and $\frac{b}{d_{11}}$ in the relevant expressions for the corresponding isotropic beam.

An isotropic beam subjected to an axial force $\widehat{N}$ and a bending moment $\widehat{M}_y$ only bends in the x–z plane. On the other hand, under these loads the cross sections of a composite beam may also twist. To determine the amount of this twist we refer to the twisting of a plate. The out-of-plane curvature of a plate (symmetrical layup) is (Eq. 3.32)

$$\kappa_{xy} = d_{16} M_x \qquad \text{plate,} \tag{6.24}$$

where κ_{xy} is defined in Eq. (3.8) and is repeated below

$$\kappa_{xy} = -\frac{2\partial^2 w^{\mathrm{o}}}{\partial x \partial y} = -2\frac{\partial \frac{\partial w^{\mathrm{o}}}{\partial y}}{\partial x}, \tag{6.25}$$

where w^{o} is the deflection of the midplane. The expression $\partial w^{\mathrm{o}}/\partial y$ in the plate corresponds to ψ in the beam (Fig. 6.8). Thus, we have

$$\kappa_{xy} = -2\frac{\partial \psi}{\partial x}. \tag{6.26}$$

Equations (6.1) and (6.26) give the rate of twist of the beam as follows:

$$\vartheta = -\frac{1}{2}\kappa_{xy}. \tag{6.27}$$

By combining Eqs. (6.20), (6.24), and (6.27), we obtain the rate of twist of a beam as follows:

$$\vartheta = \underbrace{\left(-\frac{1}{2}\frac{d_{16}}{b}\right)}_{W_{24}} \widehat{M}_y \qquad \begin{matrix}\text{composite}\\ \text{beam.}\end{matrix} \tag{6.28}$$

When only $\widehat{N}$ and $\widehat{M}_y$ act, the relevant elements of the compliance matrix are W_{11}, W_{22}, W_{23}, W_{14}, W_{24} (Eq. 6.17). The elements W_{11}, W_{22}, and W_{24} are given

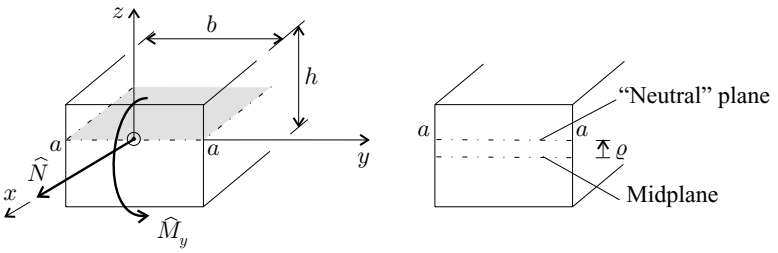

Figure 6.9: Unsymmetrical solid rectangular beam.

by Eqs. (6.22) and (6.28). Elements W_{14} and W_{23} are zero because the layup is symmetrical.

When the beam is orthotropic, d_{16} is zero (Eq. 3.37), and the rate of twist is zero ($\vartheta = 0$) when the beam is subjected to an $\widehat{M}_y$ bending moment.

6.2.2 Displacements – Unsymmetrical Layup

The layup of the laminated beam is unsymmetrical. The centroid is located at the *a–a* plane at a distance ϱ from an arbitrary reference plane. This reference plane may be chosen as the midplane (Fig. 6.9). The location of this *a–a* plane is such that an axial load does not cause a change in the curvature $1/\rho_y$, and a bending moment does not cause axial strain ϵ_x^o. Thus, the *a–a* plane is analogous to the neutral plane (which, for beams made of isotropic materials, passes through the center of gravity).

We now consider a laminated plate (unsymmetrical layup) on which an axial force N_x and a moment M_x (per unit length) act in the *a–a* plane. For this plate, the following relationships hold in the *a–a* plane (Eq. 3.22):

$$\epsilon_x^o = \alpha_{11}^{\varrho} N_x + \beta_{11}^{\varrho} M_x \qquad \kappa_x = \beta_{11}^{\varrho} N_x + \delta_{11}^{\varrho} M_x \qquad \text{plate,} \tag{6.29}$$

where α_{11}^{ϱ}, β_{11}^{ϱ}, and δ_{11}^{ϱ} are evaluated at the *a–a* "neutral" plane. According to the aforementioned definition of the "neutral" plane, ϵ_x^o depends only on N_x, and κ_x depends only on M_x. Therefore, β_{11}^{ϱ} must be equal to zero. Thus, we write (see Eq. 3.48)

$$\beta_{11}^{\varrho} = \beta_{11} + \varrho \delta_{11} = 0, \tag{6.30}$$

where β_{11} and δ_{11} are evaluated at the arbitrarily chosen reference plane that here we have taken to be the midplane. The consequence of $\beta_{11}^{\varrho} = 0$ is twofold. The first consequence is that the distance ϱ is

$$\varrho = -\frac{\beta_{11}}{\delta_{11}}. \tag{6.31}$$

The second consequence is that Eq. (6.29) reduces to

$$\epsilon_x^o = \alpha_{11}^{\varrho} N_x \qquad \kappa_x = \delta_{11}^{\varrho} M_x \qquad \text{plate.} \tag{6.32}$$

We note again that the curvature of the plate κ_x corresponds to the curvature of the beam $1/\rho_y$. Then, for a beam, Eqs. (6.20) and (6.32) yield

$$\epsilon_x^{\circ} = \underbrace{\left(\frac{\alpha_{11}^{\varrho}}{b}\right)}_{W_{11}} \widehat{N} \qquad \frac{1}{\rho_y} = \underbrace{\left(\frac{\delta_{11}^{\varrho}}{b}\right)}_{W_{22}} \widehat{M}_y \qquad \begin{matrix}\text{composite}\\ \text{beam.}\end{matrix} \tag{6.33}$$

By comparing this equation with Eq. (6.17), we see that the terms in parentheses are the W_{11} and W_{22} elements of the compliance matrix.

It follows from Eqs. (6.33) and (6.23) that the axial strain and curvature of the axis (and consequently the displacements u and w) of a composite beam (unsymmetrical layup) can be calculated by replacing EA and EI by $\frac{b}{\alpha_{11}^{\varrho}}$ and $\frac{b}{\delta_{11}^{\varrho}}$ in the relevant expressions for the corresponding isotropic beam.

When an isotropic beam is subjected to an axial force $\widehat{N}$ and to a bending moment $\widehat{M}_y$, it will only bend in the x–z plane. The cross section of a composite beam subjected to $\widehat{N}$ and $\widehat{M}_y$ may also twist. To determine the rate of twist of a composite beam, we again refer to a laminated plate. The out-of-plane curvature of a laminated plate (unsymmetrical layup) is (see Eq. 3.22)

$$\kappa_{xy} = \beta_{16}^{\varrho} N_x + \delta_{16}^{\varrho} M_x \qquad \text{plate,} \tag{6.34}$$

where β_{16}^{ϱ}, and δ_{16}^{ϱ} are evaluated at the a–a "neutral" plane. From Eq. (3.48) we have

$$\beta_{16}^{\varrho} = \beta_{16} + \varrho\delta_{16} \qquad \delta_{16}^{\varrho} = \delta_{16}. \tag{6.35}$$

From Eqs. (6.20), (6.27), and (6.34) we obtain the rate of twist of the beam:

$$\vartheta = \underbrace{\left(-\frac{1}{2}\frac{\beta_{16}^{\varrho}}{b}\right)}_{W_{14}} \widehat{N} + \underbrace{\left(-\frac{1}{2}\frac{\delta_{16}^{\varrho}}{b}\right)}_{W_{24}} \widehat{M}_y \qquad \begin{matrix}\text{composite}\\ \text{beam.}\end{matrix} \tag{6.36}$$

By comparing this equation with Eq. (6.17), we see that the terms in the parentheses are the W_{14} and W_{24} elements of the compliance matrix.

When only $\widehat{N}$ and $\widehat{M}_y$ act, the relevant elements of the compliance matrix are W_{11}, W_{22}, W_{23}, W_{14}, W_{24} (Eq. 6.17). Elements W_{11}, W_{22}, W_{14}, and W_{24} are given by Eqs. (6.33) and (6.36), and W_{23} is zero.

When the beam is orthotropic and one of the orthotropy axes is aligned with the beam's axis, δ_{16} and β_{16} are zero (Eq. 3.37). Therefore, (see Eqs. 6.35 and 6.36), the rate of twist is zero ($\vartheta = 0$) when an orthotropic beam is subjected to an axial force $\widehat{N}$ and a bending moment $\widehat{M}_y$.

6.2.3 Stresses and Strains

The stresses and strains are given in this section for a rectangular thin beam whose thickness h is small compared with its width b (Fig. 6.9). We consider only regions away from the edges and employ the laminate plate theory expressions.

Symmetrical layup. At the neutral plane (which for a symmetrical laminate coincides with the midplane), the strains and curvatures are (see Eqs. 3.31, 3.32, and 6.20)

$$\begin{Bmatrix} \epsilon_x^{\mathrm{o}} \\ \epsilon_y^{\mathrm{o}} \\ \gamma_{xy}^{\mathrm{o}} \end{Bmatrix} = \begin{bmatrix} a_{11} \\ a_{12} \\ a_{16} \end{bmatrix} \left\{ \frac{\widehat{N}}{b} \right\} \qquad \begin{Bmatrix} \kappa_x \\ \kappa_y \\ \kappa_{xy} \end{Bmatrix} = \begin{bmatrix} d_{11} \\ d_{12} \\ d_{16} \end{bmatrix} \left\{ \frac{\widehat{M}_y}{b} \right\}. \tag{6.37}$$

In a ply at a distance z from the midplane, the strains are (see Eq. 3.7)

$$\begin{Bmatrix} \epsilon_x \\ \epsilon_y \\ \gamma_{xy} \end{Bmatrix} = \begin{Bmatrix} \epsilon_x^{\mathrm{o}} \\ \epsilon_y^{\mathrm{o}} \\ \gamma_{xy}^{\mathrm{o}} \end{Bmatrix} + z \begin{Bmatrix} \kappa_x \\ \kappa_y \\ \kappa_{xy} \end{Bmatrix}. \tag{6.38}$$

The ply stresses are given by (Eq. 3.11)

$$\begin{Bmatrix} \sigma_x \\ \sigma_y \\ \tau_{xy} \end{Bmatrix} = \begin{bmatrix} \overline{Q}_{11} & \overline{Q}_{12} & \overline{Q}_{16} \\ \overline{Q}_{21} & \overline{Q}_{22} & \overline{Q}_{26} \\ \overline{Q}_{61} & \overline{Q}_{62} & \overline{Q}_{66} \end{bmatrix} \begin{Bmatrix} \epsilon_x \\ \epsilon_y \\ \gamma_{xy} \end{Bmatrix}. \tag{6.39}$$

Unsymmetrical layup. The strains and curvatures of the axis passing through the centroid (which is in the "neutral" plane) are (see Eqs. 3.22 and 6.20)

$$\begin{Bmatrix} \epsilon_x^{\mathrm{o}} \\ \epsilon_y^{\mathrm{o}} \\ \gamma_{xy}^{\mathrm{o}} \\ \kappa_x \\ \kappa_y \\ \kappa_{xy} \end{Bmatrix} = \begin{bmatrix} \alpha_{11}^{\varrho} & 0 \\ \alpha_{12}^{\varrho} & \beta_{21}^{\varrho} \\ \alpha_{16}^{\varrho} & \beta_{61}^{\varrho} \\ 0 & \delta_{11}^{\varrho} \\ \beta_{12}^{\varrho} & \delta_{12}^{\varrho} \\ \beta_{16}^{\varrho} & \delta_{16}^{\varrho} \end{bmatrix} \begin{Bmatrix} \frac{\widehat{N}}{b} \\ \frac{\widehat{M}_y}{b} \end{Bmatrix}, \tag{6.40}$$

where α^{ϱ} and β^{ϱ} are evaluated at the "neutral" plane (Fig. 6.9). The location of the "neutral" plane is given by Eq. (6.31).

In a ply at a distance z from the "neutral" plane, the strains and stresses are given by Eqs. (6.38) and (6.39).

6.1 Example. *An $L = 0.2$-m-long and $b = 0.02$-m-wide beam, with the cross section shown in Fig. 6.10, is made of graphite epoxy. The material properties are given in Table 3.6 (page 81). The layup is $[\pm 45_2^{\mathrm{f}}/0_{12}/\pm 45_2^{\mathrm{f}}]$. The beam, simply supported at each end, is loaded uniformly ($p = 1\,000$ N/m). Calculate the maximum bending moment, the maximum deflection, and the ply stresses and strains.*

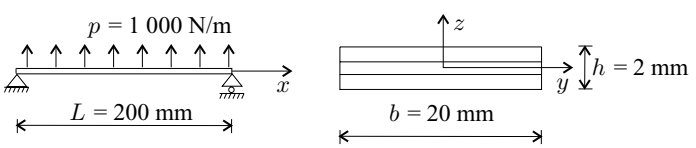

Figure 6.10: The beam in Example 6.1.

Solution. The maximum bending moment at the middle of the beam is (Table 7.3, page 332)

$$\widehat{M}_y = \frac{pL^2}{8} = 5\ \mathrm{N}\cdot\mathrm{m}. \tag{6.41}$$

The maximum deflection of the corresponding isotropic beam is (Table 7.3)

$$\widetilde{w} = \frac{5}{384}\frac{pL^4}{EI}. \tag{6.42}$$

The maximum deflection of the composite beam is obtained by replacing EI by $\frac{b}{d_{11}}$ (see page 212)

$$\widetilde{w} = \frac{5}{384}\frac{pL^4}{\frac{b}{d_{11}}}. \tag{6.43}$$

With the value of $d_{11} = 33.10 \times 10^{-3}\ \frac{1}{\mathrm{N}\cdot\mathrm{m}}$ (Table 3.8, page 85), the maximum deflection is

$$\widetilde{w} = 0.0345\ \mathrm{m} = 34.5\ \mathrm{mm}. \tag{6.44}$$

The axial force is zero ($\widehat{N} = 0$). Thus, with the compliance matrices given in Table 3.8, the midplane strains and curvatures are (see Eqs. 6.37 and 6.41)

$$\begin{Bmatrix} \epsilon_x^{\mathrm{o}} \\ \epsilon_y^{\mathrm{o}} \\ \gamma_{xy}^{\mathrm{o}} \end{Bmatrix} = \begin{Bmatrix} a_{11} \\ a_{12} \\ a_{16} \end{Bmatrix} \left\{ \frac{\widehat{N}}{b} \right\} = \begin{Bmatrix} 0 \\ 0 \\ 0 \end{Bmatrix} \tag{6.45}$$

$$\begin{aligned} \begin{Bmatrix} \kappa_x \\ \kappa_y \\ \kappa_{xy} \end{Bmatrix} &= \begin{Bmatrix} d_{11} \\ d_{12} \\ d_{16} \end{Bmatrix} \left\{ \frac{\widehat{M}_y}{b} \right\} = \begin{Bmatrix} 33.10 \\ -25.59 \\ 0 \end{Bmatrix} 10^{-3} \left\{ \frac{5}{0.02} \right\} \\ &= \begin{Bmatrix} 8.28 \\ -6.40 \\ 0 \end{Bmatrix} \frac{1}{\mathrm{m}}, \end{aligned} \tag{6.46}$$

where κ_x and κ_y are illustrated in Figure 6.11. In a ply, at a distance z from the midplane, the strains are given by Eq. (6.38) as follows:

$$\begin{Bmatrix} \epsilon_x \\ \epsilon_y \\ \gamma_{xy} \end{Bmatrix} = z \begin{Bmatrix} \kappa_x \\ \kappa_y \\ \kappa_{xy} \end{Bmatrix} = z \begin{Bmatrix} 8.27 \\ -6.40 \\ 0 \end{Bmatrix}. \tag{6.47}$$

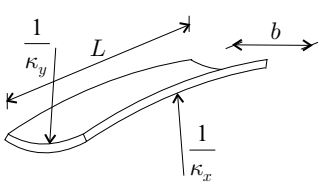

Figure 6.11: Illustration of the curvatures of the beam in Example 6.1.

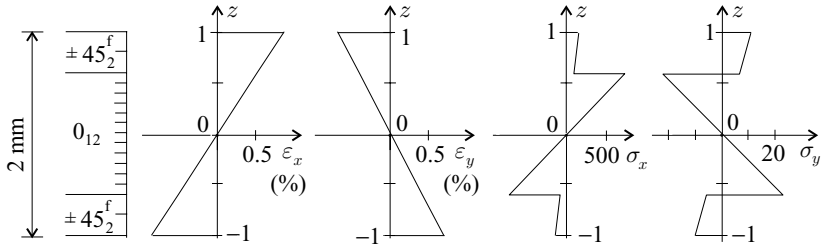

Figure 6.12: The nonzero stresses and strains in the beam in Example 6.1. The unit of σ is 10^6 N/m^2.

The stresses in the kth ply are (Eq. 6.39)

$$\begin{Bmatrix} \sigma_x \\ \sigma_y \\ \tau_{xy} \end{Bmatrix}_k = \begin{bmatrix} \overline{Q}_{11} & \overline{Q}_{12} & \overline{Q}_{16} \\ \overline{Q}_{21} & \overline{Q}_{22} & \overline{Q}_{26} \\ \overline{Q}_{61} & \overline{Q}_{62} & \overline{Q}_{66} \end{bmatrix}_k \begin{Bmatrix} \epsilon_x \\ \epsilon_y \\ \gamma_{xy} \end{Bmatrix}_k . \tag{6.48}$$

The elements of the $[\overline{Q}]$ matrix of the 0-degree ply are given by Eq. (3.65) and of the woven fabric by Eq. (3.66). The stresses are calculated with these values of the $[\overline{Q}]$ matrices and with the strains given in Eq. (6.47). The results are shown in Figure 6.12. We note again that these stresses are valid only in regions away from the edges.

6.3 Thin-Walled, Open-Section Orthotropic or Symmetrical Cross-Section Beams Subjected to Axial Load and Bending

In this section we present the deflections of, and stresses and strains in, thin-walled, open-section beams. The method is first illustrated via orthotropic T-beams with symmetrical cross section and via orthotropic L-beams. The analysis is then extended to orthotropic beams with arbitrary cross section and to nonorthotropic beams with symmetrical cross section.

6.3.1 Displacements of T-Beams

We consider a T-beam whose cross section is symmetrical with respect to the z-axis (Fig. 6.13). The layup of both the flange and the web is orthotropic and

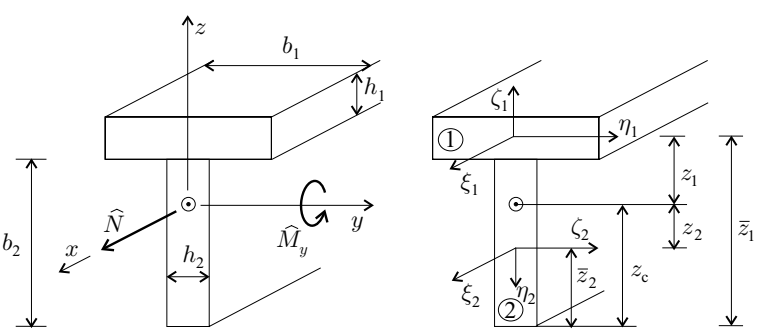

Figure 6.13: Illustration of the T-beam.

symmetrical. An axial force $\widehat{N}$ and a bending moment $\widehat{M}_y$ act at the centroid of the beam. The origin of the x–y–z coordinate system is attached to this centroid. In addition we use the ξ_1–η_1–ζ_1 and ξ_2–η_2–ζ_2 coordinate systems attached to the midpoints of the flange and the web, respectively. The flange and the web are designated by the subscripts 1 and 2.

In the following we derive the replacement stiffnesses. The displacements of a T-beam are obtained by substituting these replacement stiffnesses into the expressions for the displacements of the corresponding isotropic beam. Because the cross section is symmetrical with respect to the z-axis and the loads act in the x–z plane, the beam bends only about the y-axis. Consequently, only $\widehat{EA}$ and $\widehat{EI}_{yy}$ are of interest.

The calculation proceeds in four steps. In Step 1 we deform the axis of the beam and calculate the strains in, and the curvatures of, each wall segment; in Step 2 we calculate the forces and moments in each wall segment; in Step 3 we calculate the resultant forces and moments acting on the beam; in Step 4 we determine the replacement stiffnesses.

We treat both the flange and the web as thin plates and analyze them by the laminate plate theory.

Tensile stiffness $\widehat{EA}$ and centroid.

Step 1. The axis of the beam (passing through the centroid) is elongated, and the strain of the axis is denoted by ϵ_x^{o}. The beam does not bend, and the axial strains are the same across the cross section,

$$\epsilon_{\xi 1}^{\mathrm{o}} = \epsilon_{\xi 2}^{\mathrm{o}} = \epsilon_x^{\mathrm{o}}, \tag{6.49}$$

where $\epsilon_{\xi 1}^{\mathrm{o}}$ and $\epsilon_{\xi 2}^{\mathrm{o}}$ are the axial strains in the midplanes of the flange and the web, respectively.

Step 2. The axial strains result in distributed axial forces (per unit length) $N_{\xi 1}$, $N_{\xi 2}$ in the midplanes of the flange and the web (Fig. 6.14, left). These forces are (see Eq. 3.31)

$$N_{\xi 1} = \frac{1}{(a_{11})_1}\epsilon_{\xi 1}^{\mathrm{o}} \qquad N_{\xi 2} = \frac{1}{(a_{11})_2}\epsilon_{\xi 2}^{\mathrm{o}}, \tag{6.50}$$

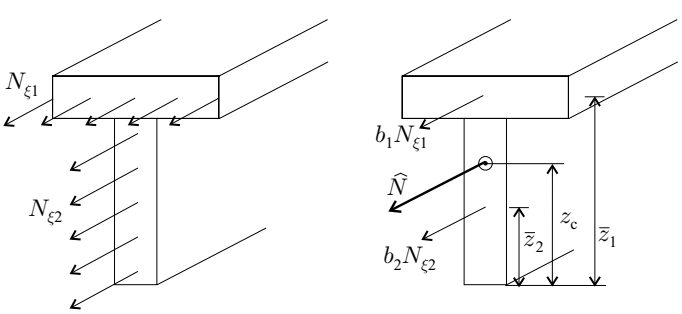

Figure 6.14: The distributed forces and the force resultants.

where $(a_{11})_1$ and $(a_{11})_2$ are evaluated in the ξ–η–ζ coordinate system at the midplanes of the flange and the web.

Step 3. The total forces acting in the flange and in the web are $b_1 N_{\xi 1}$ and $b_2 N_{\xi 2}$, respectively, and the total force acting on the beam is (Fig. 6.14, right)

$$\widehat{N} = b_1 N_{\xi 1} + b_2 N_{\xi 2}. \tag{6.51}$$

Step 4. Equations (6.49)–(6.51) give

$$\widehat{N} = \underbrace{\left(\frac{b_1}{(a_{11})_1} + \frac{b_2}{(a_{11})_2} \right)}_{\widehat{EA}} \epsilon_x^{\mathrm{o}}. \tag{6.52}$$

The term indicated by the bracket is the replacement tensile stiffness $\widehat{EA}$.

The coordinate of the centroid z_{c} is calculated by a moment balance about the bottom edge of the web (Fig. 6.14, right) as follows:

$$z_{\mathrm{c}} \widehat{N} = \overline{z}_1 b_1 N_{\xi 1} + \overline{z}_2 b_2 N_{\xi 2}. \tag{6.53}$$

The distances $\overline{z}_1$ and $\overline{z}_2$ are shown in Figure 6.14. By combining this equation with Eqs. (6.49)–(6.52), we obtain the position of the centroid:

$$z_{\mathrm{c}} = \frac{\overline{z}_1 \frac{b_1}{(a_{11})_1} + \overline{z}_2 \frac{b_2}{(a_{11})_2}}{\frac{b_1}{(a_{11})_1} + \frac{b_2}{(a_{11})_2}}. \tag{6.54}$$

The coordinates of the centers of the flange and the web with respect to the centroid are (Fig. 6.13)

$$z_1 = \overline{z}_1 - z_{\mathrm{c}} \qquad z_2 = \overline{z}_2 - z_{\mathrm{c}}. \tag{6.55}$$

Depending on where the centroid is located, z_2 is either positive or negative. In Figure 6.13, z_2 is negative.

Bending stiffness $\widehat{EI}_{yy}$. The beam is bent about the y-axis passing through the centroid (Fig. 6.15). The radius of curvature of the beam is denoted by ρ_y.

Step 1. The strain varies linearly with z as follows:

$$\epsilon_x = \frac{1}{\rho_y} z. \tag{6.56}$$

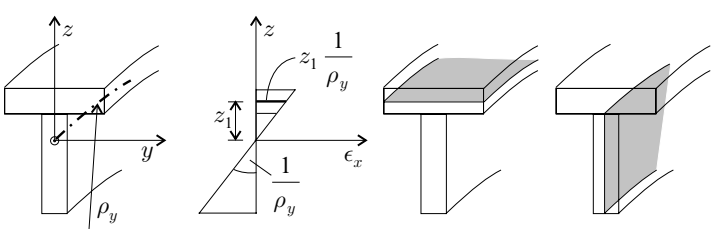

Figure 6.15: The radius of curvature ρ_y, the strain distribution, and the deformed shapes of the midplanes of the flange and the web.

At the midplane of the flange $z = z_1$ and the strain is

$$\epsilon^{\mathrm{o}}_{\xi 1} = \frac{1}{\rho_y} z_1. \tag{6.57}$$

The curvature of the midplane of the flange about the y-axis (by definition) is

$$\kappa_{\xi 1} = \frac{1}{\rho_y}. \tag{6.58}$$

In the midplane of the web, the strain $\epsilon^{\mathrm{o}}_{\xi 2}$ is

$$\epsilon^{\mathrm{o}}_{\xi 2} = \frac{1}{\rho_y} z. \tag{6.59}$$

The midplane of the web remains flat, and its curvature is zero (Fig. 6.15) as denoted by

$$\kappa_{\xi 2} = 0. \tag{6.60}$$

Step 2. The axial force $N_{\xi 1}$ and the bending moment $M_{\xi 1}$ (per unit length) acting on the flange are (Eqs. 3.31 and 3.32)

$$N_{\xi 1} = \frac{1}{(a_{11})_1} \epsilon^{\mathrm{o}}_{\xi 1} \qquad M_{\xi 1} = \frac{1}{(d_{11})_1} \kappa_{\xi 1}. \tag{6.61}$$

The preceding force and moment are illustrated in Figure 6.16 (left). The terms $(a_{11})_1$ and $(d_{11})_1$ are evaluated in the ξ–η–ζ coordinate system at the midplane of the flange.

The layup of the web is symmetrical, and $\kappa_{\xi 2} = 0$. Consequently, $M_{\xi 2}$ is zero. Thus, the only force acting in the web is $N_{\xi 2}$ (Fig. 6.16, right), and this force is

$$N_{\xi 2} = \frac{1}{(a_{11})_2} \epsilon^{\mathrm{o}}_{\xi 2}, \tag{6.62}$$

where $(a_{11})_2$ is evaluated in the ξ–η–ζ coordinate system at the midplane of the web.

Step 3. The resultant bending moment about the y-axis is (Fig. 6.16)

$$\widehat{M}_y = b_1 N_{\xi 1} z_1 + b_1 M_{\xi 1} + \int_{(b_2)} N_{\xi 2} z dz, \tag{6.63}$$

where b_1, b_2, and z are shown in Figure 6.13.

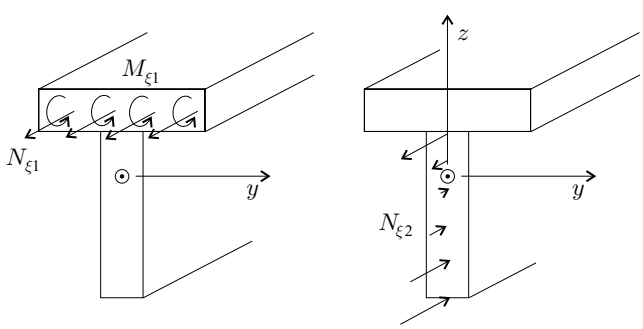

Figure 6.16: The distributed forces and moments (per unit length) in the flange and in the web of a T-beam bent about the y-axis.

Step 4. Equations (6.57)–(6.63) yield

$$\widehat{M}_y = \frac{1}{\rho_y} \underbrace{\left[z_1^2 \frac{b_1}{(a_{11})_1} + \frac{b_1}{(d_{11})_1} + \frac{1}{(a_{11})_2} \left(\frac{b_2^3}{12} + z_2^2 b_2 \right) \right]}_{\widehat{EI}_{yy}}. \tag{6.64}$$

The term indicated by the bracket is the replacement bending stiffness $\widehat{EI}_{yy}$.

6.3.2 Displacements of L-Beams

We consider an L-beam. The walls of the flanges are orthotropic, and one of the axes of orthotropy is aligned with the axis of the beam. The layups of the flanges need not be symmetrical with respect to the flanges' midplanes. The beam is subjected to an axial force $\widehat{N}$ and bending moments $\widehat{M}_y$ and $\widehat{M}_z$ acting at the centroid (Fig. 6.17).

We use an x–y–z coordinate system with its origin attached to the centroid of the beam and the ξ_1–η_1–ζ_1 and ξ_2–η_2–ζ_2 coordinate systems attached to the midpoints of the arbitrarily chosen reference planes in the horizontal and vertical flanges, respectively. The horizontal and vertical flanges are designated by the subscripts 1 and 2.

In this section the replacement stiffnesses are determined. The displacements are obtained by substituting these replacement stiffnesses into the expressions for the displacements of the corresponding isotropic beam. Because the cross section of the L-beam is unsymmetrical, all three bending stiffnesses $\widehat{EI}_{zz}$, $\widehat{EI}_{yy}$, and $\widehat{EI}_{yz}$ as well as the tensile stiffness $\widehat{EA}$ are needed to determine the displacements.

We treat the flanges as thin plates and employ the laminate plate theory equations. The calculation proceeds along the four steps used in the analysis of T-beams (page 218).

Tensile stiffness $\widehat{EA}$ and centroid. The tensile stiffness is obtained by considering the elongation of the beam while the axis of the beam remains straight.

Step 1. The axis of the beam (passing through the centroid) is elongated, and the strain of the axis is denoted by ϵ_x^{o}. In the absence of bending, the axial strains are

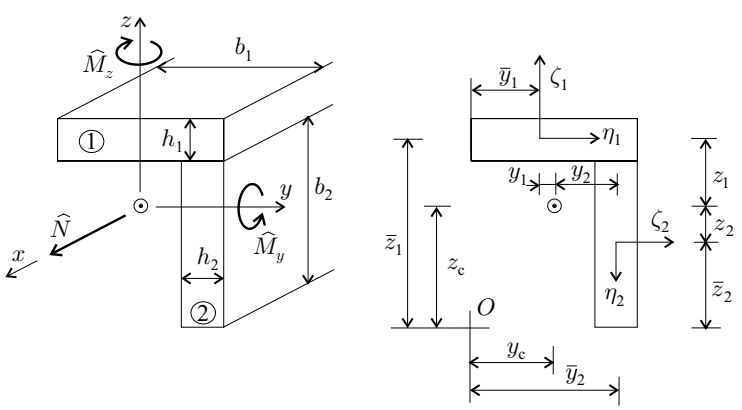

Figure 6.17: L-beam.

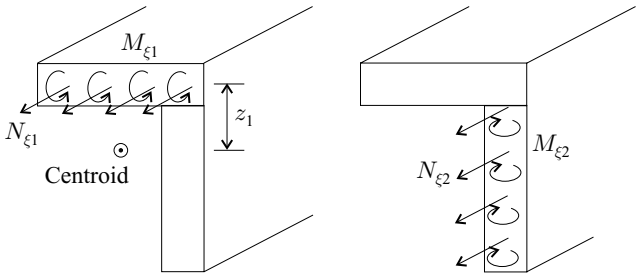

Figure 6.18: The distributed forces and moments acting in an L-beam with unsymmetrical layup when the axis of the beam is elongated.

the same across the cross section,

$$\epsilon^{\mathrm{o}}_{\xi 1} = \epsilon^{\mathrm{o}}_{\xi 2} = \epsilon^{\mathrm{o}}_{x}, \tag{6.65}$$

where $\epsilon^{\mathrm{o}}_{\xi 1}$ and $\epsilon^{\mathrm{o}}_{\xi 2}$ are the axial strains of the reference planes of the two flanges, respectively. The locations of the reference planes may be chosen arbitrarily.

Step 2. The axial forces $N_{\xi 1}$, $N_{\xi 2}$ and the bending moments $M_{\xi 1}$, $M_{\xi 2}$ (per unit length) in the flanges (Fig. 6.18) are expressed in terms of the strains $\epsilon^{\mathrm{o}}_{\xi 1}$, $\epsilon^{\mathrm{o}}_{\xi 2}$. The derivation of these expressions is discussed subsequently on pages 227–228. Here we quote the results, which are

$$N_{\xi 1} = \frac{(\delta_{11})_1}{(D)_1}\epsilon^{\mathrm{o}}_{\xi 1} \qquad N_{\xi 2} = \frac{(\delta_{11})_2}{(D)_2}\epsilon^{\mathrm{o}}_{\xi 2} \tag{6.66}$$

$$M_{\xi 1} = -\frac{(\beta_{11})_1}{(D)_1}\epsilon^{\mathrm{o}}_{\xi 1} \qquad M_{\xi 2} = -\frac{(\beta_{11})_2}{(D)_2}\epsilon^{\mathrm{o}}_{\xi 2}, \tag{6.67}$$

where D is defined in Table 6.2, and δ_{11} and β_{11} are evaluated in the ξ–η–ζ coordinate system.

Table 6.2. The axial force and moments inside the wall ($N_\eta = N_{\xi\eta} = M_\eta = 0$). The elements of the compliance matrix δ_{11}, δ_{16}, δ_{66}, β_{11}, and β_{16} are evaluated in the wall's ξ–η–ζ coordinate system.

	Arbitrary cross section		Symmetrical cross section
	Orthotropic unsymmetrical layup	Orthotropic and symmetrical layup	Arbitrary layup
N_ξ	$\frac{\delta_{11}}{D}\epsilon^{\mathrm{o}}_\xi - \frac{\beta_{11}}{D}\kappa_\xi$	$\frac{1}{a_{11}}\epsilon^{\mathrm{o}}_\xi$	$\frac{\overline{\delta}_{11}}{\overline{D}}\epsilon^{\mathrm{o}}_\xi - \frac{\overline{\beta}_{11}}{\overline{D}}\kappa_\xi$
M_ξ	$-\frac{\beta_{11}}{D}\epsilon^{\mathrm{o}}_\xi + \frac{\alpha_{11}}{D}\kappa_\xi$	$\frac{1}{d_{11}}\kappa_\xi$	$-\frac{\overline{\beta}_{11}}{\overline{D}}\epsilon^{\mathrm{o}}_\xi + \frac{\overline{\alpha}_{11}}{\overline{D}}\kappa_\xi$
$M_{\xi\eta}$	0	0	$-\frac{\beta_{16}}{\delta_{66}}N_\xi - \frac{\delta_{16}}{\delta_{66}}M_\xi$
where	$\overline{\alpha}_{11} = \left(\alpha_{11} - \frac{\beta_{16}^2}{\delta_{66}}\right)$	$\overline{\beta}_{11} = \left(\beta_{11} - \frac{\beta_{16}\delta_{16}}{\delta_{66}}\right)$	$\overline{\delta}_{11} = \left(\delta_{11} - \frac{\delta_{16}^2}{\delta_{66}}\right)$
	$D = \alpha_{11}\delta_{11} - \beta_{11}^2$	$\overline{D} = \overline{\alpha}_{11}\overline{\delta}_{11} - \overline{\beta}_{11}^2$	

Step 3. The resultant axial force is (Fig. 6.18)

$$\widehat{N} = b_1 N_{\xi 1} + b_2 N_{\xi 2}, \tag{6.68}$$

where b_1 and b_2 are shown in Figure 6.17.

Step 4. Equations (6.65)–(6.68) give

$$\widehat{N} = \underbrace{\sum_{k=1}^{2} \frac{b_k (\delta_{11})_k}{(D)_k}}_{\widehat{EA}} \epsilon_x^{\mathrm{o}}. \tag{6.69}$$

The term indicated by the bracket is the tensile stiffness $\widehat{EA}$. The terms $(D)_k$ and $(\delta_{11})_k$ are evaluated in the coordinate systems attached to the reference planes of the horizontal ($k = 1$) and vertical ($k = 2$) flanges, respectively.

The coordinates of the centroid z_{c}, y_{c} are calculated by moment equilibria about point O (Fig. 6.17). With the symbols defined in Figures 6.17 and 6.18, moment equilibria give

$$z_{\mathrm{c}} \widehat{N} = \overline{z}_1 b_1 N_{\xi 1} + \overline{z}_2 b_2 N_{\xi 2} + b_1 M_{\xi 1} \tag{6.70}$$

$$y_{\mathrm{c}} \widehat{N} = \overline{y}_1 b_1 N_{\xi 1} + \overline{y}_2 b_2 N_{\xi 2} + b_2 M_{\xi 2}. \tag{6.71}$$

By combining Eqs. (6.65)–(6.71), we obtain the coordinates of the centroid (Fig. 6.17):

$$z_{\mathrm{c}} = \frac{b_1 \left(\overline{z}_1 \frac{(\delta_{11})_1}{(D)_1} - \frac{(\beta_{11})_1}{(D)_1} \right) + \frac{\overline{z}_2 b_2 (\delta_{11})_2}{(D)_2}}{\sum_{k=1}^{2} \frac{b_k (\delta_{11})_k}{(D)_k}} \tag{6.72}$$

$$y_{\mathrm{c}} = \frac{\frac{\overline{y}_1 b_1 (\delta_{11})_1}{(D)_1} + b_2 \left(\overline{y}_2 \frac{(\delta_{11})_2}{(D)_2} - \frac{(\beta_{11})_2}{(D)_2} \right)}{\sum_{k=1}^{2} \frac{b_k (\delta_{11})_k}{(D)_k}}. \tag{6.73}$$

The coordinates of the centers of the flanges with respect to the centroid are (Fig. 6.17)

$$y_1 = \overline{y}_1 - y_{\mathrm{c}} \qquad z_1 = \overline{z}_1 - z_{\mathrm{c}} \tag{6.74}$$

$$y_2 = \overline{y}_2 - y_{\mathrm{c}} \qquad z_2 = \overline{z}_2 - z_{\mathrm{c}}. \tag{6.75}$$

The location of the centroid determines whether y_1, y_2, z_1, and z_2 are positive or negative. In Figure 6.17, y_2 and z_1 are positive and y_1 and z_2 are negative.

Bending stiffnesses $\widehat{EI}_{yy}$, $\widehat{EI}_{yz}$. To determine the bending stiffnesses $\widehat{EI}_{yy}$ and $\widehat{EI}_{yz}$ the beam is bent about the y-axis, which passes through the centroid. The radius of curvature is ρ_y (Fig. 6.19, left). This bending results in moments $\widehat{M}_y$ and $\widehat{M}_z$.

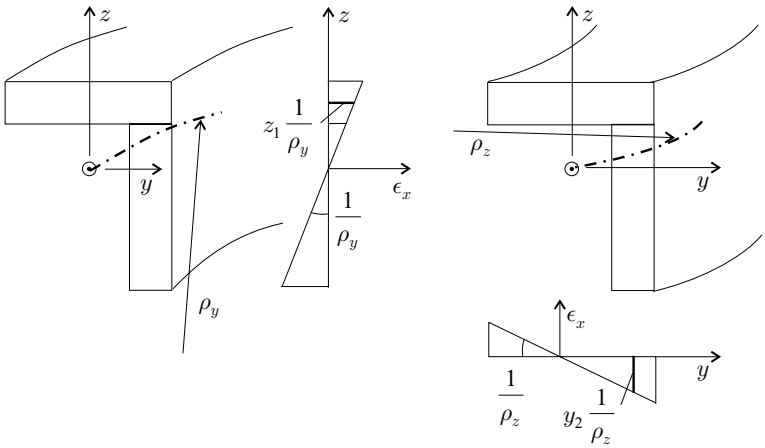

Figure 6.19: The radii of curvatures ρ_y and ρ_z and illustration of the axial strain distributions.

The bending stiffness $\widehat{EI}_{yy}$ is determined below.

Step 1. The strains and curvatures of the two flanges are identical to those of the T-beam (see Eqs. 6.57–6.60). Hence, we write

$$\epsilon^{\mathrm{o}}_{\xi 1} = \frac{1}{\rho_y} z_1 \qquad \kappa_{\xi 1} = \frac{1}{\rho_y} \tag{6.76}$$

$$\epsilon^{\mathrm{o}}_{\xi 2} = \frac{1}{\rho_y} z \qquad \kappa_{\xi 2} = 0. \tag{6.77}$$

Step 2. The axial forces $N_{\xi 1}$, $N_{\xi 2}$ and the bending moments $M_{\xi 1}$, $M_{\xi 2}$ in the flanges (Fig. 6.20) are expressed in terms of the strains $\epsilon^{\mathrm{o}}_{\xi 1}$, $\epsilon^{\mathrm{o}}_{\xi 2}$ and curvatures $\kappa_{\xi 1}$, $\kappa_{\xi 2}$. The derivation of these expressions is discussed subsequently on pages 227–228. Here we quote the results, which are

$$N_{\xi 1} = \frac{(\delta_{11})_1}{(D)_1}\epsilon^{\mathrm{o}}_{\xi 1} - \frac{(\beta_{11})_1}{(D)_1}\kappa_{\xi 1} \qquad M_{\xi 1} = -\frac{(\beta_{11})_1}{(D)_1}\epsilon^{\mathrm{o}}_{\xi 1} + \frac{(\alpha_{11})_1}{(D)_1}\kappa_{\xi 1} \tag{6.78}$$

$$N_{\xi 2} = \frac{(\delta_{11})_2}{(D)_2}\epsilon^{\mathrm{o}}_{\xi 2} - \frac{(\beta_{11})_2}{(D)_2}\kappa_{\xi 2} \qquad M_{\xi 2} = -\frac{(\beta_{11})_2}{(D)_2}\epsilon^{\mathrm{o}}_{\xi 2} + \frac{(\alpha_{11})_2}{(D)_2}\kappa_{\xi 2}. \tag{6.79}$$

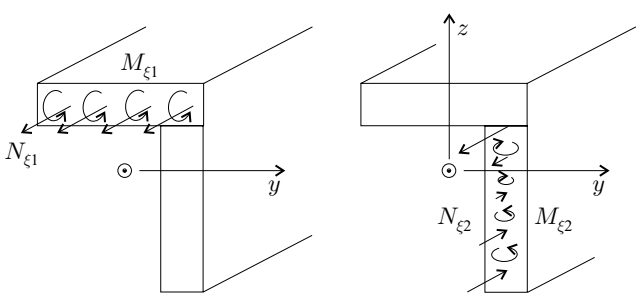

Figure 6.20: Forces and moments (per unit length) acting in the L-beam with unsymmetrical layup bent about the y-axis.

Step 3. The resulting bending moment $\widehat{M}_y$ about the y-axis is

$$\widehat{M}_y = b_1 N_{\xi 1} z_1 + b_1 M_{\xi 1} + \int_{(b_2)} N_{\xi 2} z dz. \tag{6.80}$$

Step 4. Equations (6.76)–(6.80) give

$$\widehat{M}_y = \frac{1}{\rho_y} \underbrace{\left[b_1 \left(\frac{(\delta_{11})_1}{(D)_1} z_1^2 - 2\frac{(\beta_{11})_1}{(D)_1} z_1 + \frac{(\alpha_{11})_1}{(D)_1} \right) + \frac{(\delta_{11})_2}{(D)_2} \left(\frac{b_2^3}{12} + z_2^2 b_2 \right) \right]}_{\widehat{EI}_{yy}}. \tag{6.81}$$

The term indicated by the bracket is the bending stiffness $\widehat{EI}_{yy}$.

The bending stiffness $\widehat{EI}_{yz}$ is determined below.

Steps 1 and 2. In the calculation of the bending moment $\widehat{M}_z$, the first two steps are identical to those given for the calculation of $\widehat{M}_y$.

Step 3. When the beam is bent about the y-axis, the resultant bending moment $\widehat{M}_z$ about the z-axis is (Figs. 6.20 and 6.17)

$$\widehat{M}_z = b_1 N_{\xi 1} y_1 + \int_{(b_2)} N_{\xi 2} y_2 dz + \int_{(b_2)} M_{\xi 2} dz. \tag{6.82}$$

Step 4. Equations (6.76)–(6.79) and (6.82) give

$$\widehat{M}_z = \frac{1}{\rho_y} \underbrace{\left[\left(\frac{(\delta_{11})_1}{(D)_1} z_1 - \frac{(\beta_{11})_1}{(D)_1} \right) b_1 y_1 + \left(\frac{(\delta_{11})_2}{(D)_2} y_2 - \frac{(\beta_{11})_2}{(D)_2} \right) z_2 b_2 \right]}_{\widehat{EI}_{yz}}. \tag{6.83}$$

The term indicated by the bracket is the bending stiffness $\widehat{EI}_{yz}$.

Bending stiffnesses $\widehat{EI}_{zz}$, $\widehat{EI}_{zy}$. To determine the bending stiffnesses $\widehat{EI}_{zz}$ and $\widehat{EI}_{zy}$, the beam is bent about the z-axis with a radius of curvature ρ_z (Fig. 6.19, right). Expressions for these bending moments can be derived in the same way as Eqs. (6.81) and (6.83). The results are

$$\widehat{M}_z = \frac{1}{\rho_z} \underbrace{\left[b_2 \left(\frac{(\delta_{11})_2}{(D)_2} y_2^2 - 2\frac{(\beta_{11})_2}{(D)_2} y_2 + \frac{(\alpha_{11})_2}{(D)_2} \right) + \frac{(\delta_{11})_1}{(D)_1} \left(\frac{b_1^3}{12} + y_1^2 b_1 \right) \right]}_{\widehat{EI}_{zz}} \tag{6.84}$$

$$\widehat{M}_y = \frac{1}{\rho_z} \underbrace{\left[\left(\frac{(\delta_{11})_1}{(D)_1} z_1 - \frac{(\beta_{11})_1}{(D)_1} \right) b_1 y_1 + \left(\frac{(\delta_{11})_2}{(D)_2} y_2 - \frac{(\beta_{11})_2}{(D)_2} \right) z_2 b_2 \right]}_{\widehat{EI}_{zy}}. \tag{6.85}$$

The terms indicated by the brackets are the bending stiffnesses $\widehat{EI}_{zz}$ and $\widehat{EI}_{zy}$ $(= \widehat{EI}_{yz})$.

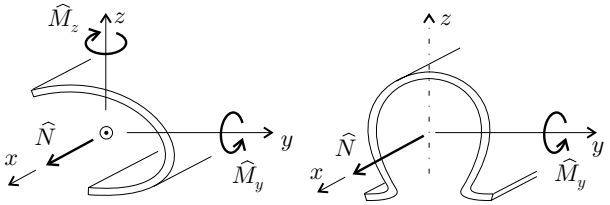

Figure 6.21: Illustration of thin-walled, open-section beams with symmetrical and unsymmetrical cross sections.

6.3.3 Displacements of Arbitrary Cross-Section Beams

In this section we treat thin-walled, open-section beams. The beams are subjected to an axial force $\widehat{N}$ and to bending moments $\widehat{M}_y$, $\widehat{M}_z$ acting at the centroid (Fig. 6.21).

Three types of beams are considered:

1. The layup of the wall is orthotropic but unsymmetrical; the beam's cross section is arbitrary.[5]
2. The layup of the wall is orthotropic and symmetrical; the beam's cross section is arbitrary.
3. The layup of the wall is arbitrary; the cross section is symmetrical with respect to the z-axis, and the loads $\widehat{N}$ and $\widehat{M}_z$ are applied in the x–z symmetry plane (Fig. 6.21, right).

There are no tension–bending–torsion couplings in any of the preceding three types of beams. In the first two types of beams these couplings are not present because the beam is orthotropic (page 207); in the third type of beam couplings are not present because the cross section is symmetrical and the loads act in the symmetry plane.

In the following we derive the replacement stiffnesses. The displacements are then obtained by substituting these replacement stiffnesses into the expressions for the displacements of the corresponding isotropic beam.

We perform the analysis for beams of the first type, that is, the layup is orthotropic but is not necessarily symmetrical and the cross section is arbitrary. We then generalize the results to the other two types of beams in the list above.

We employ three coordinate systems (Fig. 6.22). For the beam we use the x–y–z coordinate system with the origin at the centroid and the $\overline{x}$–$\overline{y}$–$\overline{z}$ coordinate system with the origin at an arbitrarily chosen point. We also define a ξ–η–ζ coordinate system with the origin at the reference plane of the wall. At each point in the wall ξ is parallel to the x coordinate, η is tangential to the circumference of the wall, and ζ is perpendicular to the circumference.

The calculation proceeds in four steps. In Step 1 we deform the axis of the beam (axial strain ϵ_x^{o} and curvatures $1/\rho_y$ and $1/\rho_z$) and calculate the strains in,

[5] J. C. Massa and E. J. Barbero, A Strength of Materials Formulation for Thin Walled Composite Beams with Torsion. *Journal of Composite Materials,* Vol. 32, 1560–1594, 1998.

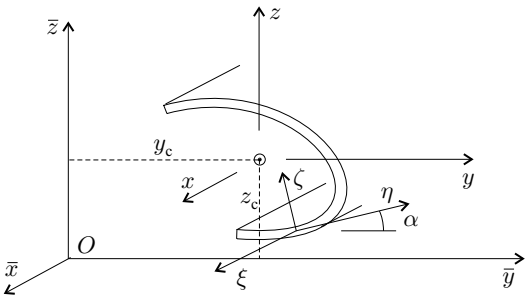

Figure 6.22: The coordinate systems.

and the curvatures of, the wall; in Step 2 we calculate the forces and moments in the wall; in Step 3 we calculate the resultant forces and moments acting on the beam; in Step 4 we determine the stiffnesses.

Step 1. The Bernoulli–Navier hypothesis states that the axial strain varies linearly with the curvatures of the beam. Thus, the axial strain $\epsilon_\xi^{\mathrm{o}}$ at a point on the arbitrarily chosen reference surface of the wall is related to the axial strain ϵ_x^{o} and curvatures $1/\rho_y$ and $1/\rho_z$ of the beam by

$$\epsilon_\xi^{\mathrm{o}} = \epsilon_x^{\mathrm{o}} + z\frac{1}{\rho_y} + y\frac{1}{\rho_z}, \tag{6.86}$$

where z and y are the coordinates of the point on the wall's reference surface. From geometry, it can be shown that the wall's curvature κ_ξ in the ξ–ζ plane is, (Fig. 6.23)

$$\kappa_\xi = \frac{1}{\rho_y}\cos\alpha - \frac{1}{\rho_z}\sin\alpha, \tag{6.87}$$

where α is the angle between the η- and y-coordinate axes (Fig. 6.23).

Step 2. In this step we express the axial force N_ξ and bending moments M_ξ and $M_{\xi\eta}$ in terms of $\epsilon_\xi^{\mathrm{o}}$ and κ_ξ. To derive the necessary expressions we observe that along the free longitudinal edges of the beam the in-plane forces and moments (per unit length) are zero: $N_\eta = N_{\xi\eta} = M_\eta = 0$ (Fig. 6.24). Since the dimensions of

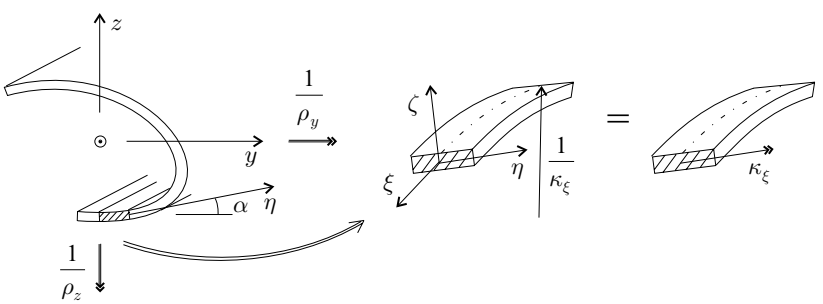

Figure 6.23: Curvatures of the beam (left) and the curvature of the wall (middle) and its vector representation (right).

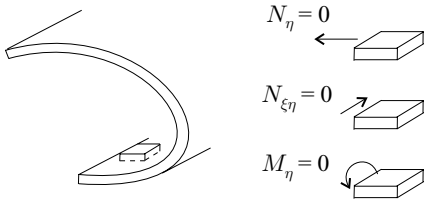

Figure 6.24: The forces and moments along the longitudinal edge of an open-section, thin-walled beam.

the cross section are small compared with the beam's length, these in-plane forces and moments are approximately zero inside the wall:

$$N_\eta = N_{\xi\eta} = M_\eta = 0. \tag{6.88}$$

We apply only axial strain and curvatures to the beam, but no twist. Therefore, the twist of the wall is zero:

$$\kappa_{\xi\eta} = 0. \tag{6.89}$$

We now recall the strain–force relationships given by Eq. (3.22) with the compliance matrix for an orthotropic material given by Eq. (3.37). To apply the relationships to the wall we replace x by ξ and y by η. The resulting generalized strain–force relationships are (orthotropic):

$$\begin{Bmatrix} \epsilon_\xi^o \\ \epsilon_\eta^o \\ \gamma_{\xi\eta}^o \\ \kappa_\xi \\ \kappa_\eta \\ \kappa_{\xi\eta} \end{Bmatrix} = \begin{bmatrix} \alpha_{11} & \alpha_{12} & 0 & \beta_{11} & \beta_{12} & 0 \\ \alpha_{12} & \alpha_{22} & 0 & \beta_{21} & \beta_{22} & 0 \\ 0 & 0 & \alpha_{66} & 0 & 0 & \beta_{66} \\ \beta_{11} & \beta_{21} & 0 & \delta_{11} & \delta_{12} & 0 \\ \beta_{12} & \beta_{22} & 0 & \delta_{12} & \delta_{22} & 0 \\ 0 & 0 & \beta_{66} & 0 & 0 & \delta_{66} \end{bmatrix} \begin{Bmatrix} N_\xi \\ N_\eta \\ N_{\xi\eta} \\ M_\xi \\ M_\eta \\ M_{\xi\eta} \end{Bmatrix}. \tag{6.90}$$

Substitution of Eqs. (6.88) and (6.89) into Eq. (6.90) yields

$$\begin{Bmatrix} \epsilon_\xi^o \\ \kappa_\xi \end{Bmatrix} = \begin{bmatrix} \alpha_{11} & \beta_{11} \\ \beta_{11} & \delta_{11} \end{bmatrix} \begin{Bmatrix} N_\xi \\ M_\xi \end{Bmatrix} + \begin{bmatrix} 0 \\ 0 \end{bmatrix} M_{\xi\eta} \tag{6.91}$$

$$\kappa_{\xi\eta} = 0 = 0 \times N_\xi + 0 \times M_\xi + \delta_{66} M_{\xi\eta}. \tag{6.92}$$

From these equations we can obtain N_ξ, M_ξ, and $M_{\xi\eta}$ in terms of ϵ_ξ^o and κ_ξ. The resulting expressions are listed in the left column of Table 6.2 (page 222).

Step 3. The resultant force and moments in the beam are (Fig. 6.25)

$$\widehat{N} = \int_{(S)} N_\xi d\eta \tag{6.93}$$

$$\widehat{M}_y = \int_{(S)} M_\xi \cos\alpha_k d\eta + \int_{(S)} z N_\xi d\eta \tag{6.94}$$

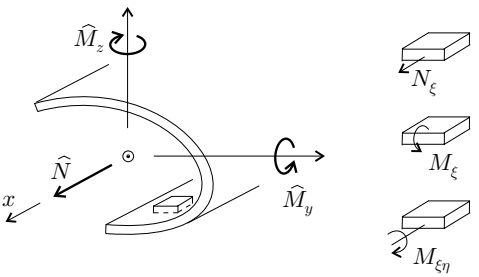

Figure 6.25: The forces and moments acting on the beam and the forces and moments (per unit length) acting inside the wall.

$$\widehat{M}_z = \int_{(S)} -M_\xi \sin\alpha_k d\eta + \int_{(S)} y N_\xi d\eta \tag{6.95}$$

$$\widehat{T} = \int_{(S)} 2M_{\xi\eta} d\eta = 0, \tag{6.96}$$

where S is the length of the circumference. The torque resultant $\widehat{T}$ is zero because, for orthotropic beams, $M_{\xi\eta}$ is zero (Eq. 6.92).

Since $\widehat{T}$ is zero for orthotropic beams, P_{14}, P_{24}, and P_{34} are zero (see Eq. 6.2). Consequently, there is no tension–bending–torsion coupling in orthotropic beams.

Step 4. We axially elongate the beam such that $1/\rho_y$ and $1/\rho_z$ remain zero. Thus, from Eqs. (6.86) and (6.87) we have

$$\epsilon_\xi^{\mathrm{o}} = \epsilon_x^{\mathrm{o}} \qquad \kappa_\xi = 0. \tag{6.97}$$

For a beam with orthotropic and unsymmetrical layup (arbitrary cross section) Eqs. (6.93) and (6.97), together with the expression for N_ξ in Table 6.2, left column, yield

$$\widehat{N} = \underbrace{\int_{(S)} \frac{\delta_{11}}{D} d\eta}_{\widehat{EA}} \epsilon_x^{\mathrm{o}}. \tag{6.98}$$

The coordinates of the centroid are obtained by taking a moment about point O shown in Figure 6.22:

$$\widehat{N} y_{\mathrm{c}} = \int_{(S)} N_\xi \overline{y} d\eta - \int_{(S)} M_\xi \sin\alpha_k d\eta \tag{6.99}$$

$$\widehat{N} z_{\mathrm{c}} = \int_{(S)} N_\xi \overline{z} d\eta + \int_{(S)} M_\xi \cos\alpha_k d\eta, \tag{6.100}$$

where $\overline{y}$ and $\overline{z}$ are the coordinates of a point on the wall's reference surface in the $\overline{x}, \overline{y}, \overline{z}$ coordinate system. By setting $1/\rho_y = 1/\rho_z = 0$ and by using Eqs. (6.86), (6.98), and the expression for N_ξ in Table 6.2 (page 222), left column, we obtain the coordinates of the centroid as follows:

$$y_c = \frac{\int\limits_{(S)} \left(\overline{y}_k \frac{\delta_{11}}{D} + \frac{\beta_{11}}{D} \sin\alpha\right) d\eta}{\int\limits_{(S)} \frac{\delta_{11}}{D} d\eta} \qquad z_c = \frac{\int\limits_{(S)} \left(\overline{z}_k \frac{\delta_{11}}{D} - \frac{\beta_{11}}{D} \cos\alpha\right) d\eta}{\int\limits_{(S)} \frac{\delta_{11}}{D} d\eta}. \tag{6.101}$$

Next we determine the bending stiffnesses. First, we set ϵ_x^o equal to zero in Eqs. (6.86) and (6.87). Then, Eqs. (6.86), (6.87), (6.94), and (6.95) together with the expressions in Table 6.2 give the following resultant moments of a beam with orthotropic and unsymmetrical layup (arbitrary cross section):

$$\widehat{M}_y = \underbrace{\int\limits_{(S)} \left[\frac{\delta_{11}}{D} z^2 - \frac{2\beta_{11}}{D} z\cos\alpha_k + \frac{\alpha_{11}}{D} \cos^2\alpha\right] d\eta}_{\widehat{EI}_{yy}} \frac{1}{\rho_y} + \underbrace{\int\limits_{(S)} \left[\frac{\delta_{11}}{(D)} yz + \frac{\beta_{11}}{D} (z\sin\alpha - y\cos\alpha) - \frac{\alpha_{11}}{D} \cos\alpha\sin\alpha\right] d\eta}_{\widehat{EI}_{yz}} \frac{1}{\rho_z} \tag{6.102}$$

$$\widehat{M}_z = \underbrace{\int\limits_{(S)} \left[\frac{\delta_{11}}{(D)} yz + \frac{\beta_{11}}{D} (z\sin\alpha - y\cos\alpha) - \frac{\alpha_{11}}{D} \cos\alpha\sin\alpha\right] d\eta}_{\widehat{EI}_{yz}} \frac{1}{\rho_y} + \underbrace{\int\limits_{(S)} \left[\frac{\delta_{11}}{D} y^2 + \frac{2\beta_{11}}{D} y\sin\alpha + \frac{\alpha_{11}}{D} \sin^2\alpha\right] d\eta}_{\widehat{EI}_{zz}} \frac{1}{\rho_z}. \tag{6.103}$$

The tensile stiffnesses, the coordinates of the centroid, and the bending stiffnesses of beams with orthotropic and symmetrical layup (arbitrary cross section) and with arbitrary layup (symmetrical cross section) are obtained similarly. The main difference is in Step 2, where the appropriate stress–strain relationships must be used instead of Eq. (6.90). The results are given in Tables 6.3–6.5.

Choice of the reference surface. The expressions of the replacement stiffnesses simplify when the properties are not evaluated at an arbitrary reference surface but at a "neutral" surface, where β_{11} (orthotropic layup – arbitrary cross section) or $\overline{\beta}_{11}$ (arbitrary layup – symmetrical cross section) is zero. The surface is "neutral" in the sense that a bending moment M_ξ does not cause axial strain ϵ_ξ in this surface. (However, it is not a real neutral surface because, unlike in an isotropic beam, in this reference surface the strain perpendicular to the beam's axis ϵ_η is not zero.)

Table 6.3. The tensile and bending stiffnesses and the coordinates of the centroid of open- and closed-section beams with curved walls. The cross section is arbitrary, and the layup of the wall is orthotropic and symmetrical; a_{11} and d_{11} are evaluated at the midsurface.

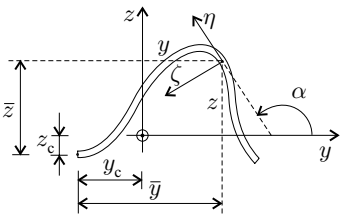

arbitrary cross section
orthotropic
symmetrical layup

Tensile stiffness

$$\widehat{EA} = \int_{(S)} \frac{1}{a_{11}} d\eta$$

Coordinates of the centroid

$$y_c = \frac{\int_{(S)} \overline{y} \frac{1}{a_{11}} d\eta}{\int_{(S)} \frac{1}{a_{11}} d\eta} \qquad z_c = \frac{\int_{(S)} \overline{z} \frac{1}{a_{11}} d\eta}{\int_{(S)} \frac{1}{a_{11}} d\eta}$$

Bending stiffnesses

$$\widehat{EI}_{yy} = \int_{(S)} \left(\frac{1}{a_{11}} z^2 + \frac{1}{d_{11}} \cos^2\alpha \right) d\eta$$

$$\widehat{EI}_{zz} = \int_{(S)} \left(\frac{1}{a_{11}} y^2 + \frac{1}{d_{11}} \sin^2\alpha \right) d\eta$$

$$\widehat{EI}_{yz} = \int_{(S)} \left(\frac{1}{a_{11}} yz + \frac{1}{d_{11}} \sin\alpha \cos\alpha \right) d\eta$$

The 11 component of the compliance matrix corresponding to the "neutral" surface is (Eq. 3.48)

$$\beta_{11}^{\varrho} = \beta_{11} + \varrho \delta_{11}, \tag{6.104}$$

where β_{11} and δ_{11} are the components of the compliance matrices in the arbitrarily chosen reference surface and ϱ is the location of the "neutral" surface (Fig. 6.26). At the "neutral" surface $\beta_{11}^{\varrho} = 0$, and the preceding equation yields

$$\widetilde{\varrho} = -\frac{\beta_{11}}{\delta_{11}} \qquad \begin{matrix} \text{orthotropic layup} \\ \text{arbitrary cross section.} \end{matrix} \tag{6.105}$$

This equation applies to orthotropic beams with symmetrical as well as unsymmetrical cross sections.

For beams with arbitrary layup (symmetrical cross section), Eq. (3.48) and the expression for $\overline{\beta}_{11}$ in Table 6.2 (page 222) yield

$$\overline{\beta}_{11}^{\varrho} = \left(\beta_{11}^{\varrho} + \varrho \delta_{11}\right) - \frac{\left(\beta_{16} + \varrho \delta_{16}\right) \delta_{16}}{\delta_{66}} = \overline{\beta}_{11} + \varrho \overline{\delta}_{11}. \tag{6.106}$$

Table 6.4. The tensile and bending stiffnesses and the coordinates of the centroid of open- and closed-section beams with curved walls. The cross section is arbitrary, and the layup of the wall is orthotropic and unsymmetrical; δ_{11}, β_{11}, and α_{11} are evaluated in the wall's ξ–η–ζ coordinate system; D is defined in Table 6.2 and $\widehat{\delta}_{11}$ and $\widehat{D}$ are defined by Eq. (6.157).

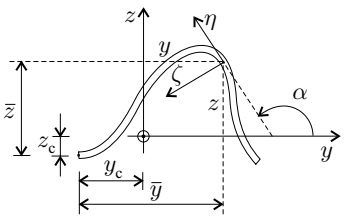

arbitrary cross section
orthotropic
unsymmetrical layup

Tensile stiffness

Open section: $\widehat{EA} = \int\limits_{(S)} \frac{\delta_{11}}{D}\, d\eta$ Closed section: $\widehat{EA} = \int\limits_{(S)} \frac{\widehat{\delta}_{11}}{\widehat{D}}\, d\eta$

Coordinates of the centroid

$$y_c = \frac{\int\limits_{(S)} \left(\bar{y}_k \frac{\delta_{11}}{D} + \frac{\beta_{11}}{D} \sin\alpha\right) d\eta}{\int\limits_{(S)} \frac{\delta_{11}}{D}\, d\eta} \qquad z_c = \frac{\int\limits_{(S)} \left(\bar{z}_k \frac{\delta_{11}}{D} - \frac{\beta_{11}}{D} \cos\alpha\right) d\eta}{\int\limits_{(S)} \frac{\delta_{11}}{D}\, d\eta}$$

Bending stiffnesses

$$\widehat{EI}_{yy} = \int\limits_{(S)} \left(\frac{\delta_{11}}{D} z^2 - \frac{2\beta_{11}}{D} z\cos\alpha_k + \frac{\alpha_{11}}{D} \cos^2\alpha\right) d\eta$$

$$\widehat{EI}_{zz} = \int\limits_{(S)} \left(\frac{\delta_{11}}{D} y^2 + \frac{2\beta_{11}}{D} y\sin\alpha + \frac{\alpha_{11}}{D} \sin^2\alpha\right) d\eta$$

$$\widehat{EI}_{yz} = \int\limits_{(S)} \left(\frac{\delta_{11}}{(D)} yz + \frac{\beta_{11}}{D} (z\sin\alpha - y\cos\alpha) - \frac{\alpha_{11}}{D} \cos\alpha\sin\alpha\right) d\eta$$

Table 6.5. The tensile and bending stiffnesses and the coordinates of the centroid of open-section beams with symmetrical cross section. The layup of the wall is unsymmetrical and nonorthotropic; $\overline{D}$, $\overline{\delta}_{11}$, and $\overline{\beta}_{11}$ are defined in Table 6.2. The elements of the compliance matrix are evaluated in the wall's ξ–η–ζ coordinate system.

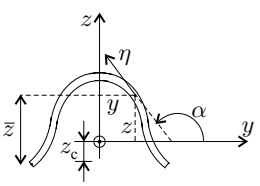

symmetrical cross section
nonorthotropic
unsymmetrical layup

Tensile stiffness

$$\widehat{EA} = \int\limits_{(S)} \frac{\overline{\delta}_{11}}{\overline{D}}\, d\eta$$

Coordinates of the centroid

$$y_c = 0 \qquad z_c = \frac{\int\limits_{(S)} \left(\overline{z}_k \frac{\overline{\delta}_{11}}{\overline{D}} - \frac{\overline{\beta}_{11}}{\overline{D}} \cos\alpha\right) d\eta}{\int\limits_{(S)} \frac{\overline{\delta}_{11}}{\overline{D}}\, d\eta}$$

Bending stiffness

$$\widehat{EI}_{yy} = \int\limits_{(S)} \left(\frac{\overline{\delta}_{11}}{\overline{D}} z^2 - \frac{2\overline{\beta}_{11}}{\overline{D}} z\cos\alpha_k + \frac{\overline{\alpha}_{11}}{\overline{D}} \cos^2\alpha\right) d\eta$$

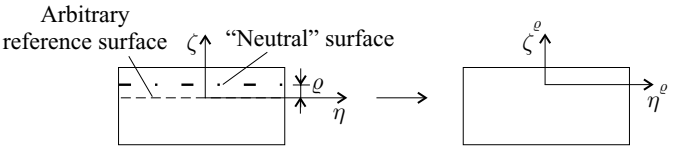

Figure 6.26: The "neutral" surface where $\widetilde{\beta}_{11}^{\varrho}$ (orthotropic layup – arbitrary cross section) or $\overline{\beta}_{11}^{\varrho}$ (arbitrary layup – symmetrical cross section) is zero.

From the condition $\overline{\beta}_{11}^{\varrho} = 0$ we obtain the location of the "neutral" surface of the wall as follows:

$$\overline{\varrho} = -\frac{\overline{\beta}_{11}}{\overline{\delta}_{11}} \qquad \begin{array}{c}\text{arbitrary layup} \\ \text{symmetrical cross section.}\end{array} \tag{6.107}$$

For selected cross sections the replacement stiffnesses and the location of the centroid are given in Tables A.1–A.4.

Segmented wall. The beam's wall may consist of several flat wall segments (Fig. 6.27). The thickness of each wall segment is small compared with the width of the segment. The wall segments are designated by the subscript k ($k = 1, 2, \ldots, K$, where K is the total number of wall segments). The layup of each wall segment may be symmetrical or unsymmetrical with respect to the wall segment's midsurface.

When the wall consists of segments and each segment is flat, the integrals in Tables 6.3–6.5 may be replaced by summations

$$\int_{(S)} (\quad) d\eta = \sum_{k=1}^{K} \int_{-b_k/2}^{b_k/2} (\quad) d\eta, \tag{6.108}$$

where b_k is the width of the kth wall segment. For each wall segment we define a ξ–η–ζ coordinate system, where ξ is parallel to the x coordinate, η is along the circumference of the wall, and ζ is perpendicular to the wall (Fig. 6.27). The origin of this coordinate system may be at an arbitrarily chosen reference surface but must be at the middle of the width of the wall segment. By performing the integrations in Tables 6.3–6.5 we obtain the expressions given in Tables 6.6–6.8.

6.3.4 Stresses and Strains

In a thin-walled isotropic beam subjected to an axial load and to bending in the x–z plane there is only axial stress σ_x. In a thin-walled composite beam, in addition to the axial stress σ_ξ, transverse normal σ_η and shear $\tau_{\xi\eta}$ stresses are also present.

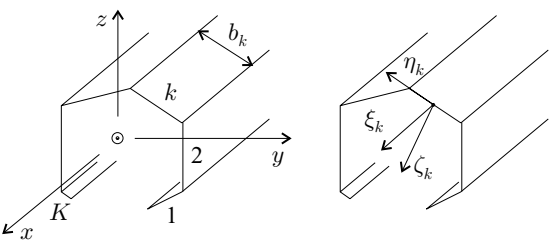

Figure 6.27: Thin-walled, open-section beams with segmented wall.

Table 6.6. The tensile and bending stiffnesses and the coordinates of the centroid of open- and closed-section beams with flat walls. The cross section is arbitrary, and the layup of each wall segment is orthotropic and symmetrical; a_{11} and d_{11} are evaluated at the wall's midplanes.

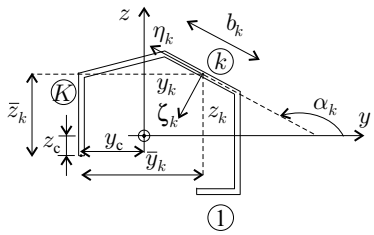

arbitrary cross section
orthotropic
symmetrical layup

Tensile stiffness

$$\widehat{EA} = \sum_{k=1}^{K} \frac{b_k}{(a_{11})_k}$$

Coordinates of the centroid

$$y_c = \frac{\sum_{k=1}^{K} \bar{y}_k \frac{b_k}{(a_{11})_k}}{\sum_{k=1}^{K} \frac{b_k}{(a_{11})_k}} \qquad z_c = \frac{\sum_{k=1}^{K} \bar{z}_k \frac{b_k}{(a_{11})_k}}{\sum_{k=1}^{K} \frac{b_k}{(a_{11})_k}}$$

Bending stiffnesses

$$\widehat{EI}_{yy} = \sum_{k=1}^{K} \left[\frac{1}{(a_{11})_k} \left(b_k z_k^2 + \frac{b_k^3 \sin^2 \alpha_k}{12} \right) + \frac{b_k}{(d_{11})_k} \cos^2 \alpha_k \right]$$

$$\widehat{EI}_{zz} = \sum_{k=1}^{K} \left[\frac{1}{(a_{11})_k} \left(b_k y_k^2 + \frac{b_k^3 \cos^2 \alpha_k}{12} \right) + \frac{b_k}{(d_{11})_k} \sin^2 \alpha_k \right]$$

$$\widehat{EI}_{yz} = \sum_{k=1}^{K} \frac{1}{(a_{11})_k} \left(b_k y_k z_k + \frac{b_k^3 \cos \alpha_k \sin \alpha_k}{12} \right) - \frac{b_k}{(d_{11})_k} \cos \alpha_k \sin \alpha_k$$

These stresses are illustrated in Fig. 6.28. However, the shear flow, defined as the integral of the shear stress across the thickness, is zero,

$$q = \int_{(h)} \tau_{\xi\eta} d\zeta = 0, \tag{6.109}$$

where h is the thickness of the wall. In the following subsections, we present analyses for calculating the three stress components $\sigma_\xi, \sigma_\eta, \tau_{\xi\eta}$ inside composite beams.

Orthotropic layup (arbitrary cross section). When the layup of the wall is orthotropic, the axial strain and the curvatures of the beam's axis passing through the centroid are (Eqs. 6.17 and 6.19)

$$\epsilon_x^o = \frac{\widehat{N}}{\widehat{EA}} \tag{6.110}$$

$$\frac{1}{\rho_y} = \frac{\widehat{EI}_{zz}\widehat{M}_y - \widehat{EI}_{yz}\widehat{M}_z}{\widehat{EI}_{yy}\widehat{EI}_{zz} - (\widehat{EI}_{yz})^2} \tag{6.111}$$

$$\frac{1}{\rho_z} = \frac{-\widehat{EI}_{yz}\widehat{M}_y + \widehat{EI}_{yy}\widehat{M}_z}{\widehat{EI}_{yy}\widehat{EI}_{zz} - (\widehat{EI}_{yz})^2}. \tag{6.112}$$

Table 6.7. The tensile and bending stiffnesses and the coordinates of the centroid of open- and closed-section beams with flat walls. The cross section is arbitrary, and the layup of each wall segment is orthotropic and unsymmetrical; δ_{11}, β_{11}, and α_{11} are evaluated in the wall's ξ–η–ζ coordinate system; D is defined in Table 6.2. The parameters $\widehat{\delta}_{11}$ and $\widehat{D}$ are defined by Eq. (6.157).

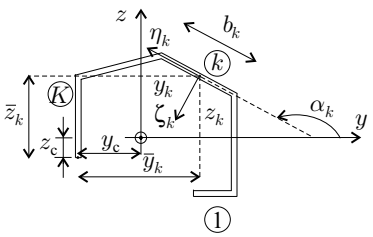

arbitrary cross section
orthotropic
unsymmetrical layup

Tensile stiffness

Open section: $\widehat{EA} = \sum_{k=1}^{K} \frac{(\delta_{11})_k b_k}{(D)_k}$ Closed section: $\widehat{EA} = \sum_{k=1}^{K} \frac{(\widehat{\delta}_{11})_k b_k}{(\widehat{D})_k}$

Coordinates of the centroid

$$y_c = \frac{\sum_{k=1}^{K} b_k \left(\bar{y}_k \frac{(\delta_{11})_k}{(D)_k} + \frac{(\beta_{11})_k}{(D)_k} \sin\alpha_k \right)}{\sum_{k=1}^{K} \frac{b_k (\delta_{11})_k}{(D)_k}} \qquad z_c = \frac{\sum_{k=1}^{K} b_k \left(\bar{z}_k \frac{(\delta_{11})_k}{(D)_k} - \frac{(\beta_{11})_k}{(D)_k} \cos\alpha_k \right)}{\sum_{k=1}^{K} \frac{b_k (\delta_{11})_k}{(D)_k}}$$

Bending stiffnesses

$$\widehat{EI}_{yy} = \sum_{k=1}^{K} \frac{(\delta_{11})_k}{(D)_k} \left(b_k z_k^2 + \frac{b_k^3 \sin^2\alpha_k}{12} \right) - \frac{2(\beta_{11})_k}{(D)_k} b_k z_k \cos\alpha_k + \frac{(\alpha_{11})_k}{(D)_k} b_k \cos^2\alpha_k$$

$$\widehat{EI}_{zz} = \sum_{k=1}^{K} \frac{(\delta_{11})_k}{(D)_k} \left(b_k y_k^2 + \frac{b_k^3 \cos^2\alpha_k}{12} \right) + \frac{2(\beta_{11})_k}{(D)_k} b_k y_k \sin\alpha_k + \frac{(\alpha_{11})_k}{(D)_k} b_k \sin^2\alpha_k$$

$$\widehat{EI}_{yz} = \sum_{k=1}^{K} \frac{(\delta_{11})_k}{(D)_k} \left(b_k y_k z_k + \frac{b_k^3 \cos\alpha_k \sin\alpha_k}{12} \right) + \frac{(\beta_{11})_k}{(D)_k} b_k (z_k \sin\alpha_k - y_k \cos\alpha_k) - \frac{(\alpha_{11})_k}{(D)_k} b_k \cos\alpha_k \sin\alpha_k$$

At an arbitrary point on the reference surface of the wall, the axial strain ϵ_ξ^o and curvature κ_ξ are related to the strain and curvatures of the beam by Eqs. (6.86) and (6.87).

$$\epsilon_\xi^o = \epsilon_x^o + y\frac{1}{\rho_z} + z\frac{1}{\rho_y} \tag{6.113}$$

$$\kappa_\xi = -\frac{1}{\rho_z}\sin\alpha + \frac{1}{\rho_y}\cos\alpha, \tag{6.114}$$

where α is the angle between the tangent of the wall (coordinate η) and the y-axis (Fig. 6.22).

The layup of the wall is orthotropic, and hence the following forces and moments are zero (see Eqs. 6.88 and 6.92):

$$N_\eta = N_{\xi\eta} = M_\eta = M_{\xi\eta} = 0. \tag{6.115}$$

Table 6.8. The tensile and bending stiffnesses and the coordinates of the centroid of open-section beams with symmetrical cross section. The layup of each wall segment is nonorthotropic and unsymmetrical; $\overline{D}$, $\overline{\delta}_{11}$, and $\overline{\beta}_{11}$ are defined in Table 6.2. The elements of the compliance matrix are evaluated in the wall's ξ–η–ζ coordinate system.

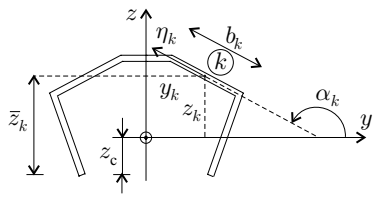

symmetrical cross section
nonorthotropic
unsymmetrical layup

Tensile stiffness

$$\widehat{EA} = \sum_{k=1}^{K} \frac{(\overline{\delta}_{11})_k b_k}{(\overline{D})_k}$$

Coordinates of the centroid

$$y_c = 0 \qquad z_c = \frac{\sum_{k=1}^{K} b_k \left(\overline{z}_k \frac{(\overline{\delta}_{11})_k}{(\overline{D})_k} - \frac{(\overline{\beta}_{11})_k}{(\overline{D})_k} \cos\alpha_k \right)}{\sum_{k=1}^{K} \frac{b_k (\overline{\delta}_{11})_k}{(\overline{D})_k}}$$

Bending stiffness

$$\widehat{EI}_{yy} = \sum_{k=1}^{K} \frac{(\overline{\delta}_{11})_k}{(\overline{D})_k} \left(b_k z_k^2 + \frac{b_k^3 \sin^2\alpha_k}{12} \right) - \frac{2(\overline{\beta}_{11})_k}{(\overline{D})_k} b_k z_k \cos\alpha_k + \frac{(\overline{\alpha}_{11})_k}{(\overline{D})_k} b_k \cos^2\alpha_k$$

The axial force N_ξ and the moment M_ξ (per unit length) in the wall are (Table 6.2, page 222)

$$N_\xi = \frac{\delta_{11}}{D} \epsilon_\xi^o - \frac{\beta_{11}}{D} \kappa_\xi \tag{6.116}$$

$$M_\xi = -\frac{\beta_{11}}{D} \epsilon_\xi^o + \frac{\alpha_{11}}{D} \kappa_\xi . \tag{6.117}$$

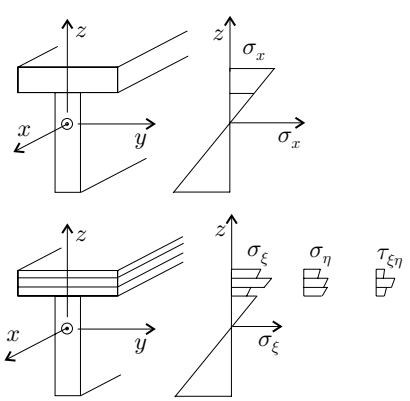

Figure 6.28: Illustration of the stresses in an isotropic (top) and a composite (bottom) T-beam subjected to bending in the x–z plane.

Equations (6.110) and (6.113)–(6.117) yield

$$N_\xi = \frac{1}{\rho_y}\left(z\frac{\delta_{11}}{D} - \cos\alpha\frac{\beta_{11}}{D}\right) + \frac{1}{\rho_z}\left(y\frac{\delta_{11}}{D} + \sin\alpha\frac{\beta_{11}}{D}\right) + \frac{\widehat{N}}{\widehat{EA}}\frac{\delta_{11}}{D} \tag{6.118}$$

$$M_\xi = \frac{1}{\rho_y}\left(-z\frac{\beta_{11}}{D} + \cos\alpha\frac{\alpha_{11}}{D}\right) - \frac{1}{\rho_z}\left(y\frac{\beta_{11}}{D} + \sin\alpha\frac{\alpha_{11}}{D}\right) - \frac{\widehat{N}}{\widehat{EA}}\frac{\beta_{11}}{D}, \tag{6.119}$$

where $1/\rho_y$ and $1/\rho_z$ are given by Eqs. (6.111) and (6.112). The strain–force relationships are (see Eq. 6.90)

$$\begin{Bmatrix} \epsilon_\xi^{\mathrm{o}} \\ \epsilon_\eta^{\mathrm{o}} \\ \gamma_{\xi\eta}^{\mathrm{o}} \\ \kappa_\xi \\ \kappa_\eta \\ \kappa_{\xi\eta} \end{Bmatrix} = \begin{bmatrix} \alpha_{11} & \beta_{11} \\ \alpha_{12} & \beta_{21} \\ 0 & 0 \\ \beta_{11} & \delta_{11} \\ \beta_{12} & \delta_{12} \\ 0 & 0 \end{bmatrix} \begin{Bmatrix} N_\xi \\ M_\xi \end{Bmatrix}. \tag{6.120}$$

By applying the results of the laminate plate theory (see Eq. 3.7), we obtain the following expression for the strains in each ply:

$$\begin{Bmatrix} \epsilon_\xi \\ \epsilon_\eta \\ \gamma_{\xi\eta} \end{Bmatrix} = \begin{Bmatrix} \epsilon_\xi^{\mathrm{o}} \\ \epsilon_\eta^{\mathrm{o}} \\ \gamma_{\xi\eta}^{\mathrm{o}} \end{Bmatrix} + \zeta \begin{Bmatrix} \kappa_\xi \\ \kappa_\eta \\ \kappa_{\xi\eta} \end{Bmatrix}. \tag{6.121}$$

The stresses from Eq. (3.11) are (orthotropic laminate, $\overline{Q}_{16} = \overline{Q}_{26} = 0$)

$$\begin{Bmatrix} \sigma_\xi \\ \sigma_\eta \\ \tau_{\xi\eta} \end{Bmatrix} = \begin{bmatrix} \overline{Q}_{11} & \overline{Q}_{12} & 0 \\ \overline{Q}_{21} & \overline{Q}_{22} & 0 \\ 0 & 0 & \overline{Q}_{66} \end{bmatrix} \begin{Bmatrix} \epsilon_\xi \\ \epsilon_\eta \\ \gamma_{\xi\eta} \end{Bmatrix}. \tag{6.122}$$

Equation (6.120) shows that $\gamma_{\xi\eta}^{\mathrm{o}}$ and $\kappa_{\xi\eta}$ are zero. Consequently, $\gamma_{\xi\eta}$ (Eq. 6.121) is also zero, and the ply shear stress $\tau_{\xi\eta}$ (Eq. 6.122) is zero.

Orthotropic and symmetrical layup (arbitrary cross section). The layup of the wall is orthotropic and symmetrical. For orthotropic layup, the following forces and moments are zero (Eqs. 6.88 and 6.92):

$$N_\eta = N_{\xi\eta} = M_\eta = M_{\xi\eta} = 0. \tag{6.123}$$

The axial force N_ξ and the moment M_ξ (per unit length) in the wall are (see Table 6.2, page 222)

$$N_\xi = \frac{1}{a_{11}}\epsilon_\xi^{\mathrm{o}} \qquad M_\xi = \frac{1}{d_{11}}\kappa_\xi. \tag{6.124}$$

Equations (6.110), (6.113), (6.114), and (6.124) yield

$$N_\xi = \frac{1}{\rho_y} z \frac{1}{a_{11}} + \frac{1}{\rho_z} y \frac{1}{a_{11}} + \frac{\widehat{N}}{\widehat{EA}} \frac{1}{a_{11}} \tag{6.125}$$

$$M_\xi = \frac{1}{\rho_y} \cos\alpha \frac{1}{d_{11}} - \frac{1}{\rho_z} \sin\alpha \frac{1}{d_{11}}. \tag{6.126}$$

For orthotropic and symmetrical layup the elements of the $[\alpha]$ and $[\delta]$ matrices are $\alpha_{ij} = a_{ij}, \delta_{ij} = d_{ij}$, whereas $\beta_{ij} = 0$. Thus, the strain–force relationships (Eqs. 6.90 and 3.28) give

$$\begin{Bmatrix} \epsilon_\xi^{\mathrm{o}} \\ \epsilon_\eta^{\mathrm{o}} \\ \gamma_{\xi\eta}^{\mathrm{o}} \\ \kappa_\xi \\ \kappa_\eta \\ \kappa_{\xi\eta} \end{Bmatrix} = \begin{bmatrix} a_{11} & 0 \\ a_{12} & 0 \\ 0 & 0 \\ 0 & d_{11} \\ 0 & d_{12} \\ 0 & 0 \end{bmatrix} \begin{Bmatrix} N_\xi \\ M_\xi \end{Bmatrix}. \tag{6.127}$$

The ply strains and stresses are given by Eqs. (6.121) and (6.122).

Arbitrary layup (symmetrical cross section). The layup of the wall is arbitrary, and the cross section is symmetrical about the z-axis. The loads are applied in the x–z symmetry plane. Such a beam bends only about the y-axis. Correspondingly, $1/\rho_z$ is zero and we have (Eq. 6.6)

$$\epsilon_x^{\mathrm{o}} = \frac{\widehat{N}}{\widehat{EA}} \qquad \frac{1}{\rho_y} = \frac{\widehat{M}_y}{\widehat{EI}_{yy}} \qquad \frac{1}{\rho_z} = 0. \tag{6.128}$$

With these substitutions, Eqs. (6.113) and (6.114) simplify to

$$\epsilon_\xi^{\mathrm{o}} = \epsilon_x^{\mathrm{o}} + z\frac{1}{\rho_y} \qquad \kappa_\xi = \frac{1}{\rho_y}\cos\alpha. \tag{6.129}$$

In the walls of an open cross-section beam, the following forces and moment are zero (see Eq. 6.88):

$$N_\eta = N_{\xi\eta} = M_\eta = 0. \tag{6.130}$$

The axial force N_ξ and the moments M_ξ and $M_{\xi\eta}$ (per unit length) inside the wall are (Table 6.2, page 222)

$$N_\xi = \frac{\overline{\delta}_{11}}{\overline{D}}\epsilon_\xi^{\mathrm{o}} - \frac{\overline{\beta}_{11}}{\overline{D}}\kappa_\xi \tag{6.131}$$

$$M_\xi = -\frac{\overline{\beta}_{11}}{\overline{D}}\epsilon_\xi^{\mathrm{o}} + \frac{\overline{\alpha}_{11}}{\overline{D}}\kappa_\xi \tag{6.132}$$

$$M_{\xi\eta} = -\frac{\beta_{16}}{\delta_{66}}N_\xi - \frac{\delta_{16}}{\delta_{66}}M_\xi. \tag{6.133}$$

Equations (6.128)–(6.133) may be rearranged to yield the axial force N_ξ and the moment M_ξ (per unit length) in terms of applied force and moment:

$$N_\xi = \frac{\widehat{M}_y}{\widehat{EI}_{yy}}\left(z\frac{\overline{\delta}_{11}}{\overline{D}} - \cos\alpha\frac{\overline{\beta}_{11}}{\overline{D}}\right) + \frac{\widehat{N}}{\widehat{EA}}\frac{\overline{\delta}_{11}}{\overline{D}} \tag{6.134}$$

$$M_\xi = \frac{\widehat{M}_y}{\widehat{EI}_{yy}}\left(-z\frac{\overline{\beta}_{11}}{\overline{D}} + \cos\alpha\frac{\overline{\alpha}_{11}}{\overline{D}}\right) - \frac{\widehat{N}}{\widehat{EA}}\frac{\overline{\beta}_{11}}{\overline{D}}. \tag{6.135}$$

The strain–force relationships in the x, y, z coordinate system are given by Eq. (3.22). We apply this equation in the ξ, η, ζ coordinate system with $N_\eta = N_{\xi\eta} = M_\eta = 0$. Thus, we write

$$\begin{Bmatrix} \epsilon_\xi^{\mathrm{o}} \\ \epsilon_\eta^{\mathrm{o}} \\ \gamma_{\xi\eta}^{\mathrm{o}} \\ \kappa_\xi \\ \kappa_\eta \\ \kappa_{\xi\eta} \end{Bmatrix} = \begin{bmatrix} \alpha_{11} & \beta_{11} & \beta_{16} \\ \alpha_{12} & \beta_{21} & \beta_{26} \\ \alpha_{16} & \beta_{61} & \beta_{66} \\ \beta_{11} & \delta_{11} & \delta_{16} \\ \beta_{12} & \delta_{12} & \delta_{26} \\ \beta_{16} & \delta_{16} & \delta_{66} \end{bmatrix} \begin{Bmatrix} N_\xi \\ M_\xi \\ M_{\xi\eta} \end{Bmatrix}. \tag{6.136}$$

The ply strains are calculated by Eqs. (6.121). The ply stresses are (Eq. 3.11)

$$\begin{Bmatrix} \sigma_\xi \\ \sigma_\eta \\ \tau_{\xi\eta} \end{Bmatrix} = \begin{bmatrix} \overline{Q}_{11} & \overline{Q}_{12} & \overline{Q}_{16} \\ \overline{Q}_{21} & \overline{Q}_{22} & \overline{Q}_{26} \\ \overline{Q}_{61} & \overline{Q}_{62} & \overline{Q}_{66} \end{bmatrix} \begin{Bmatrix} \epsilon_\xi \\ \epsilon_\eta \\ \gamma_{\xi\eta} \end{Bmatrix}. \tag{6.137}$$

The elements of matrix $[\overline{Q}]$ are evaluated in the ξ, η, ζ coordinate system.

6.2 Example. *An $L = 0.6$-m-long T-section beam with the cross section shown in Figure 6.29 is made of graphite epoxy. The material properties are given in Table 3.6 (page 81). The layup is $[\pm 45_2^{\mathrm{f}}/0_{12}/\pm 45_2^{\mathrm{f}}]$. The beam is built-in at both ends. The beam is subjected to a uniformly distributed load ($p = -1\,500$ N/m) acting in the plane of symmetry. Calculate the maximum deflection and the ply stresses and strains.*

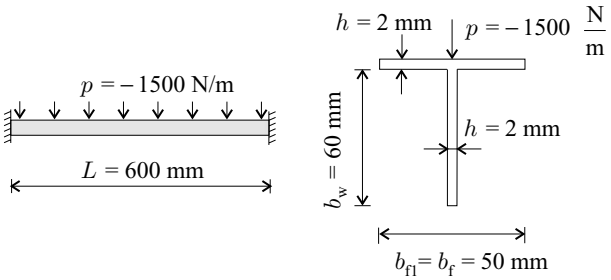

Figure 6.29: The T-beam in Example 6.2.

Solution. From Table A.2, with b_{f2} set equal to zero, the tensile stiffness and the location of the centroid are

$$\begin{aligned} \widehat{EA} &= \frac{b_{f1}}{(\alpha_{11})_{f1}} + \frac{b_w}{(a_{11})_w} = 21.22 \times 10^6 \text{ N} \\ z_c &= \frac{1}{\widehat{EA}} \left(\frac{b_{f1}}{(\alpha_{11})_{f1}} d + \frac{b_w}{(a_{11})_w} \frac{b_w}{2} \right) = 0.0441 \text{ m}. \end{aligned} \tag{6.138}$$

For symmetrical layup (which is the case here), α_{11} is replaced by a_{11}. The element a_{11} for both the web and the flange is $(a_{11})_w = (a_{11})_{f1} = 5.18 \times 10^{-9} \frac{\text{m}}{\text{N}}$ (Table 3.8, page 85). The dimensions $b_{f1} = b_f = 0.05\,\text{m}$, $b_w = 0.06\,\text{m}$, and $d = 0.061\,\text{m}$ are shown in Figures 6.29 and 6.30. Setting b_{f2} equal to zero in the expression given in Table A.2 results in the following bending stiffness:

$$\widehat{EI}_{yy} = \frac{b_{f1}}{(\alpha_{11})_{f1}} (d - z_c)^2 + \frac{b_{f1}}{(\delta_{11})_{f1}} + \frac{1}{(a_{11})_w} \left(\frac{b_{w1}^3 + b_{w2}^3}{3} \right). \tag{6.139}$$

For symmetrical layup (which is the case here) δ_{11} is replaced by d_{11}. The element d_{11} for both the web and the flange is $(d_{11})_w = (d_{11})_{f1} = 33.10 \times 10^{-3} \frac{1}{\text{N} \cdot \text{m}}$ (Table 3.8, page 85). Equation (6.139), with $b_{w2} = z_c = 0.0441\,\text{m}$ and $b_{w1} = b_w - z_c = 0.0159\,\text{m}$, yields

$$\widehat{EI}_{yy} = 8\,530\,\text{N} \cdot \text{m}^2. \tag{6.140}$$

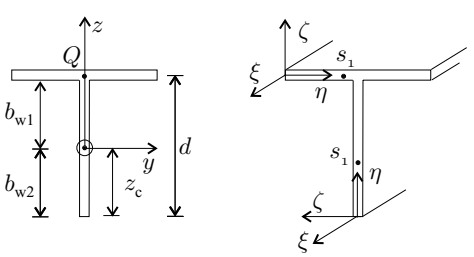

Figure 6.30: The cross section of the beam in Example 6.2.

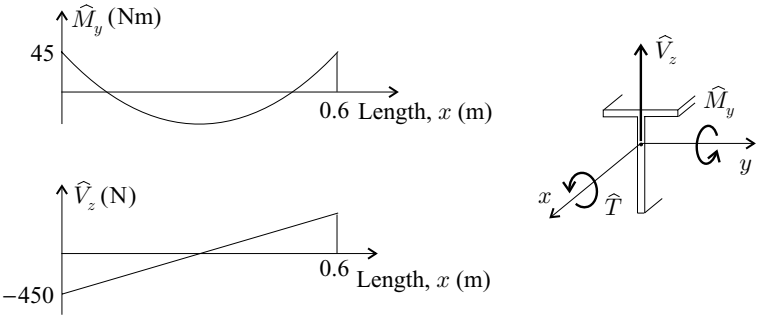

Figure 6.31: Bending moment $\widehat{M}_y$ and shear force $\widehat{V}_z$ for the beam in Example 6.2.

The distributed load is $p = -1\,500$ N/m. The corresponding bending moment $\widehat{M}_y$ and shear force $\widehat{V}_z$ diagrams are given in Fig. 6.31. The maximum values are

$$\widehat{M}_y^{\max} = -\frac{pL^2}{12} = 45\,\mathrm{N}\cdot\mathrm{m} \tag{6.141}$$

$$\widehat{V}_z^{\max} = \frac{pL}{2} = -450\,\mathrm{N}.$$

The maximum deflection is (Table 7.3, page 332)

$$\widetilde{w} = \frac{1}{384}\frac{pL^4}{\widehat{E}\widehat{I}_{yy}} = -0.0593 \times 10^{-3}\,\mathrm{m} = -0.0593\,\mathrm{mm}. \tag{6.142}$$

The axial force N_ξ and the moment M_ξ (per unit length) in the wall are (see Eqs. 6.125, 6.126, 6.111, and 6.112)

$$\begin{aligned} N_\xi &= \frac{\widehat{M}_y}{\widehat{E}\widehat{I}_{yy}} z \frac{1}{a_{11}} \\ M_\xi &= \frac{\widehat{M}_y}{\widehat{E}\widehat{I}_{yy}} \cos\alpha \frac{1}{d_{11}}, \end{aligned} \tag{6.143}$$

where z is shown in Figure 6.30 and cos α is zero for the web and $+1$ for the flange. For completeness we also calculate the shear flow, which will be discussed in Section 6.7. The shear flow is (Eq. 6.282)

$$q^{\mathrm{op}}(s_1) = N_{\xi\eta} = -\frac{\widehat{V}_z}{\widehat{E}\widehat{I}_{yy}} \int_0^{s_1} \left(z \frac{1}{a_{11}} \right) d\eta. \tag{6.144}$$

The η coordinate is shown in Figure 6.30. We next determine the forces at point Q, which is at the intersection of the flange and the web ($z = d - z_{\mathrm{c}}$) at the built-in end ($x = 0$, $\widehat{M}_y = \widehat{M}_y^{\max}$, and $\widehat{V}_z = \widehat{V}_z^{\max}$). At point Q the forces and moments are

$$N_\xi = \frac{\widehat{M}_y^{\max}}{\widehat{E}\widehat{I}_{yy}}(d - z_{\mathrm{c}})\frac{1}{a_{11}} = 17\,209\,\frac{\mathrm{N}}{\mathrm{m}} \qquad M_\xi = \frac{\widehat{M}_y^{\max}}{\widehat{E}\widehat{I}_{yy}}\frac{1}{d_{11}} = 0.1594\,\frac{\mathrm{N}\cdot\mathrm{m}}{\mathrm{m}}$$

$$q^{\mathrm{op}} = N_{\xi\eta} = \mp\frac{\widehat{V}_z^{\max}}{\widehat{E}\widehat{I}_{yy}}\frac{b_{\mathrm{f}}}{2}(d - z_{\mathrm{c}})\frac{1}{a_{11}} = \pm 2\,151\,\frac{\mathrm{N}}{\mathrm{m}}. \tag{6.145}$$

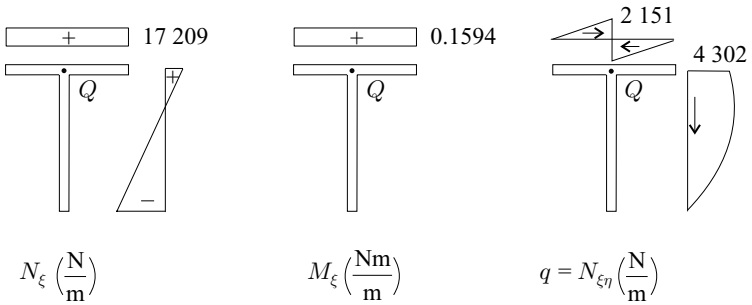

Figure 6.32: The axial force N_ξ, the moment M_ξ, and the shear force $N_{\xi\eta}$ in the flange and the web at the built-in end of the beam in Example 6.2.

The plus and minus values of the shear flow refer to the left and right of Q (Fig. 6.32). We also calculated these forces and moments around the entire cross section at $x = 0$. The results are shown in Figure 6.32.

The relevant elements of the compliance matrices are (Table 3.8, page 85)

$$a_{11} = 5.18 \times 10^{-9}\,\frac{\mathrm{m}}{\mathrm{N}} \qquad a_{12} = -3.52 \times 10^{-9}\,\frac{\mathrm{m}}{\mathrm{N}} \qquad a_{66} = 27.77 \times 10^{-9}\,\frac{\mathrm{m}}{\mathrm{N}}$$

$$d_{11} = 33.10 \times 10^{-3}\,\frac{1}{\mathrm{N}\cdot\mathrm{m}} \quad d_{12} = -25.59 \times 10^{-3}\,\frac{1}{\mathrm{N}\cdot\mathrm{m}} \quad d_{66} = 48.51 \times 10^{-3}\,\frac{1}{\mathrm{N}\cdot\mathrm{m}}.$$

At point Q the strains are calculated by the strain–force relationships (see Eq. 6.90 with α replaced by a, δ replaced by d, and β is zero)

$$\begin{Bmatrix} \epsilon_\xi^{\mathrm{o}} \\ \epsilon_\eta^{\mathrm{o}} \\ \gamma_{\xi\eta}^{\mathrm{o}} \\ \kappa_\xi \\ \kappa_\eta \\ \kappa_{\xi\eta} \end{Bmatrix} = \begin{bmatrix} a_{11} & 0 & 0 \\ a_{12} & 0 & 0 \\ 0 & a_{66} & 0 \\ 0 & 0 & d_{11} \\ 0 & 0 & d_{12} \\ 0 & 0 & 0 \end{bmatrix} \begin{Bmatrix} N_\xi \\ N_{\xi\eta} \\ M_\xi \end{Bmatrix} = \begin{Bmatrix} 0.000\,0892 \\ -0.000\,0606 \\ -0.000\,0597 \\ 0.005\,28 \\ -0.004\,08 \\ 0 \end{Bmatrix}, \tag{6.146}$$

where κ_ξ, κ_η, and $\kappa_{\xi\eta}$ are in 1/m. With the preceding strains, the ply stresses are calculated by Eqs. (6.121) and (6.122). The results are given in Figure 6.33.

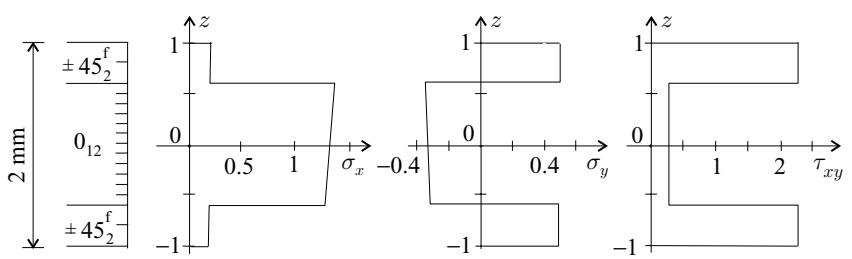

Figure 6.33: The ply stresses in the beam at the built-in end just left of the vertical symmetry axis of the flange in Example 6.2. The unit of the stresses is 10^6 N/m^2. (Just to the right of the symmetry axis, τ_{xy} is negative.)

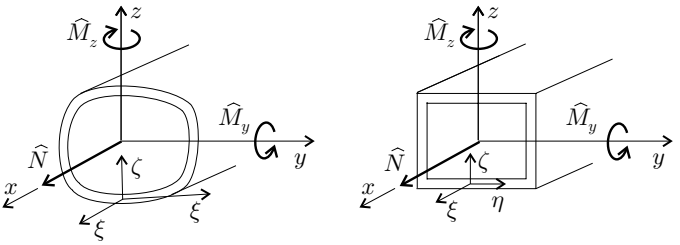

Figure 6.34: Thin-walled, closed section beams with curved and straight wall segments subjected to axial load and bending moments.

6.4 Thin-Walled, Closed-Section Orthotropic Beams Subjected to Axial Load and Bending

In this section we treat thin-walled, closed-section beams subjected to axial load and bending. The beam may consist of flat and curved walls (Fig. 6.34). The beams are subjected to an axial force $\widehat{N}$ and to bending moments $\widehat{M}_y$, $\widehat{M}_z$.

Two types of beams are considered:

1. The layup of the wall is orthotropic and symmetrical; the beam's cross section is arbitrary.
2. The layup of the wall is orthotropic but unsymmetrical; the beam's cross section is arbitrary.

There are no tension–bending–torsion couplings in either of the latter types of beams because the beam is orthotropic (page 207).

We define a ξ–η–ζ coordinate system along the wall. At each point ξ is parallel to the x coordinate, η is along the circumference of the wall, and ζ is perpendicular to the wall (Fig. 6.34). The origin of this coordinate system is in an arbitrarily chosen reference surface.

Displacements – symmetrical layup. The layup of the wall is orthotropic and symmetrical. Under the action of the applied loads $\widehat{N}$, $\widehat{M}_y$, and $\widehat{M}_z$, the shape of the cross section changes. To examine the change in shape we first look at an isotropic beam. The changed shape of the cross section of a solid isotropic beam is shown in Figure 6.35. The changed shape of a thin-walled isotropic beam is the same as that of a solid beam with the same initial cross section. There is only axial stress in the beam, and therefore, the cross-sectional shape would not be altered if the beam were cut.

A thin-walled composite beam with orthotropic and symmetrical layup behaves similarly to an isotropic beam, namely, under the actions of an axial load and bending the change in shape of the cross section of a closed-section beam is nearly the same as the change in shape of the cross section of an open-section beam (Fig. 6.36, middle). This implies that closed-section beams respond to the applied loads in much the same way as open-section beams. Therefore, we may treat thin-walled, closed-section beams with orthotropic and symmetrical layup

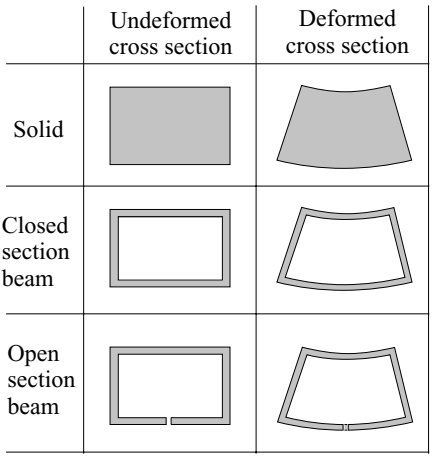

Figure 6.35: The changes of the cross sections of solid and thin-walled open- and closed-section isotropic beams subjected to axial load and bending.

in the same way as we treat open-section beams and calculate the displacements with the replacement stiffnesses given in Table 6.3 (page 231).

Displacements – unsymmetrical layup. The layup of the wall is orthotropic but unsymmetrical. When such a beam is subjected to loads $\widehat{N}$, $\widehat{M}_y$, and $\widehat{M}_z$, the shape of the cross sections changes significantly, as shown in Figure 6.36. In this case we can no longer approximate closed-section beams as open-section beams. An open-section beam would "open up" under the axial load and bending, as shown in Figure 6.36 (right). Similarly, if a closed section beam were cut, the two cut edges would move relative to each other, as shown in Figure 6.37. In a closed-section beam these displacements are prevented by a shear force $N_{\xi\eta}$, a bending moment M_η, a normal force N_η, and a transverse shear force V_η acting along the cut. Since the walls are orthotropic, (a) the beam does not twist ($\kappa_{\xi\eta} = 0$), and (b) the two "cut" edges do not move relative to each other in the axial direction. In the absence of these motions no shear force arises along the cut ($N_{\xi\eta} = 0$). The forces N_η and V_η are generally small and can be neglected ($N_\eta = 0$, $V_\eta = 0$). Thus,

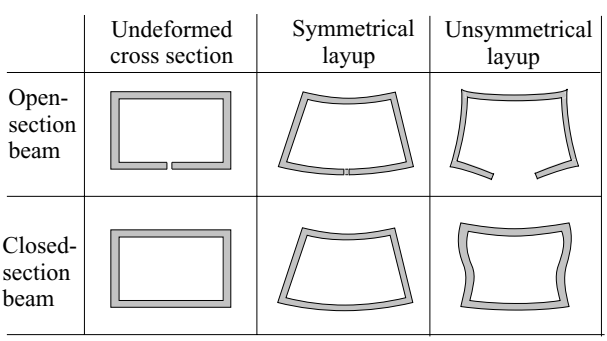

Figure 6.36: The changes of the cross sections of thin-walled open- and closed-section composite beams subjected to axial load and bending.

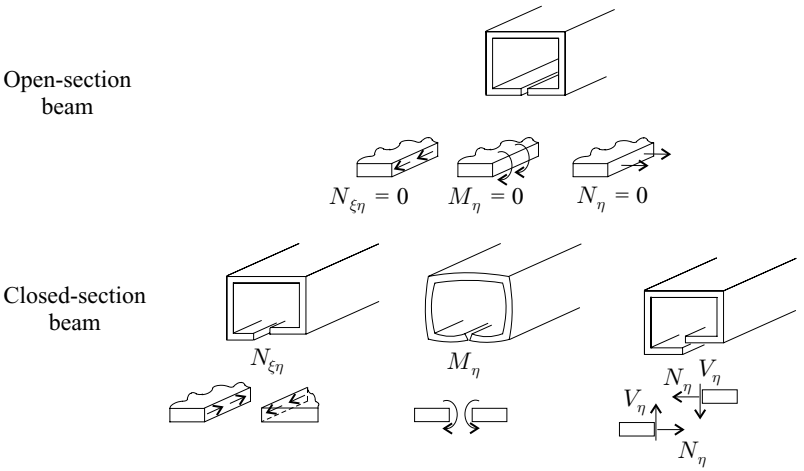

Figure 6.37: The forces along the lengthwise edges of an open-section beam (top) and along the cut of a closed-section beam (bottom).

in the case of orthotropic walls we have

$$\begin{aligned} N_\eta &= N_{\xi\eta} = 0 \\ \kappa_{\xi\eta} &= 0 \qquad\qquad \text{closed-section.} \\ V_\eta &= 0 \end{aligned} \tag{6.147}$$

There is a bending moment M_η along the cut that prevents rotation of the edges relative to each other. The slope of the wall must be the same to the left and to the right of the cut (Figure 6.38)

$$\left.\frac{\partial w^{\mathrm{o}}}{\partial \eta}\right|_{\text{right}} = \left.\frac{\partial w^{\mathrm{o}}}{\partial \eta}\right|_{\text{left}}, \tag{6.148}$$

where w^{o} is the displacement of the wall perpendicular to its reference surface. The change in curvature of the wall is

$$\kappa_\eta = -\frac{\partial^2 w^{\mathrm{o}}}{\partial \eta^2}. \tag{6.149}$$

By integrating this equation from an arbitrary point $\eta = 0$ to s_1, we have

$$\int_0^{s_1} \kappa_\eta d\eta = -\left[\frac{\partial w^{\mathrm{o}}}{\partial \eta}\right]_0^{s_1}. \tag{6.150}$$

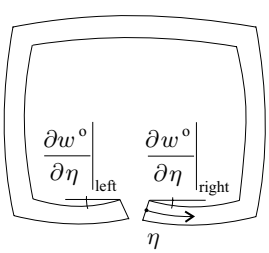

Figure 6.38: Relative rotation of the cut edges.

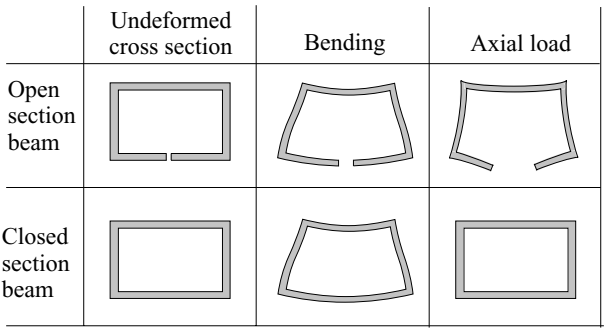

Figure 6.39: The changes of the cross sections of thin-walled open- and closed-section beams subjected to axial load and bending. Each wall has the same othotropic unsymmetrical layup.

By performing the integration along the entire circumference ($s_1 = S$), we obtain (see Eq. 6.148)

$$\int_0^S \kappa_\eta d\eta = \oint \kappa_\eta d\eta = -\left.\frac{\partial w^{\mathrm{o}}}{\partial \eta}\right|_{\text{right}} + \left.\frac{\partial w^{\mathrm{o}}}{\partial \eta}\right|_{\text{left}} = 0. \tag{6.151}$$

This compatibility condition must be enforced for closed-section beams. An analysis that takes this condition into account is presented in Section 6.6. This exact analysis is complex. In the next paragraph we present a simpler way to determine the replacement stiffnesses when the layup is the same around the circumference.

To establish the bending replacement stiffnesses, we observe that bending the cross-sectional shape of a closed cross-section beam with uniform layup around the circumference is similar to the shape of an open-section beam (Fig. 6.39). In this case the replacement stiffnesses $\widehat{EI}_{yy}$, $\widehat{EI}_{zz}$, and $\widehat{EI}_{yz}$ may be approximated by the expressions obtained for open-section beams (Tables 6.4 and 6.7, pages 232 and 235).

To establish the tensile replacement stiffness, we observe that the beam with uniform layup does not deform under tension (Fig. 6.39). In this case the change in curvature is zero along the circumference

$$\kappa_\eta \approx 0 \qquad \begin{matrix}\text{closed-section} \\ \text{in tension.}\end{matrix} \tag{6.152}$$

By substituting Eqs. (6.147) and (6.152) into Eq. (6.90), after algebraic manipulations, we obtain

$$N_\xi = \left(\frac{\widehat{\delta}_{11}}{\widehat{D}}\right)\epsilon_\xi^{\mathrm{o}} - \left(\frac{\widehat{\beta}_{11}}{\widehat{D}}\right)\kappa_\xi \tag{6.153}$$

$$M_\xi = -\left(\frac{\widehat{\beta}_{11}}{\widehat{D}}\right)\epsilon_\xi^{\mathrm{o}} + \left(\frac{\widehat{\alpha}_{11}}{\widehat{D}}\right)\kappa_\xi \tag{6.154}$$

$$M_\eta = -\frac{\beta_{12}}{\delta_{22}}N_\xi - \frac{\delta_{12}}{\delta_{22}}M_\xi, \tag{6.155}$$

where $\widehat{\alpha}_{11}$, $\widehat{\beta}_{11}$, $\widehat{\delta}_{11}$, and $\widehat{D}$ are defined as

$$\widehat{\alpha}_{11} = \left(\alpha_{11} - \frac{\beta_{12}^2}{\delta_{22}}\right) \qquad \widehat{\beta}_{11} = \left(\beta_{11} - \frac{\beta_{12}\delta_{12}}{\delta_{22}}\right) \tag{6.156}$$

$$\widehat{\delta}_{11} = \left(\delta_{11} - \frac{\delta_{12}^2}{\delta_{22}}\right) \qquad \widehat{D} = \widehat{\alpha}_{11}\widehat{\delta}_{11} - \widehat{\beta}_{11}^2. \tag{6.157}$$

By comparing Eq. (6.153) with the expression for N_ξ given for open-section beams in Table 6.2 (page 222), we see that they differ only by the terms in the brackets. Therefore, the tensile stiffness $\widehat{EA}$ of thin-walled closed-section beams (orthotropic but unsymmetrical layup) may be calculated from the expressions of open-section beams (Tables 6.4 and 6.7, pages 232 and 235) by replacing δ_{11}, D by $\widehat{\delta}_{11}$, $\widehat{D}$.

The W_{11}, W_{22}, $W_{23}(= W_{32})$, W_{33} elements of the compliance matrix are then determined by substituting the replacement stiffnesses (given in Tables 6.4 and 6.7) into Eq. (6.19).

The expressions for $\widehat{EA}$, $\widehat{EI}_{yy}$, $\widehat{EI}_{zz}$, and $\widehat{EI}_{yz}$ in Tables 6.4 and 6.7 are also reasonable approximations when the layup is not uniform but the wall is "thin."

Stresses and strains. As with displacements, the stresses and strains in closed-section beams with orthotropic and symmetrical layup can be calculated by the same expressions used for the stresses and strains in open-section beams (see Section 6.3.4, orthotropic and symmetrical layup).

When a closed-section beam with orthotropic but unsymmetrical layup is in bending, the stresses and strains can be calculated by the same expressions used for the stresses and strains in open-section beams (see Section 6.3.4, orthotropic layup, arbitrary cross section).

When a closed-section beam with orthotropic but unsymmetrical layup is in tension, we determine the stresses and strains as follows. At an arbitrary point on the reference surface of the wall the axial strain is related to the strain of the beam's axis by (Eq. 6.113) as follows:

$$\epsilon_\xi^{\mathrm{o}} = \epsilon_x^{\mathrm{o}}. \tag{6.158}$$

When the layup of the wall is orthotropic, $N_\eta = N_{\xi\eta} = M_{\xi\eta} = 0$, and the axial force and the moment (per unit length) in the wall are given by Eqs. (6.153) and (6.154). Thus, we have

$$N_\xi = \frac{\widehat{N}}{\widehat{EA}}\frac{\widehat{\delta}_{11}}{\widehat{D}} \qquad M_\xi = -\frac{\widehat{N}}{\widehat{EA}}\frac{\widehat{\beta}_{11}}{\widehat{D}}. \tag{6.159}$$

The strain–force relationships (see Eq. 6.90) give the strains

$$\begin{Bmatrix} \epsilon_\xi^{\mathrm{o}} \\ \epsilon_\eta^{\mathrm{o}} \\ \gamma_{\xi\eta}^{\mathrm{o}} \\ \kappa_\xi \\ \kappa_\eta \\ \kappa_{\xi\eta} \end{Bmatrix} = \begin{bmatrix} \alpha_{11} & \beta_{11} & \beta_{12} \\ \alpha_{12} & \beta_{21} & \beta_{22} \\ 0 & 0 & 0 \\ \beta_{11} & \delta_{11} & \delta_{12} \\ \beta_{12} & \delta_{12} & \delta_{22} \\ 0 & 0 & 0 \end{bmatrix} \begin{Bmatrix} N_\xi \\ M_\xi \\ M_\eta \end{Bmatrix}, \tag{6.160}$$

where M_η is given by Eq. (6.155).

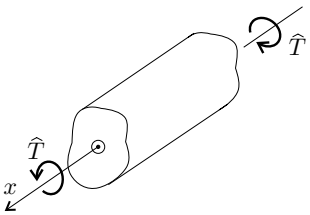

Figure 6.40: Beam subjected to torque $\widehat{T}$.

The strains and stresses inside the wall (orthotropic, unsymmetrical layup) are calculated by Eqs. (6.121) and (6.137).

6.5 Torsion of Thin-Walled Beams

We consider thin-walled, open- and closed-section beams subjected to pure torque (Fig. 6.40). Because of the torque, the beam twists about an axis that passes through the center of twist. When the beam is isotropic, the twist axis remains straight. For a composite beam the twist axis becomes curved, except when the beam is orthotropic.

The stresses differ in thin-walled isotropic and composite beams. Under the action of pure torque there are only shear stresses inside the wall of an isotropic beam, whereas there are also normal stresses inside the wall of a composite beam.

Under the action of the torque, each cross section rotates (twists) as a rigid body in its own plane about the center of twist. In addition, the cross sections suffer warping displacements normal to their (cross-sectional) planes. We are interested in the twist, the warping displacements, and the stresses inside the walls.

Stiffness and rate of twist. Under the action of pure torsion (no axial constraint), the rate of twist of an isotropic beam is (Eq. 6.4)

$$\vartheta = \frac{\widehat{T}}{GI_{\mathrm{t}}} \qquad \text{isotropic.} \tag{6.161}$$

Similarly, for a composite beam we write

$$\vartheta = \frac{\widehat{T}}{\widehat{GI}_{\mathrm{t}}} \qquad \text{composite.} \tag{6.162}$$

With these definitions the rate of twist of composite beams can be obtained by replacing the stiffnesses GI_{t} by $\widehat{GI}_{\mathrm{t}}$ in the expressions for the torsion of isotropic beams. In the following we obtain expressions for $\widehat{GI}_{\mathrm{t}}$.

6.5.1 Thin Rectangular Cross Section

We consider a solid, rectangular, thin beam (Fig. 6.41). The layup of the beam is arbitrary. The width of the beam b is large compared with its thickness h ($b >> h$). The applied torque gives rise to shear stresses in the beam that may be represented by a resultant shear flow q, the unit of which is force per length. This induced shear

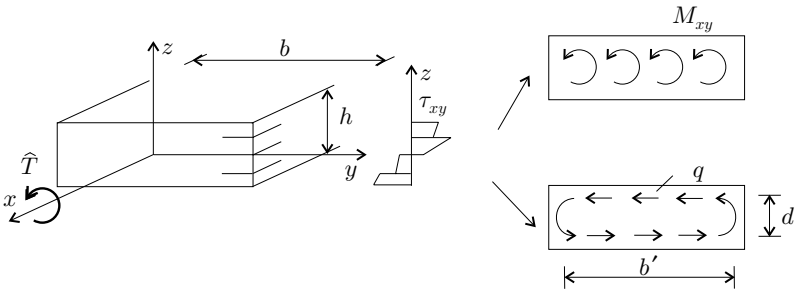

Figure 6.41: The shear stress distribution, the twist moment, and the shear flow in a solid thin beam under torsion.

equilibrates the applied torque (Fig. 6.41),

$$\widehat{T} = (qd)b' + (qb')d, \tag{6.163}$$

where d and b' are the length and width of the path of the resultant shear flow. The latter is taken to be approximately equal to the width of the beam ($b' \approx b$). The twist moment M_{xy} (per unit length) in the cross section is

$$M_{xy} = -qd. \tag{6.164}$$

Equations (6.163) and (6.164), with the approximation $b' = b$, yield

$$\widehat{T} = -2bM_{xy}. \tag{6.165}$$

When the beam is treated as a plate, the out-of-plane curvature κ_{xy} is (see Eqs. 3.22)

$$\kappa_{xy} = \delta_{66} M_{xy}. \tag{6.166}$$

The rate of twist ϑ is (Eq. 6.27)

$$\vartheta = \frac{\partial \psi}{\partial x} = -\frac{1}{2}\kappa_{xy}. \tag{6.167}$$

By combining Eqs. (6.166), (6.167), and (6.165), we obtain the rate of twist

$$\vartheta = \frac{\delta_{66}}{4b}\widehat{T}, \tag{6.168}$$

where δ_{66} is evaluated at an arbitrarily chosen reference plane. By comparing Eqs. (6.162) and (6.168), we see that the torsional stiffness of a flat thin-walled beam is

$$\widehat{GI}_{\mathrm{t}} = \frac{4b}{\delta_{66}}. \tag{6.169}$$

For a thin-walled isotropic beam, $\delta_{66} = d_{66} = 12/Gh^3$ (Eq. 3.43), and the torsional stiffness in Eq. (6.169) becomes $\widehat{GI}_{\mathrm{t}} = GI_{\mathrm{t}} = G\frac{bh^3}{3}$.

When the wall is not flat but is curved, the torsional stiffness may be approximated by

$$\widehat{GI}_{\mathrm{t}} = 4 \int_0^S \frac{1}{\delta_{66}} d\eta, \tag{6.170}$$

where η is the coordinate along the circumference of the wall and S is the length of the entire circumference.

Although the beam is subjected to pure torque, there are axial ϵ_x^{o} and shear strains γ_{xy}^{o}, and there is a change in the curvature κ_x given by (see Eq. 3.22)

$$\begin{Bmatrix} \epsilon_x^{\mathrm{o}} \\ \gamma_{xy}^{\mathrm{o}} \\ \kappa_x \end{Bmatrix} = \begin{bmatrix} \beta_{16} \\ \beta_{66} \\ \delta_{16} \end{bmatrix} M_{xy}. \tag{6.171}$$

This equation together with Eq. (6.165) yields

$$\begin{Bmatrix} \epsilon_x^{\mathrm{o}} \\ \gamma_{xy}^{\mathrm{o}} \\ \kappa_x \end{Bmatrix} = - \begin{bmatrix} \beta_{16} \\ \beta_{66} \\ \delta_{16} \end{bmatrix} \frac{\widehat{T}}{2b}. \tag{6.172}$$

To determine W_{14}, W_{24}, and W_{44} elements of the compliance matrix, we rearrange Eqs. (6.168) and (6.172) in the form

$$\begin{Bmatrix} \epsilon_x^{\mathrm{o}} \\ \kappa_x = 1/\rho_y \\ \vartheta \end{Bmatrix} = \begin{Bmatrix} -\frac{1}{2b}\beta_{16} \\ -\frac{1}{2b}\delta_{16} \\ \frac{\delta_{66}}{4b} \end{Bmatrix} \widehat{T}. \tag{6.173}$$

By comparing this equation with Eq. (6.17), we see that the terms in brackets are the $W_{14}(= -\beta_{16}/2b)$, $W_{24}(= -\delta_{16}/2b)$, and $W_{44}(= \delta_{66}/4b)$ elements of the compliance matrix.

When the layup is symmetrical, β_{66} is zero and there is no shear strain. When the layup is orthotropic, β_{16} and δ_{16} are zero, and there is neither axial strain nor a change in curvature. When the layup is both orthotropic and symmetrical, there are neither axial nor shear strains and there is no change in curvature.

6.5.2 Open-Section Orthotropic Beams

The wall of an open-section beam may be considered to consist of thin wall segments (Fig. 6.27). The torsional stiffness of a thin-walled, open-section isotropic beam may be approximated by

$$GI_{\mathrm{t}} = (GI_{\mathrm{t}})_1 + (GI_{\mathrm{t}})_2 + \ldots + (GI_{\mathrm{t}})_K, \tag{6.174}$$

where the subscript refers to the kth segment. Similarly, we approximate the torsional stiffness of a composite beam with orthotropic walls by

$$\widehat{GI}_{\mathrm{t}} = (\widehat{GI}_{\mathrm{t}})_1 + (\widehat{GI}_{\mathrm{t}})_2 + \ldots + (\widehat{GI}_{\mathrm{t}})_K. \tag{6.175}$$

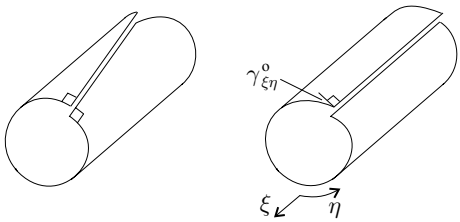

Figure 6.42: Warping of an open-section composite beam due to torsion and due to shear strain.

For flat and curved segments, $(\widehat{GI}_{\mathrm{t}})_k$ are given by Eqs. (6.169) and (6.170).

The rate of twist is calculated by

$$\vartheta = \frac{\widehat{T}}{\widehat{GI}_{\mathrm{t}}}. \tag{6.176}$$

Stresses and strains. In each wall segment we employ a ξ–η–ζ coordinate system. The origin of each coordinate system is at the wall segment's reference surface. The out-of-plane curvature of each wall segment is obtained from Eq. (6.167) by replacing x and y by ξ and η as follows:

$$\kappa_{\xi\eta} = -2\vartheta. \tag{6.177}$$

We consider only $M_{\xi\eta}$ resulting from the torque. Thus we have (see Eq. 6.90)

$$\gamma^{\mathrm{o}}_{\xi\eta} = \beta_{66} M_{\xi\eta} \qquad \kappa_{\xi\eta} = \delta_{66} M_{\xi\eta} \tag{6.178}$$

$$\epsilon^{\mathrm{o}}_{\xi} = \epsilon^{\mathrm{o}}_{\eta} = \kappa_{\xi} = \kappa_{\eta} = 0. \tag{6.179}$$

Equations (6.178) and (6.177) give

$$M_{\xi\eta} = \frac{1}{\delta_{66}} \kappa_{\xi\eta} = -\frac{2}{\delta_{66}} \vartheta. \tag{6.180}$$

Equations (6.121) and (6.122) together with Eq. (6.179) yield the strains and stresses

$$\begin{Bmatrix} \epsilon_{\xi} \\ \epsilon_{\eta} \\ \gamma_{\xi\eta} \end{Bmatrix} = \begin{Bmatrix} 0 \\ 0 \\ \gamma^{\mathrm{o}}_{\xi\eta} \end{Bmatrix} + \zeta \begin{Bmatrix} 0 \\ 0 \\ \kappa_{\xi\eta} \end{Bmatrix} \tag{6.181}$$

$$\begin{Bmatrix} \sigma_{\xi} \\ \sigma_{\eta} \\ \tau_{\xi\eta} \end{Bmatrix} = \begin{bmatrix} 0 \\ 0 \\ \overline{Q}_{66} \end{bmatrix} \gamma_{\xi\eta}. \tag{6.182}$$

Warping. A thin-walled, open-section beam warps when subjected to a pure torque. Under torsion the wall of a beam (no shear deformation) warps, as shown in Figure 6.42, (left). The axial displacement u relative to an arbitrarily chosen reference point ($\eta = 0$) is[6]

$$u(s_1) - u(0) = -2A_{\mathrm{s}_1}\vartheta, \tag{6.183}$$

[6] T. H. G. Megson, *Aircraft Structures for Engineering Students*. 3rd edition. Halsted Press, John Wiley & Sons, New York, 1999, p. 318.

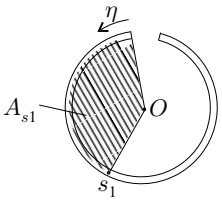

Figure 6.43: The swept area.

where ϑ is the rate of twist, and A_{s_1} is the swept area from $\eta = 0$ to $\eta = s_1$ (Fig. 6.43) about the center of twist (point O). For thin-walled beams the center of twist and the shear center coincide. The shear center is defined such that a transverse load acting at the shear center of an orthotropic beam does not cause twist (see Section 6.7.3).

When there is no shear strain the angle between the circumferential and the longitudinal edges remains 90 degrees (Fig. 6.42). For a composite beam the shear strain is zero when β_{66} is zero (see Eq. 6.178). When β_{66} is not zero the originally 90-degree angle between the circumferential and the longitudinal edges becomes $90^\circ + \gamma^\circ_{\xi\eta}$. This change in angle introduces the additional axial displacement along the circumference

$$u(s_1) - u(0) = \int_0^{s_1} \gamma^{\mathrm{o}}_{\xi\eta} d\eta. \tag{6.184}$$

The total relative axial displacement (warping) is (see Eqs. 6.183 and 6.184)

$$\Delta u = u(s_1) - u(0) = -2A_{s_1}\vartheta + \int_0^{s_1} \gamma^{\mathrm{o}}_{\xi\eta} d\eta. \tag{6.185}$$

For a thin-walled, open-section beam with orthotropic layup $\gamma^{\mathrm{o}}_{\xi\eta}$ is given by Eq. (6.178).

When the layup of each wall segment is symmetrical, $\gamma^{\mathrm{o}}_{\xi\eta}$ is zero, and such composite beams warp similarly to that of isotropic beams.

6.5.3 Closed-Section Orthotropic Beams – Single Cell

For a thin-walled, closed-section beam, the points $\eta = 0$ and $\eta = S$ coincide (Fig. 6.44), and thus the warping is

$$\Delta u = u(0) - u(S) = 0, \tag{6.186}$$

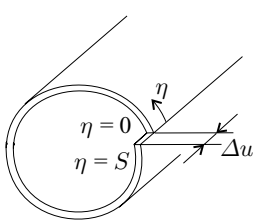

Figure 6.44: The relative displacement at the "cut" of a closed-section beam subjected to pure torque.

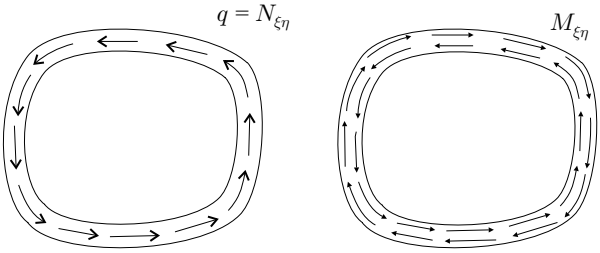

Figure 6.45: The torque carried by $N_{\xi\eta}$ and by $M_{\xi\eta}$.

where S is the length of the circumference. By employing Eq. (6.185), we write

$$\Delta u = -2A\vartheta + \int_0^S \gamma^{\circ}_{\xi\eta} d\eta = -2A\vartheta + \oint \gamma^{\circ}_{\xi\eta} d\eta = 0, \tag{6.187}$$

where A is the enclosed area and $\gamma^{\circ}_{\xi\eta}$ is the shear strain. From this equation the rate of twist is

$$\vartheta = \frac{1}{2A} \oint \gamma^{\circ}_{\xi\eta} d\eta. \tag{6.188}$$

In thin-walled, closed-section beams the torque due to the induced twist moment $M_{\xi\eta}$ is small compared with the torque due to the induced shear force $N_{\xi\eta}$ (Fig. 6.45). In the following we neglect the twist moment $M_{\xi\eta}$.

We introduce the shear flow q defined as the integral of the shear stress across the thickness

$$q = \int_{(h)} \tau_{\xi\eta} d\zeta \equiv N_{\xi\eta}, \tag{6.189}$$

where h is the thickness of the wall. The torque produced by q (or $N_{\xi\eta}$) is (Fig. 6.46)

$$\widehat{T} = \oint qp d\eta = 2Aq, \tag{6.190}$$

where p is the distance between an arbitrary point and the tangent to the wall. Accordingly, the shear flow is

$$q = \frac{\widehat{T}}{2A}. \tag{6.191}$$

Equation (6.191) is the same as the Bredt–Batho formula[7] developed for thin-walled, closed-section isotropic beams.

Equation (6.90) yields

$$\gamma^{\circ}_{\xi\eta} = \alpha_{66} N_{\xi\eta} + \beta_{66} M_{\xi\eta}. \tag{6.192}$$

To simplify this expression we select a reference surface at which β_{66} (denoted by β^{v}_{66}) is zero. The 66 component of the compliance matrix corresponding to this

[7] T. H. G. Megson, *Aircraft Structures for Engineering Students*. 3rd edition. Halsted Press, John Wiley & Sons, New York, 1999, p. 307.

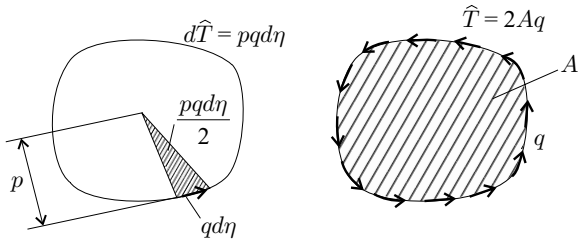

Figure 6.46: The torque carried by the shear flow q.

surface, which we refer to as the "torque neutral" surface, is (Eq. 3.48)

$$\beta_{66}^{\nu} = \beta_{66} + \nu\delta_{66}, \tag{6.193}$$

where β_{66} and δ_{66} are the components of the compliance matrices in the arbitrarily chosen reference surface, and ν is the location of the "torque neutral" surface (Fig. 6.47). For $\beta_{66}^{\nu} = 0$, Eq. (6.193) yields

$$\nu = -\frac{\beta_{66}}{\delta_{66}}. \tag{6.194}$$

By applying Eq. (6.192) at the "torque neutral" surface, we have

$$\gamma_{\xi\eta}^{\mathrm{o}} = \alpha_{66}^{\nu} N_{\xi\eta} = \alpha_{66}^{\nu} q, \tag{6.195}$$

where the superscript ν refers to the "torque neutral" surface (Eq. 6.194), and α_{66}^{ν} is given by Eqs. (3.48) and (6.194) as follows:

$$\alpha_{66}^{\nu} = \alpha_{66} + 2\nu\beta_{66} + \nu^2\delta_{66} = \alpha_{66} - \frac{\beta_{66}^2}{\delta_{66}}. \tag{6.196}$$

By combining Eqs. (6.188)–(6.195), we obtain

$$\vartheta = \widehat{T}\frac{1}{4A^2}\oint \alpha_{66}^{\nu} d\eta. \tag{6.197}$$

With reference to Eq. (6.162), we see that the replacement torsional stiffness $\widehat{GI}_{\mathrm{t}}$ is

$$\widehat{GI}_{\mathrm{t}} = \frac{4A^2}{\oint \alpha_{66}^{\nu} d\eta}. \tag{6.198}$$

When the wall's layup is symmetrical, $\alpha_{66}^{\nu} = a_{66}$. For a thin-walled isotropic beam, $\alpha_{66}^{\nu} = a_{66} = 1/Gh$ (Eq. 3.43), and the torsional stiffness (Eq. 6.198) becomes $\widehat{GI}_{\mathrm{t}} = GI_{\mathrm{t}} = G\frac{4A^2}{\oint(1/h)d\eta}$.

The W_{44} element of the compliance matrix is $W_{44} = 1/\widehat{GI}_{\mathrm{t}}$.

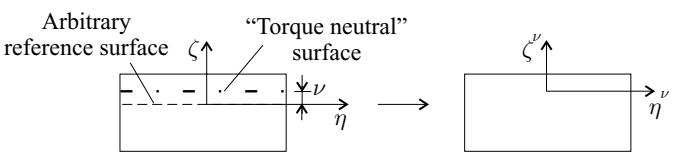

Figure 6.47: The torque neutral surface where $\widetilde{\beta}_{66}^{\nu}$ is zero.

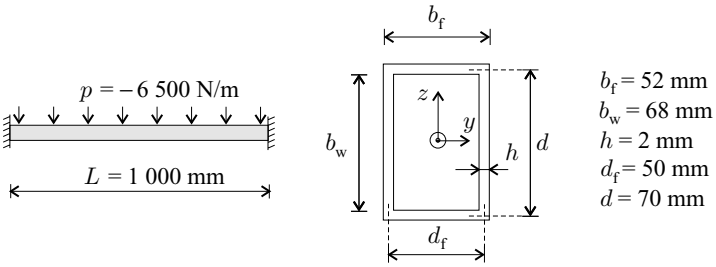

Figure 6.48: The beam in Example. 6.3.

Stresses and strain. The strains and curvature in each ply at the "torque neutral" surface are given by (see Eq. 6.90)

$$\begin{Bmatrix} \epsilon_\xi^o \\ \epsilon_\eta^o \\ \gamma_{\xi\eta}^o \\ \kappa_\xi \\ \kappa_\eta \\ \kappa_{\xi\eta} \end{Bmatrix} = \begin{bmatrix} 0 \\ 0 \\ \alpha_{66}^v \\ 0 \\ 0 \\ 0 \end{bmatrix} N_{\xi\eta}, \tag{6.199}$$

where $N_{\xi\eta} \equiv q$ is the shear flow calculated by Eq. (6.191).

With the preceding strains and curvatures, the stresses are calculated by Eqs. (6.181) and (6.182).

6.3 Example. *An $L = 1.0$-m-long box beam, with the cross section shown in Figure 6.48, is made of graphite epoxy. The material properties are given in Table 3.6 (page 81). The layup is $[\pm 45_2^f/0_{12}/\pm 45_2^f]$. The beam, built-in at each end, is subjected to a uniformly distributed load ($p = -6\ 500$ N/m) acting at the midplane of the left web (Fig. 6.49). By neglecting the effects of axial restraint, calculate the maximum deflection and the maximum twist.*

Solution. The cross section is doubly symmetrical, and both the centroid and the shear center (see Section 6.7.3) coincide with the center of the cross section. The

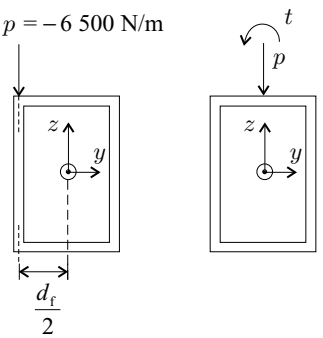

Figure 6.49: Loading on the box beam in Example 6.3 (left), and the loading with respect to the shear center (right).

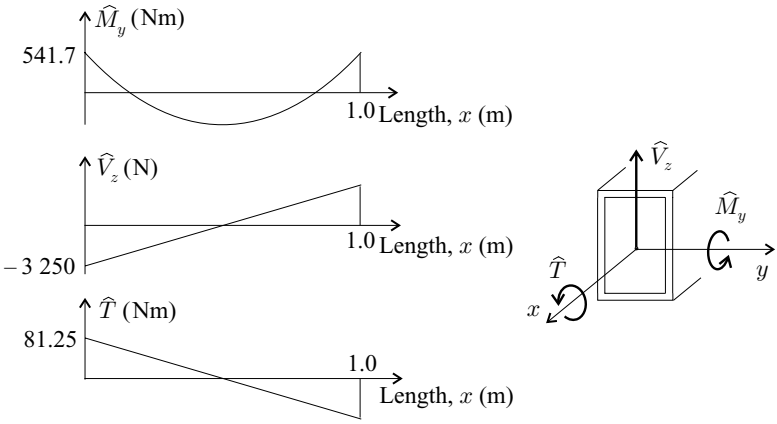

Figure 6.50: The bending moment $\widehat{M}_y$, shear force $\widehat{V}_z$, and torque $\widehat{T}$ diagrams for the beam in Example 6.3.

loads with respect to the shear center are (Fig. 6.49)

$$\begin{aligned} p &= -6\,500\,\frac{\mathrm{N}}{\mathrm{m}} && \text{(distributed load)} \\ t &= -p \times \frac{d_\mathrm{f}}{2} = 162.5\,\frac{\mathrm{N}\cdot\mathrm{m}}{\mathrm{m}} && \text{(distributed torque).} \end{aligned} \tag{6.200}$$

The corresponding bending moment $\widehat{M}_y$, shear force $\widehat{V}_z$, and torque $\widehat{T}$ diagrams are shown in Figure 6.50. The maximum values are

$$\begin{aligned} \widehat{M}_y^{\max} &= -\frac{pL^2}{12} = 541.7\ \mathrm{N}\cdot\mathrm{m} \\ \widehat{V}_z^{\max} &= \frac{pL}{2} = -3\,250\ \mathrm{N} \\ \widehat{T}^{\max} &= \frac{tL}{2} = 81.25\ \mathrm{N}\cdot\mathrm{m}. \end{aligned} \tag{6.201}$$

The compliance matrices for the flange and the web are the same, and their relevant elements are (Table 3.8, page 85)

$$a_{11} = 5.18 \times 10^{-9}\,\frac{\mathrm{m}}{\mathrm{N}} \qquad a_{66} = 27.77 \times 10^{-9}\,\frac{\mathrm{m}}{\mathrm{N}} \qquad d_{11} = 33.10 \times 10^{-3}\,\frac{1}{\mathrm{N}\cdot\mathrm{m}}.$$

The dimensions are (Fig. 6.48) $b_\mathrm{f} = 0.052\,\mathrm{m}$, $b_\mathrm{w} = 0.068\,\mathrm{m}$, $d = 0.07\,\mathrm{m}$, $d_\mathrm{f} = 0.05\,\mathrm{m}$.

From Table A.1 the bending stiffnesses are

$$\begin{aligned} \widehat{EI}_{yy} &= \frac{b_\mathrm{f}}{(a_{11})_\mathrm{f}}\frac{d^2}{2} + \frac{2b_\mathrm{f}}{(d_{11})_\mathrm{f}} + \frac{2b_\mathrm{w}^3}{12(a_{11})_\mathrm{w}} = 34\,692\ \mathrm{N}\cdot\mathrm{m}^2 \\ \widehat{EI}_{zz} &= \frac{b_\mathrm{w}}{(a_{11})_\mathrm{w}}\frac{d_\mathrm{f}^2}{2} + \frac{2b_\mathrm{w}}{(d_{11})_\mathrm{w}} + \frac{2b_\mathrm{f}^3}{12(a_{11})_\mathrm{f}} = 20\,924\ \mathrm{N}\cdot\mathrm{m}^2. \end{aligned} \tag{6.202}$$

The torsional stiffness $\widehat{GI}_\mathrm{t}$ is (Table A.6, with α_{66}^v replaced by a_{66})

$$\widehat{GI}_\mathrm{t} = \frac{2d_\mathrm{f}^2 d^2}{a_{66}(d_\mathrm{f} + d)} = 7\,352\ \mathrm{N}\cdot\mathrm{m}^2. \tag{6.203}$$

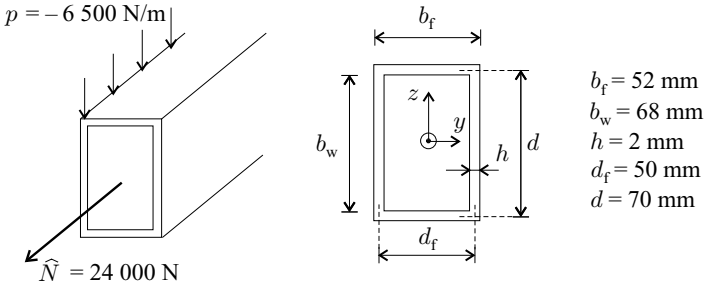

Figure 6.51: Cross section of the beam in Example 6.4 and the load applied on the beam.

The maximum deflection is (Table 7.3, page 332)

$$\widetilde{w} = \frac{1}{384}\frac{pL^4}{\widehat{EI}_{yy}} = -0.000\,488\,\text{m} = -0.488\,\text{mm}. \tag{6.204}$$

The maximum twist is at $x = L/2$ and is

$$\psi = \int_0^{L/2} \vartheta\, dx = \int_0^{L/2} \frac{\widehat{T}}{\widehat{GI}_t} dx. \tag{6.205}$$

The torque $\widehat{T}$ varies linearly with x, and the preceding integral yields

$$\psi = \frac{\widehat{T}^{\max} L}{4\widehat{GI}_t} = 0.002\,76\,\text{rad} = 0.158^\circ. \tag{6.206}$$

6.4 Example. *An $L = 1.0$-m-long box beam, with the cross section shown in Figure 6.51, is made of graphite epoxy. The material properties are given in Table 3.6 (page 81). The layup is $[\pm 45_5^f/0_{10}]$. The fabric is on the outside of the wall. The beam, built-in at each end, is subjected to a uniformly distributed load ($p = -6\,500$ N/m) acting along the midplane of the left web and to an axial load $\widehat{N} = 24\,000$ N. By neglecting the effects of axial restraint, calculate the maximum deflection and the maximum twist.*

Solution. The cross section is doubly symmetrical, and the centroid and the shear center (see Section 6.7.3) coincide with the center of the cross section. The loads with respect to the shear center and the corresponding bending moment $\widehat{M}_y$, shear force $\widehat{V}_z$, and torque $\widehat{T}$ are given in Example 6.3 (page 255).

The layup of each wall is orthotropic and unsymmetrical. The compliance matrices for the flange and the web are the same, and their relevant elements are (see Table 3.9, page 86).

$$\alpha_{11}^{MP} = 11.65 \times 10^{-9}\,\frac{\text{m}}{\text{N}} \qquad \alpha_{66}^{MP} = 43.70 \times 10^{-9}\,\frac{\text{m}}{\text{N}}$$

$$\beta_{11}^{MP} = -13.97 \times 10^{-6}\,\frac{1}{\text{N}} \qquad \beta_{12}^{MP} = 12.22 \times 10^{-6}\,\frac{1}{\text{N}} \qquad \beta_{66}^{MP} = 51.60 \times 10^{-6}\,\frac{1}{\text{N}}$$

$$\delta_{11}^{MP} = 34.94 \times 10^{-3}\,\frac{1}{\text{N}\cdot\text{m}} \qquad \delta_{12}^{MP} = -25.74\,\frac{1}{\text{N}\cdot\text{m}} \qquad \delta_{22}^{MP} = 98.83\,\frac{1}{\text{N}\cdot\text{m}},$$

$$\delta_{66}^{MP} = 131.11 \times 10^{-3}\,\frac{1}{\text{N}\cdot\text{m}}$$

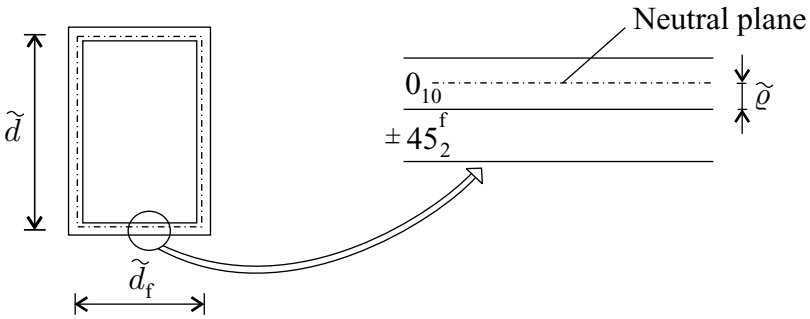

Figure 6.52: The neutral plane of the beam in Example 6.4.

where MP refers to the midplane of the wall. The dimensions of the beam are (Fig. 6.51) $b_{\mathrm{f}} = 0.052\,\mathrm{m}$, $b_{\mathrm{w}} = 0.068\,\mathrm{m}$, $d = 0.07$ m, and $d_{\mathrm{f}} = 0.05\,\mathrm{m}$.

To evaluate the bending stiffnesses, we determine the position of the neutral plane (Eq. 6.105 and Fig. 6.52) as follows:

$$\widetilde{\varrho} = -\frac{\beta_{11}^{\mathrm{MP}}}{\delta_{11}^{\mathrm{MP}}} = 0.0004\ \mathrm{m} = 0.400\ \mathrm{mm}. \tag{6.207}$$

At the $\widetilde{\varrho}$ reference plane the compliances of the flanges and the webs are (Eq. 3.48)

$$\begin{aligned} \alpha_{11} &= \alpha_{11}^{\mathrm{MP}} + 2\widetilde{\varrho}\beta_{11}^{\mathrm{MP}} + \widetilde{\varrho}^2\delta_{11}^{\mathrm{MP}} = 6.056 \times 10^{-9}\,\frac{\mathrm{m}}{\mathrm{N}} \\ \beta_{66} &= \beta_{66}^{\mathrm{MP}} + \widetilde{\varrho}\delta_{66}^{\mathrm{MP}} = 104.04 \times 10^{-6}\,\frac{1}{\mathrm{N}} \qquad \text{at } \widetilde{\varrho} \\ \delta_{11} &= \delta_{11}^{\mathrm{MP}} = 34.94 \times 10^{-3}\,\frac{1}{\mathrm{N}\cdot\mathrm{m}}. \end{aligned} \tag{6.208}$$

From Table A.3 the bending stiffnesses are

$$\widehat{EI}_{yy} = \frac{b_{\mathrm{f}}}{(\alpha_{11})_{\mathrm{f}}}\frac{\widetilde{d}^2}{2} + \frac{2b_{\mathrm{f}}}{(\delta_{11})_{\mathrm{f}}} + \frac{2b_{\mathrm{w}}^3}{12(\alpha_{11})_{\mathrm{w}}} = 29\,214\ \mathrm{N}\cdot\mathrm{m}^2 \tag{6.209}$$

$$\widehat{EI}_{zz} = \frac{b_{\mathrm{w}}}{(\alpha_{11})_{\mathrm{w}}}\frac{\widetilde{d}_{\mathrm{f}}^2}{2} + \frac{2b_{\mathrm{w}}}{(\delta_{11})_{\mathrm{w}}} + \frac{2b_{\mathrm{f}}^3}{12(\alpha_{11})_{\mathrm{f}}} = 17\,463\ \mathrm{N}\cdot\mathrm{m}^2, \tag{6.210}$$

where the dimensions $\widetilde{d}$ and $\widetilde{d}_{\mathrm{f}}$ are (Fig. 6.52) $\widetilde{d} = d - 2\widetilde{\varrho} = 0.0692$ m, $\widetilde{d}_{\mathrm{f}} = d_{\mathrm{f}} - 2\widetilde{\varrho} = 0.0492\,\mathrm{m}$.

The torsional stiffness $\widehat{GI}_{\mathrm{t}}$ is given in Table A.6 with reference to the $\widetilde{\varrho}$ neutral plane as

$$\widehat{GI}_{\mathrm{t}} = \frac{2d_{\mathrm{f}}^2 d^2}{\alpha_{66}^{\nu}(d_{\mathrm{f}} + d)} = 8\,726\ \mathrm{N}\cdot\mathrm{m}^2, \tag{6.211}$$

where α_{66}^{ν} is (Eq. 6.196)

$$\alpha_{66}^{\nu} = \alpha_{66}^{\mathrm{MP}} - \frac{(\beta_{66}^{\mathrm{MP}})^2}{\delta_{66}^{\mathrm{MP}}} = 23.40 \times 10^{-9}\frac{\mathrm{m}}{\mathrm{N}}. \tag{6.212}$$

The accuracy of $\widehat{GI}_{\mathrm{t}}$, as calculated by Eq. (6.211), is improved when $\widehat{GI}_{\mathrm{t}}$ is evaluated in reference to the "torque neutral" surface. Equation (6.194) gives $\nu = -\beta_{66}^{\mathrm{MP}}/\delta_{66}^{\mathrm{MP}} = -0.394\,\mathrm{mm}$. When d and d_{f} are replaced by $d - 2\nu = 0.0708$ and $d_{\mathrm{f}} - 2\nu = 0.0508\,\mathrm{m}$, respectively, Eq. (6.211) results in $\widehat{GI}_{\mathrm{t}} = 9\,087\ \mathrm{N}\cdot\mathrm{m}^2$.

Next, we calculate the tensile stiffness. From Eqs. (6.156) and (6.157), we have

$$\begin{aligned}\widehat{\beta}_{11}^{\mathrm{MP}} &= \left(\beta_{11}^{\mathrm{MP}} - \frac{\beta_{12}^{\mathrm{MP}}\delta_{12}^{\mathrm{MP}}}{\delta_{22}^{\mathrm{MP}}}\right) = -10.79 \times 10^{-6}\,\frac{1}{\mathrm{N}} \\ \widehat{\delta}_{11}^{\mathrm{MP}} &= \left(\delta_{11}^{\mathrm{MP}} - \frac{\left(\delta_{12}^{\mathrm{MP}}\right)^2}{\delta_{22}^{\mathrm{MP}}}\right) = 28.23 \times 10^{-3}\,\frac{1}{\mathrm{N}\cdot\mathrm{m}}.\end{aligned} \tag{6.213}$$

The location of the reference surface is (Eq. A.3)

$$\widehat{\varrho} = -\frac{\widehat{\beta}_{11}^{\mathrm{MP}}}{\widehat{\delta}_{11}^{\mathrm{MP}}} = 0.000\,382\ \mathrm{m} = 0.382\ \mathrm{mm}. \tag{6.214}$$

At the $\widehat{\varrho}$ reference surface, the compliances of the flanges and the webs are (Eq. 3.48)

$$\begin{aligned}\alpha_{11} &= \alpha_{11}^{\mathrm{MP}} + 2\widehat{\varrho}\beta_{11}^{\mathrm{MP}} + \widehat{\varrho}^2\delta_{11}^{\mathrm{MP}} = 6.067 \times 10^{-9}\,\frac{\mathrm{m}}{\mathrm{N}} \\ \beta_{12} &= \beta_{12}^{\mathrm{MP}} + \widehat{\varrho}\delta_{12}^{\mathrm{MP}} = 2.380 \times 10^{-6}\,\frac{1}{\mathrm{N}} \\ \delta_{11} &= \delta_{11}^{\mathrm{MP}} = 34.94 \times 10^{-3}\,\frac{1}{\mathrm{N}\cdot\mathrm{m}} \\ \delta_{12} &= \delta_{12}^{\mathrm{MP}} = -25.74 \times 10^{-3}\,\frac{1}{\mathrm{N}\cdot\mathrm{m}} \\ \delta_{22} &= \delta_{22}^{\mathrm{MP}} = 98.83 \times 10^{-3}\,\frac{1}{\mathrm{N}\cdot\mathrm{m}}.\end{aligned} \tag{6.215}$$

With these compliances from Eqs. (6.156) and (6.157), for both the flange and the web we have

$$\begin{aligned}\widehat{\alpha}_{11} &= \left(\alpha_{11} - \frac{(\beta_{12})^2}{\delta_{22}}\right) = 6.01 \times 10^{-9}\,\frac{\mathrm{m}}{\mathrm{N}} \\ \widehat{\delta}_{11} &= \left(\delta_{11} - \frac{(\delta_{12})^2}{\delta_{22}}\right) = 28.23 \times 10^{-3}\,\frac{1}{\mathrm{N}\cdot\mathrm{m}}.\end{aligned} \tag{6.216}$$

From Table A.3 the tensile stiffness is

$$\widehat{EA} = \frac{2b_{\mathrm{f}}}{(\widehat{\alpha}_{11})_{\mathrm{f}}} + \frac{2b_{\mathrm{w}}}{(\widehat{\alpha}_{11})_{\mathrm{w}}} = 39.934 \times 10^{6}\ \mathrm{N}. \tag{6.217}$$

The maximum deflection is (Table 7.3, page 332)

$$\widetilde{w} = \frac{1}{384}\frac{pL^4}{\widehat{EI}_{yy}} = -0.000\,579\ \mathrm{m} = -0.579\ \mathrm{mm}. \tag{6.218}$$

The maximum twist is at $x = L/2$ and is

$$\psi = \int_0^{L/2} \vartheta\, dx = \int_0^{L/2} \frac{\widehat{T}}{\widehat{GI}_{\mathrm{t}}} dx. \tag{6.219}$$

Torque $\widehat{T}$ varies linearly with x, thus, the integral above yields

$$\psi = \frac{\widehat{T}^{\max} L}{4\widehat{GI}_{\mathrm{t}}} = 0.002\,33\ \mathrm{rad} = 0.133^{\circ}, \tag{6.220}$$

where $\widehat{T}^{\max} = 81.25\ \frac{\mathrm{N\cdot m}}{\mathrm{m}}$ (Eq. 6.201). The elongation of the beam is

$$\Delta L = \int_0^L \varepsilon_x dx = \int_0^L \frac{\widehat{N}}{\widehat{EA}} dx = \frac{\widehat{N}L}{\widehat{EA}} = 0.000\,601\,\mathrm{m} = 0.601\,\mathrm{mm}. \quad (6.221)$$

6.5.4 Closed Section Orthotropic Beams – Multicell

For multicell composite beams the rate of twist and the shear flows are determined in the same way as for isotropic beams. Accordingly, for a beam consisting of L cells the torque is

$$\widehat{T} = \sum_{l=1}^{L} 2A_l q_l, \quad (6.222)$$

where A_l is the enclosed area of the lth cell and q_l is the shear flow in the lth cell (Fig. 6.53). The shear strain $\gamma^{\mathrm{o}}_{\xi\eta}$ in each wall segment is calculated by (Eq. 6.195)

$$\gamma^{\mathrm{o}}_{\xi\eta} = \alpha^{v}_{66} q, \quad (6.223)$$

where q is the shear flow in the wall segment. Then, the rate of twist of each cell is (Eq. 6.188)

$$\begin{aligned}
\vartheta_1 &= \frac{1}{2A_1} \oint_{\text{cell } 1} \alpha^{v}_{66} q\, d\eta \\
\vartheta_2 &= \frac{1}{2A_2} \oint_{\text{cell } 2} \alpha^{v}_{66} q\, d\eta \\
&\vdots \\
\vartheta_L &= \frac{1}{2A_L} \oint_{\text{cell } L} \alpha^{v}_{66} q\, d\eta.
\end{aligned} \quad (6.224)$$

For a wall that belongs to one cell only, q is equal to the shear flow of the appropriate cell ($q = q_l$). For a wall that belongs to two cells, the shear flow is the sum of the shear flows of the adjacent cells, as illustrated in Figure 6.53.

The rate of twist of each cell is the same

$$\vartheta = \vartheta_1 = \vartheta_2 = \ldots = \vartheta_L. \quad (6.225)$$

There are $L+1$ equations (Eqs. 6.224 and 6.222) that can be solved for the $L+1$ unknowns: q_l ($l = 1, 2, \ldots, L$) and ϑ.

The stresses in the walls are calculated as for a single-cell beam.

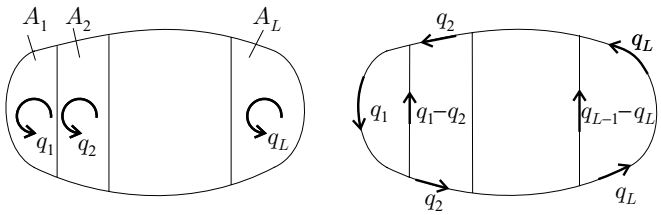

Figure 6.53: Shear flow in multicell beams.

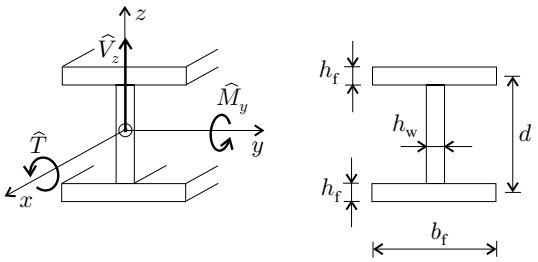

Figure 6.54: Thin-walled I-beam.

6.5.5 Restrained Warping – Open-Section Orthotropic Beams

When an isotropic beam is subjected to pure torsion and the cross sections of the beam are free to warp, the torque is (Eq. 6.161)

$$\widehat{T} = (GI_t)\,\vartheta. \tag{6.226}$$

When the beam is axially constrained at one of its cross sections (for example at a built-in end), then, at this cross section, warping cannot occur. The shorter the beam, the more important are the effects of restrained warping. Furthermore, the effects of restrained warping are more pronounced for thin-walled open-section beams than for thin-walled closed-section beams and for solid cross-section beams. Therefore, in this section, we consider only restrained warping of open-section beams.

We illustrate the analysis through the example of a symmetrical I-beam (Fig. 6.54).

Isotropic I beams. Under pure torque, in the absence of axial constraint, the shear stress distribution in an isotropic I-beam is as shown in Figure 6.55. When the beam is axially restrained, axial forces N_ξ (per unit length) are introduced in the wall (Fig. 6.56, bottom). These axial forces create a bending moment $\widehat{M}_f$[8]

$$\widehat{M}_f = -\frac{d^2 v_f}{dx^2} EI_f, \tag{6.227}$$

where I_f is the moment of inertia of the flange about the z-axis denoted by

$$I_f = \frac{h_f b_f^3}{12}, \tag{6.228}$$

b_f and h_f are the width and the thickness of the flanges (Fig. 6.54), respectively; v_f is the displacement of the flange due to the rotation about the x-axis (Fig. 6.57),

$$v_f = \psi \frac{d}{2}, \tag{6.229}$$

where d is the distance between the midplanes of the flanges. We recall that

[8] T. H. G. Megson, *Aircraft Structures for Engineering Students*. 3rd edition. Halsted Press, John Wiley & Sons, New York, 1999, p. 467.

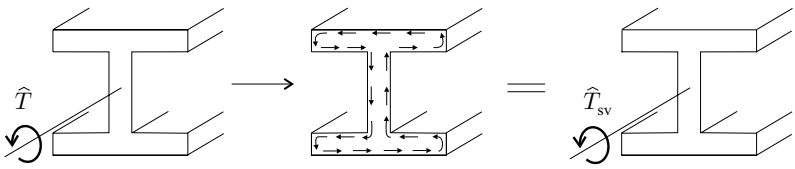

Figure 6.55: Isotropic I-beam under pure torque with no axial constraint.

$\vartheta = d\psi/dx$ (Eq. 6.1). Thus, we have

$$\frac{dv_f}{dx} = \vartheta \frac{d}{2}. \tag{6.230}$$

The bending moment $\widehat{M}_f$ may now be expressed as

$$\widehat{M}_f = -\frac{d\vartheta}{dx} E \frac{h_f b_f^3}{12} \frac{d}{2}. \tag{6.231}$$

We now introduce the bimoment $\widehat{M}_\omega$ defined for an I-beam as

$$\widehat{M}_\omega = \widehat{M}_f d. \tag{6.232}$$

The last two equations give

$$\widehat{M}_\omega = -\frac{d\vartheta}{dx} \underbrace{\left(\frac{E h_f b_f^3}{24} d^2\right)}_{EI_\omega}. \tag{6.233}$$

The term indicated by the bracket is the warping stiffness EI_ω.

Owing to the axial constraint, the bending moment $\widehat{M}_f$ varies along the x-axis of the beam. Correspondingly, there is a shear force in the flanges. The relationship between the flange shear force and the flange bending moment is

$$\widehat{V}_f = \frac{d\widehat{M}_f}{dx}. \tag{6.234}$$

The shear force results in a torque $\widehat{T}_\omega$ (Fig. 6.56, bottom) defined by

$$\widehat{T}_\omega = \widehat{V}_f d. \tag{6.235}$$

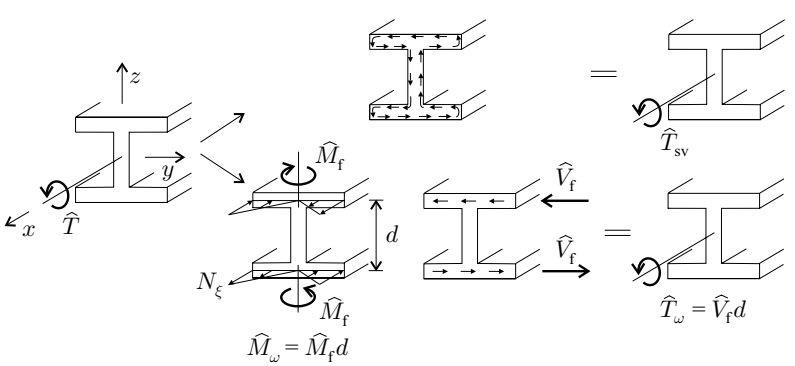

Figure 6.56: Isotropic I-beam under pure torque with axial constraint.

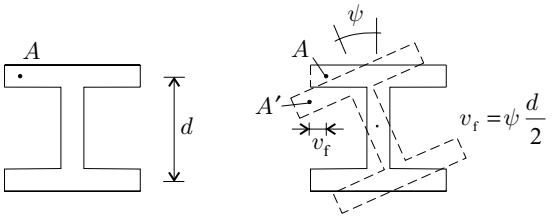

Figure 6.57: Rotation of an I-beam about the x-axis.

Equations (6.232), (6.234), and (6.235) give

$$\widehat{T}_\omega = \frac{d\widehat{M}_\omega}{dx}. \tag{6.236}$$

From Eqs. (6.236) and (6.233) we have

$$\widehat{T}_\omega = -EI_\omega \frac{d^2\vartheta}{dx^2}, \tag{6.237}$$

where the warping stiffness EI_ω is (see Eq. 6.233)

$$EI_\omega = \frac{Eh_f b_f^3}{24} d^2. \tag{6.238}$$

The total torque is

$$\widehat{T} = \underbrace{(GI_t)\,\vartheta}_{\widehat{T}_{sv}} + \underbrace{(EI_\omega)\left(-\frac{d^2\vartheta}{dx^2}\right)}_{\widehat{T}_\omega}, \tag{6.239}$$

where $\widehat{T}_{sv}$ and $\widehat{T}_\omega$ are referred to as the "Saint-Venant" and the "restrained–warping-induced" torques, respectively.

Orthotropic I-beams. The expression for the torque of orthotropic beams is similar to the expression for isotropic I-beams (Eq. 6.239) as follows:

$$\widehat{T} = \underbrace{\widehat{GI}_t\vartheta}_{\widehat{T}_{sv}} + \underbrace{\widehat{EI}_\omega\left(-\frac{d^2\vartheta}{dx^2}\right)}_{\widehat{T}_\omega}. \tag{6.240}$$

The torsional stiffness $\widehat{GI}_t$ presented in Section 6.5.2 is unaffected by the axial constraint and is given by Eq. (6.175).

It remains to determine the warping stiffness $\widehat{EI}_\omega$. By referring to Eq. (6.238), we see that the warping stiffness of an isotropic I-beam is a function of the product of the flange's modulus E and thickness h ($\widehat{EI}_\omega \sim Eh$). This Eh is related to the axial force (per unit length) in the flange as follows:

$$N_\xi = h\sigma_\xi = Eh\epsilon_\xi^o. \tag{6.241}$$

For a beam with orthotropic layup, N_ξ is (see Table 6.2, page 222)

$$N_\xi = \frac{\delta_{11}}{D}\epsilon_\xi^o - \frac{\beta_{11}}{D}\kappa_\xi. \tag{6.242}$$

Table 6.9. Boundary conditions for beams in torsion.

Warping restrained	$\vartheta = 0$
unrestrained	$\widehat{M}_\omega = 0$
Rotationally restrained	$\psi = 0$
unrestrained	$\widehat{T} = 0$

This equation applies at a reference plane chosen arbitrarily. At the "neutral" plane (see Eq. 6.105) $\beta_{11} = 0$, and, hence (see Table 6.2, page 222), we have that $\delta_{11}/D = 1/\alpha_{11}^{\varrho}$, where the superscript ϱ indicates that α_{11}^{ϱ} is evaluated at the flange's "neutral" plane. With these substitutions the preceding equation becomes

$$N_\xi = \frac{1}{\alpha_{11}^{\varrho}} \epsilon_\xi^{\mathrm{o}}. \tag{6.243}$$

By comparing Eqs. (6.243) and (6.241), we see that an orthotropic beam's tensile stiffness $1/\alpha_{11}^{\varrho}$ corresponds to an isotropic beam's tensile stiffness Eh. We use this correspondence and evaluate the warping stiffness of an orthotropic I-beam by replacing Eh by $1/\alpha_{11}^{\varrho}$ in Eq. (6.238). The result is

$$\widehat{EI}_\omega = \frac{\frac{1}{\alpha_{11}^{\varrho}} b_{\mathrm{f}}^3}{24} d^2. \tag{6.244}$$

Orthotropic beam – arbitrary cross section. Equation (6.240) can also be used for thin-walled beams with other cross-sectional shapes by using the appropriate torsional and warping stiffnesses. The torsional stiffness $\widehat{GI}_{\mathrm{t}}$ is given by Eqs. (6.170) and (6.175). The warping stiffness $\widehat{EI}_\omega$ of an orthotropic beam is obtained by replacing Eh by $1/\alpha_{11}^{\varrho}$ in the appropriate expressions[9] for the corresponding isotropic beam. The warping stiffnesses $\widehat{EI}_\omega$ of frequently used cross sections are included in Table A.5.

Boundary conditions. When the warping of the cross section at the end of a beam is restrained, the distortion is zero. When warping is not restrained, the bimoment is zero.

When the end may rotate, the torque is zero. When the end is rotationally restrained, the rate of twist is zero.

The preceding boundary conditions are summarized in Table 6.9.

6.5.6 Restrained Warping – Closed-Section Orthotropic Beams

Warping of closed-section beams is often negligible. Warping may become significant, though, when the shear stiffnesses of different wall segments are markedly different. This is illustrated in Figure 6.58.

[9] S. P. Timoshenko and J. Gere, *Theory of Elastic Stability.* 2nd edition. McGraw-Hill, New York, 1961, p. 530.

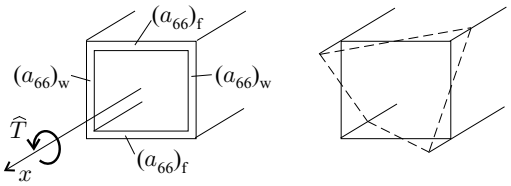

Figure 6.58: Warping of a box beam subjected to torsion when $(a_{66})_f \ll (a_{66})_w$.

6.6 Thin-Walled Beams with Arbitrary Layup Subjected to Axial Load, Bending, and Torsion

In this section we treat thin-walled, open- and closed-section beams. The beam's wall consists of flat segments (Fig. 6.59) designated by the subscript k ($k = 1, 2, \ldots,$ K, where K is the total number of wall segments). The cross section may be symmetrical or unsymmetrical, and the layup of the beam is arbitrary, that is, the layers are not necessarily orthotropic.

The beam is subjected to an axial force $\widehat{N}$, bending moments $\widehat{M}_y$, $\widehat{M}_z$, and torque $\widehat{T}$ acting at the centroid.

We employ two coordinate systems (Fig. 6.60) for the beam; the x–y–z coordinate system with its origin at the centroid and the $\overline{x}$–$\overline{y}$–$\overline{z}$ coordinate system with its origin at an arbitrarily chosen point. The location of the centroid with respect to the origin of the $\overline{x}$–$\overline{y}$–$\overline{z}$ coordinate system is given in Section 6.6.3.

The displacements of the longitudinal axis, passing through the centroid, are u, v, w, ψ (Fig. 6.3), where u is the axial displacement, v and w are the transverse displacements in the y and z directions, and ψ is the twist of the cross section. In the x–y–z coordinate system the relationships between these displacements, the axial strain ϵ_x^o, the curvatures $1/\rho_y$, $1/\rho_z$ of the x-axis, and the rate of twist ϑ (Eq. 6.1) are

$$\frac{\partial u}{\partial x} = \epsilon_x^o \qquad \frac{\partial^2 v}{\partial x^2} = -\frac{1}{\rho_z} \qquad \frac{\partial^2 w}{\partial x^2} = -\frac{1}{\rho_y} \qquad \frac{\partial \psi}{\partial x} = \vartheta. \tag{6.245}$$

In the $\overline{x}$–$\overline{y}$–$\overline{z}$ coordinate system these relationships become

$$\frac{\partial \overline{u}}{\partial \overline{x}} = \epsilon_{\overline{x}}^o \qquad \frac{\partial^2 \overline{v}}{\partial \overline{x}^2} = -\frac{1}{\rho_{\overline{z}}} \qquad \frac{\partial^2 \overline{w}}{\partial \overline{x}^2} = -\frac{1}{\rho_{\overline{y}}} \qquad \frac{\partial \overline{\psi}}{\partial \overline{x}} = \overline{\vartheta}, \tag{6.246}$$

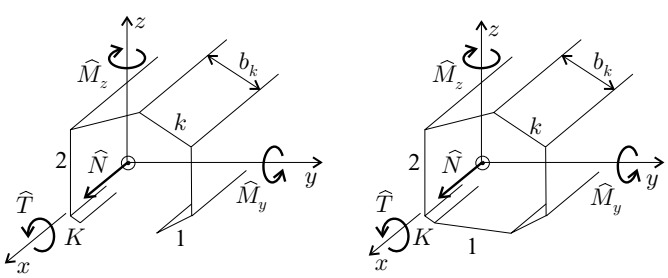

Figure 6.59: Forces on open and closed cross-section, thin-walled beams with flat wall segments.

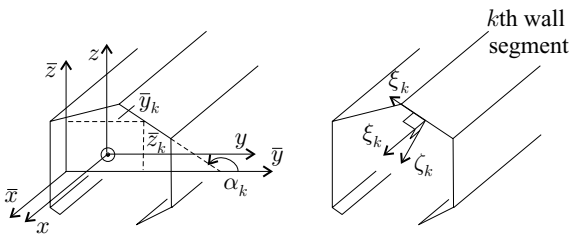

Figure 6.60: The coordinate systems employed in the analysis of thin-walled beams with arbitrary layup.

where $\epsilon^{\mathrm{o}}_{\overline{x}}$, $1/\rho_{\overline{y}}$, $1/\rho_{\overline{z}}$ are the axial strain and the curvatures of the longitudinal axis passing through the origin of the $\overline{x}$–$\overline{y}$–$\overline{z}$ coordinate system, and $\overline{u}$, $\overline{v}$, $\overline{w}$, and $\overline{\psi}$ are the displacements of the $\overline{x}$-axis.

The force, moment, and torque resultants at the origin of the bar coordinate system $\widehat{N}_{\overline{x}}$, $\widehat{M}_{\overline{y}}$, $\widehat{M}_{\overline{z}}$, $\widehat{T}_{\overline{x}}$ are related to the force applied at the centroid by the expressions,

$$\widehat{N}_{\overline{x}} = \widehat{N} \qquad \widehat{M}_{\overline{y}} = \widehat{M}_y + z_{\mathrm{c}}\widehat{N} \qquad \widehat{M}_{\overline{z}} = \widehat{M}_z + y_{\mathrm{c}}\widehat{N} \qquad \widehat{T}_{\overline{x}} = \widehat{T}, \tag{6.247}$$

where z_{c} and y_{c} are the coordinates of the centroid in the bar coordinate system (Fig. 6.61). For both open- and closed-section beams the force–strain and strain–force relationships in the x–y–z coordinate system are (Eqs. 6.2 and 6.17)

$$\begin{Bmatrix} \widehat{N}_x \\ \widehat{M}_y \\ \widehat{M}_z \\ \widehat{T} \end{Bmatrix} = \begin{bmatrix} P_{11} & P_{12} & P_{13} & P_{14} \\ P_{12} & P_{22} & P_{23} & P_{24} \\ P_{13} & P_{23} & P_{33} & P_{34} \\ P_{14} & P_{24} & P_{34} & P_{44} \end{bmatrix} \begin{Bmatrix} \epsilon^{\mathrm{o}}_x \\ \frac{1}{\rho_y} \\ \frac{1}{\rho_z} \\ \vartheta \end{Bmatrix} \tag{6.248}$$

$$\begin{Bmatrix} \epsilon^{\mathrm{o}}_x \\ \frac{1}{\rho_y} \\ \frac{1}{\rho_z} \\ \vartheta \end{Bmatrix} = \begin{bmatrix} W_{11} & 0 & 0 & W_{14} \\ 0 & W_{22} & W_{23} & W_{24} \\ 0 & W_{23} & W_{33} & W_{34} \\ W_{14} & W_{24} & W_{34} & W_{44} \end{bmatrix} \begin{Bmatrix} \widehat{N}_x \\ \widehat{M}_y \\ \widehat{M}_z \\ \widehat{T} \end{Bmatrix}. \tag{6.249}$$

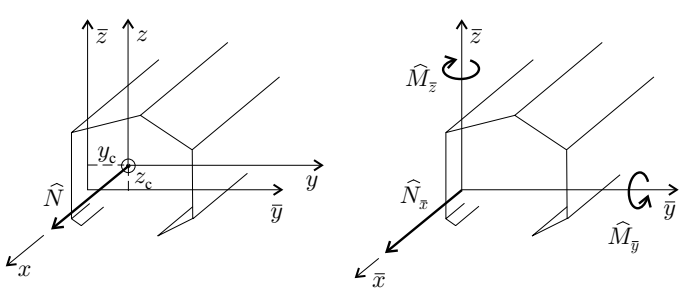

Figure 6.61: Beam subjected to an axial force at the centroid and the resultant axial force and moments in the $\overline{x}$–$\overline{y}$–$\overline{z}$ coordinate system.

In the bar coordinate system these relationships are written as

$$\begin{Bmatrix} \widehat{N}_{\overline{x}} \\ \widehat{M}_{\overline{y}} \\ \widehat{M}_{\overline{z}} \\ \widehat{T}_{\overline{x}} \end{Bmatrix} = \begin{bmatrix} \overline{P}_{11} & \overline{P}_{12} & \overline{P}_{13} & \overline{P}_{14} \\ \overline{P}_{12} & \overline{P}_{22} & \overline{P}_{23} & \overline{P}_{24} \\ \overline{P}_{13} & \overline{P}_{23} & \overline{P}_{33} & \overline{P}_{34} \\ \overline{P}_{14} & \overline{P}_{24} & \overline{P}_{34} & \overline{P}_{44} \end{bmatrix} \begin{Bmatrix} \epsilon^{\mathrm{o}}_{\overline{x}} \\ \frac{1}{\rho_{\overline{y}}} \\ \frac{1}{\rho_{\overline{z}}} \\ \vartheta \end{Bmatrix} \tag{6.250}$$

$$\begin{Bmatrix} \epsilon^{\mathrm{o}}_{\overline{x}} \\ \frac{1}{\rho_{\overline{y}}} \\ \frac{1}{\rho_{\overline{z}}} \\ \vartheta \end{Bmatrix} = \begin{bmatrix} \overline{W}_{11} & \overline{W}_{12} & \overline{W}_{13} & \overline{W}_{14} \\ \overline{W}_{12} & \overline{W}_{22} & \overline{W}_{23} & \overline{W}_{24} \\ \overline{W}_{13} & \overline{W}_{23} & \overline{W}_{33} & \overline{W}_{34} \\ \overline{W}_{14} & \overline{W}_{24} & \overline{W}_{34} & \overline{W}_{44} \end{bmatrix} \begin{Bmatrix} \widehat{N}_{\overline{x}} \\ \widehat{M}_{\overline{y}} \\ \widehat{M}_{\overline{z}} \\ \widehat{T}_{\overline{x}} \end{Bmatrix}, \tag{6.251}$$

where $[P]$, $[\overline{P}]$, $[W]$, and $[\overline{W}]$ are the stiffness and compliance matrices in the centroid x–y–z and bar $\overline{x}$–$\overline{y}$–$\overline{z}$ coordinate systems. These matrices are obtained by reasoning similar to that used in the derivations of the stiffness and compliance matrices of orthotropic beams (Sections 6.3.3 and 6.4). For beams with arbitrary layup the algebraic steps are long and laborious[10] and their presentation is beyond the scope of this book. The results are summarized in Table 6.10.

The compliances $\alpha_{ij}, \beta_{ij}, \delta_{ij}$, which appear in Table 6.10, are evaluated in the local ξ–η–ζ coordinate system. For the kth segment we employ the ξ_k–η_k–ζ_k coordinate system with the origin at the midpoint of the reference plane of the kth segment, where ξ is parallel to the x coordinate, η is along the circumference of the wall, and ζ is perpendicular to the circumference; $\overline{y}_k$ and $\overline{z}_k$ are the coordinates of the ξ_k–η_k–ζ_k coordinate system's origin, which is at the midpoint of the reference plane (Fig. 6.60). For closed-section beams, η_k points in the counterclockwise direction (Fig. 6.62), α_k is the angle between the η_k and $\overline{y}$ coordinate axes, and b_k is the width of the wall segment (Fig. 6.59).

We observe that for orthotropic beams the expressions in Table 6.10 yield the stiffness matrix given in Eq. (6.7).

6.6.1 Displacements of Open- and Closed-Section Beams

In the analysis we must take into account that thin-walled beams with arbitrary layup respond to loads differently than beams with orthotropic layup. For example, an orthotropic beam subjected to an axial load deforms, as shown in Figure 6.63 (left). A thin-walled beam with arbitrary layup deforms as shown in Figure 6.63 (right). Thus, the cross sections of beams with arbitrary layup do not remain plane, and the Bernoulli–Navier hypothesis is inapplicable. Nonetheless, in a long body, such as a beam, the strains may be considered to be constant in the axial direction, and we may apply the plane–strain condition (Section 2.4) in the analysis.

The displacements are then calculated with this approximation from the governing equations together with the force–strain relationship given in Table 6.10.

[10] L. P. Kollár and A. Pluzsik, Analysis of Thin Walled Composite Beams with Arbitrary Layup, *Journal of Reinforced Plastics and Composites*, Vol. 21, 1423–1465, 2002.

Table 6.10. Stiffness and compliance matrices in the bar ($[\overline{P}]$, $[\overline{W}]$) and centroid ($[P]$, $[W]$) coordinate systems of open- and closed-section beams with arbitrary layup. The elements α_{ij}, β_{ij}, δ_{ij} are evaluated at the ξ_k–η_k–ζ_k coordinate system of each wall segment. The enclosed area of closed-section beams is denoted by A. The superscript T denotes transpose.

Bar coordinate system: $[\overline{W}] = [\overline{P}]^{-1}$

Open-section beam: $[\overline{P}] = \sum_{k=1}^{K} [R_k]^{\mathrm{T}} [\omega_k]^{-1} [R_k]$

Closed-section beam: $[\overline{P}] = \sum_{k=1}^{K} ([R_k]^{\mathrm{T}} [\omega_k]^{-1} [R_k]) + [L]^{\mathrm{T}} [F]^{-1} [L]$

Centroid coordinate system: $[W] = [R_{\mathrm{b}}]^{\mathrm{T}} [\overline{W}] [R_{\mathrm{b}}] \qquad [P] = [W]^{-1}$

$$[R_k] = \begin{bmatrix} 1 & \overline{z}_k & \overline{y}_k & 0 \\ 0 & \cos\alpha_k & -\sin\alpha_k & 0 \\ 0 & \sin\alpha_k & \cos\alpha_k & 0 \\ 0 & 0 & 0 & 1 \end{bmatrix} \qquad \begin{bmatrix} \widetilde{A}_{11} & \widetilde{A}_{12} & \widetilde{A}_{13} \\ \widetilde{A}_{12} & \widetilde{A}_{22} & \widetilde{A}_{23} \\ \widetilde{A}_{13} & \widetilde{A}_{23} & \widetilde{A}_{33} \end{bmatrix}_k = \begin{bmatrix} \alpha_{11} & \beta_{11} & \beta_{16} \\ \beta_{11} & \delta_{11} & \delta_{16} \\ \beta_{16} & \delta_{16} & \delta_{66} \end{bmatrix}_k^{-1}$$

$$[\omega_k] = \frac{1}{b_k} \begin{bmatrix} \alpha_{11} & \beta_{11} & 0 & -\frac{1}{2}\beta_{16} \\ \beta_{11} & \delta_{11} & 0 & -\frac{1}{2}\delta_{16} \\ 0 & 0 & \frac{12}{(\widetilde{A}_{11})_k b_k^2} & 0 \\ -\frac{1}{2}\beta_{16} & -\frac{1}{2}\delta_{16} & 0 & \frac{1}{4}\delta_{66} \end{bmatrix} \qquad [R_{\mathrm{b}}] = \begin{bmatrix} 1 & 0 & 0 & 0 \\ z_{\mathrm{c}} & 1 & 0 & 0 \\ y_{\mathrm{c}} & 0 & 1 & 0 \\ 0 & 0 & 0 & 1 \end{bmatrix}$$

$$[I] = \sum_{k=1}^{K} \begin{bmatrix} \alpha_{16} & \beta_{61} & 0 & -\frac{1}{2}\beta_{66} \\ \beta_{12} & \delta_{12} & 0 & -\frac{1}{2}\delta_{26} \end{bmatrix}_k [\omega_k]^{-1} [R_k] \qquad [L] = \begin{bmatrix} 0 & 0 & 0 & 2A \\ 0 & 0 & 0 & 0 \end{bmatrix} - [I]$$

$$[F] = \sum_{k=1}^{K} \left(b_k \begin{bmatrix} \alpha_{66} & \beta_{62} \\ \beta_{62} & \delta_{22} \end{bmatrix}_k - \begin{bmatrix} \alpha_{16} & \beta_{61} & 0 & -\frac{1}{2}\beta_{66} \\ \beta_{12} & \delta_{12} & 0 & -\frac{1}{2}\delta_{26} \end{bmatrix}_k [\omega_k]^{-1} \begin{bmatrix} \alpha_{16} & \beta_{12} \\ \beta_{61} & \delta_{12} \\ 0 & 0 \\ -\frac{1}{2}\beta_{66} & -\frac{1}{2}\delta_{26} \end{bmatrix}_k \right)$$

$$[R_\eta] = \begin{bmatrix} 1 & 0 & \eta & 0 \\ 0 & 1 & 0 & 0 \\ 0 & 0 & 0 & -2 \end{bmatrix} \qquad [\widetilde{\mu}_k] = \begin{bmatrix} \alpha_{11} & \beta_{11} & \beta_{16} \\ \beta_{11} & \delta_{11} & \delta_{16} \\ \beta_{16} & \delta_{16} & \delta_{66} \end{bmatrix}_k \qquad [\widetilde{\nu}_k] = \begin{bmatrix} \alpha_{16} & \beta_{12} \\ \beta_{61} & \delta_{12} \\ \beta_{66} & \delta_{26} \end{bmatrix}_k$$

6.6.2 Stresses and Strains in Open- and Closed-Section Beams

We describe the stresses and strains inside the wall with reference to each wall segment's ξ_k–η_k–ζ_k coordinate system (Fig. 6.60). The forces and moments inside the wall are shown in Figure 6.64.

By applying the results of the laminate plate theory, the strains and stresses in the kth wall segment are obtained by replacing x by ξ, y by η, and z by ζ in

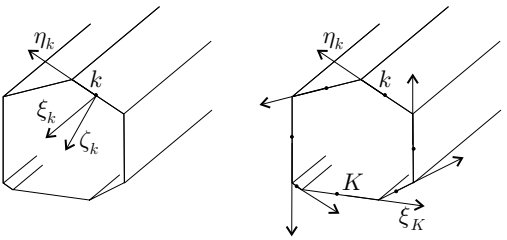

Figure 6.62: The local coordinate system attached to the kth wall segment (left) and the directions of the η coordinates (right) in a closed-section beam.

Eqs. (3.7) and (3.11) as follows:

$$\begin{Bmatrix} \epsilon_\xi \\ \epsilon_\eta \\ \gamma_{\xi\eta} \end{Bmatrix}_k = \begin{Bmatrix} \epsilon_\xi^{\mathrm{o}} \\ \epsilon_\eta^{\mathrm{o}} \\ \gamma_{\xi\eta}^{\mathrm{o}} \end{Bmatrix}_k + \zeta \begin{Bmatrix} \kappa_\xi \\ \kappa_\eta \\ \kappa_{\xi\eta} \end{Bmatrix}_k \tag{6.252}$$

$$\begin{Bmatrix} \sigma_\xi \\ \sigma_\eta \\ \tau_{\xi\eta} \end{Bmatrix}_k = \begin{bmatrix} \overline{Q}_{11} & \overline{Q}_{12} & \overline{Q}_{16} \\ \overline{Q}_{21} & \overline{Q}_{22} & \overline{Q}_{26} \\ \overline{Q}_{16} & \overline{Q}_{26} & \overline{Q}_{66} \end{bmatrix}_k \begin{Bmatrix} \epsilon_\xi \\ \epsilon_\eta \\ \gamma_{\xi\eta} \end{Bmatrix}_k , \tag{6.253}$$

where $[\overline{Q}]_k$ is evaluated in the kth wall segment's ξ_k–η_k–ζ_k coordinate system.

In the kth segment's reference plane the strains and curvatures are calculated from the strain–force relationships (Eq. 3.22), which, for convenience, are reproduced as follows:

$$\begin{Bmatrix} \epsilon_\xi^{\mathrm{o}} \\ \epsilon_\eta^{\mathrm{o}} \\ \gamma_{\xi\eta}^{\mathrm{o}} \\ \kappa_\xi \\ \kappa_\eta \\ \kappa_{\xi\eta} \end{Bmatrix}_k = \begin{bmatrix} \alpha_{11} & \alpha_{12} & \alpha_{16} & \beta_{11} & \beta_{12} & \beta_{16} \\ \alpha_{12} & \alpha_{22} & \alpha_{26} & \beta_{21} & \beta_{22} & \beta_{26} \\ \alpha_{16} & \alpha_{26} & \alpha_{66} & \beta_{61} & \beta_{62} & \beta_{66} \\ \beta_{11} & \beta_{21} & \beta_{61} & \delta_{11} & \delta_{12} & \delta_{16} \\ \beta_{12} & \beta_{22} & \beta_{62} & \delta_{12} & \delta_{22} & \delta_{26} \\ \beta_{16} & \beta_{26} & \beta_{66} & \delta_{16} & \delta_{26} & \delta_{66} \end{bmatrix}_k \begin{Bmatrix} N_\xi \\ N_\eta \\ N_{\xi\eta} \\ M_\xi \\ M_\eta \\ M_{\xi\eta} \end{Bmatrix}_k , \tag{6.254}$$

where the k subscript refers to the kth segment and α_{ij}, β_{ij}, δ_{ij} are evaluated in the kth wall segment's ξ_k–η_k–ζ_k coordinate system. The preceding expressions apply both to open- and closed-section beams. The difference in the two types of beams is in the expressions used to calculate the forces and moment (per unit length)

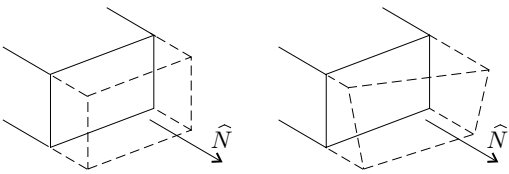

Figure 6.63: Displacements of an orthotropic beam (left) and a beam with arbitrary layup (right) under tension.

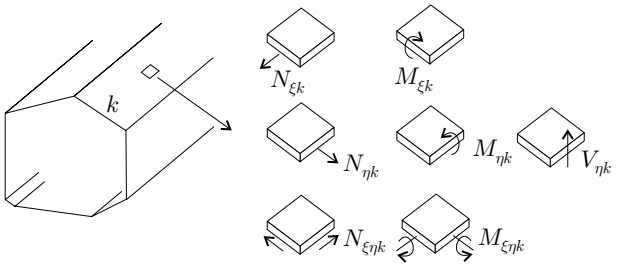

Figure 6.64: The forces and moments (per unit length) acting in the kth wall of an open- or closed-section beam.

inside the wall. The relevant expressions, derived by Pluzsik and Kollár,[11] are summarized in the remainder of this section.

Open-section beam. Along the free longitudinal edges of the beam, the in-plane forces and moments (per unit length) are zero: $N_\eta = N_{\xi\eta} = M_\eta = 0$ (Fig. 6.24). Since the dimensions of the cross section are small compared with the beam's length, these in-plane forces and moments are approximately zero inside the wall:

$$N_\eta = N_{\xi\eta} = M_\eta = 0. \tag{6.255}$$

The expressions for N_ξ, M_ξ, $M_{\xi\eta}$ are

$$\begin{Bmatrix} N_\xi \\ M_\xi \\ M_{\xi\eta} \end{Bmatrix}_k = [\widetilde{\mu}_k]^{-1}\,[R_\eta]\,[R_k]\,[\overline{W}] \begin{Bmatrix} \widehat{N}_{\overline{x}} \\ \widehat{M}_{\overline{y}} \\ \widehat{M}_{\overline{z}} \\ \widehat{T}_{\overline{x}} \end{Bmatrix}, \tag{6.256}$$

where $[\widetilde{\mu}_k]$, $[R_\eta]$, and $[R_k]$ are defined in Table 6.10.

Closed-section beam. In a closed-section beam, N_η is negligible; thus,

$$N_{\eta k} = 0. \tag{6.257}$$

The remaining forces and moments are

$$\begin{Bmatrix} N_{\xi\eta} \\ M_\eta \end{Bmatrix}_k = [F]^{-1}\,[L] \begin{Bmatrix} \epsilon^{\mathrm{o}}_{\overline{x}} \\ \frac{1}{\rho_{\overline{y}}} \\ \frac{1}{\rho_{\overline{z}}} \\ \vartheta \end{Bmatrix} = [F]^{-1}[L][\overline{W}] \begin{Bmatrix} \widehat{N}_{\overline{x}} \\ \widehat{M}_{\overline{y}} \\ \widehat{M}_{\overline{z}} \\ \widehat{T}_{\overline{x}} \end{Bmatrix} \tag{6.258}$$

$$\begin{Bmatrix} N_\xi \\ M_\xi \\ M_{\xi\eta} \end{Bmatrix}_k = [\widetilde{\mu}_k]^{-1}\,([R_\eta]\,[R_k] - [\widetilde{\nu}_k]\,[F]^{-1}\,[L]\,)[\overline{W}] \begin{Bmatrix} \widehat{N}_{\overline{x}} \\ \widehat{M}_{\overline{y}} \\ \widehat{M}_{\overline{z}} \\ \widehat{T}_{\overline{x}} \end{Bmatrix}, \tag{6.259}$$

where $[\widetilde{\mu}_k]$, $[R_\eta]$, $[R_k]$, $[\widetilde{\nu}_k]$, $[F]$, and $[L]$ are defined in Table 6.10.

[11] Ibid.

6.6.3 Centroid

The centroid is located such that the beam's axis remains straight when an axial force $\widehat{N}$ is applied at the centroid. Although this axis remains straight, the beam may twist about the axis of twist, which does not necessarily coincide with the axis passing through the centroid.

From Eqs. (6.251) and (6.247), the curvatures of the axis, passing through the origin of the bar coordinate system, are

$$\begin{Bmatrix} \frac{1}{\rho_{\bar{y}}} \\ \frac{1}{\rho_{\bar{z}}} \end{Bmatrix} = \begin{bmatrix} \overline{W}_{12} & \overline{W}_{22} & \overline{W}_{23} \\ \overline{W}_{13} & \overline{W}_{23} & \overline{W}_{33} \end{bmatrix} \begin{Bmatrix} 1 \\ z_{\mathrm{c}} \\ y_{\mathrm{c}} \end{Bmatrix} \widehat{N}_{\bar{x}}. \tag{6.260}$$

Since $\widehat{N}_{\bar{x}}$ is applied at the centroid, the curvatures of the axis passing through the centroid are zero ($1/\rho_y = 1/\rho_z = 0$). Furthermore, the curvatures of the axis passing through the centroid are the same as the curvatures of the axis passing through the origin of the bar coordinate system. Thus we have

$$\frac{1}{\rho_y} = \frac{1}{\rho_z} = \frac{1}{\rho_{\bar{y}}} = \frac{1}{\rho_{\bar{z}}} = 0. \tag{6.261}$$

Equations (6.260) and (6.261) yield the coordinates z_{c}, y_{c} of the centroid with respect to the origin of the bar coordinate system as follows:

$$\begin{Bmatrix} z_{\mathrm{c}} \\ y_{\mathrm{c}} \end{Bmatrix} = -\begin{bmatrix} \overline{W}_{22} & \overline{W}_{23} \\ \overline{W}_{23} & \overline{W}_{33} \end{bmatrix}^{-1} \begin{bmatrix} \overline{W}_{12} \\ \overline{W}_{13} \end{bmatrix}. \tag{6.262}$$

6.6.4 Restrained Warping

When restrained warping is taken into account and the layup of each wall is balanced, the force–strain relationships may be approximated by[12]

$$\begin{Bmatrix} \widehat{N}_x \\ \widehat{M}_y \\ \widehat{M}_z \\ \widehat{T}_{\mathrm{sv}} \\ \widehat{T}_{\omega} \end{Bmatrix} = \begin{bmatrix} P_{11} & P_{12} & P_{13} & P_{14} & 0 \\ P_{12} & P_{22} & P_{23} & P_{24} & 0 \\ P_{13} & P_{23} & P_{33} & P_{34} & 0 \\ P_{14} & P_{24} & P_{34} & P_{44} & 0 \\ 0 & 0 & 0 & 0 & \widehat{EI}_{\omega} \end{bmatrix} \begin{Bmatrix} \epsilon_x^{\mathrm{o}} \\ \frac{1}{\rho_y} \\ \frac{1}{\rho_z} \\ \vartheta \\ -\dfrac{d^2\vartheta}{dx^2} \end{Bmatrix}, \tag{6.263}$$

where $\widehat{EI}_{\omega}$ is to be calculated as for orthotropic beams. The effects of restrained warping on the displacements and stresses of beams with unbalanced layup are discussed by Bould and Tzeng.[13]

[12] A. Pluzsik and L. P. Kollár, Effect of Shear Deformation and Restrained Warping on the Displacements of Composite Beams, *Journal of Reinforced Plastics and Composites*, Vol. 21, 2002 (in press).

[13] N. R. Bould and L. Tzeng, A Vlasov Theory for Fiber-Reinforced Beams with Thin-Walled Cross-Sections. *International Journal of Solids and Structures*, Vol. 20, 277–297, 1984.

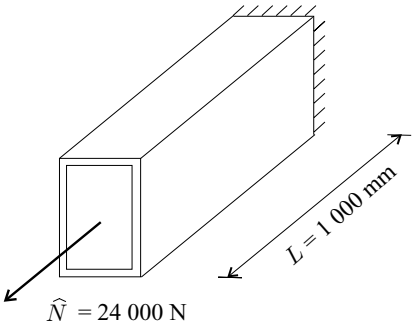

Figure 6.65: The box beam in Example 6.5.

6.5 Example. *An $L = 1$-m-long box-beam, with the cross section shown in Fig. 6.65, is made of graphite epoxy unidirectional plies. The material properties are given in Table 3.6 (page 81). The layup is $[0_{10}/45_{10}]$, with the 0-degree ply on the outside of the wall. The beam, built-in at one end and free at the other end, is subjected to an axial load of 24 000 N. By neglecting the effects of axial restraint, find the position of the centroid and calculate the maximum axial displacement and the maximum twist.*

Solution. The analysis follows the steps in Table 6.10 (page 268). From Table 6.10 we have

$$[R_k] = \begin{bmatrix} 1 & \overline{z}_k & \overline{y}_k & 0 \\ 0 & \cos\alpha_k & -\sin\alpha_k & 0 \\ 0 & \sin\alpha_k & \cos\alpha_k & 0 \\ 0 & 0 & 0 & 1 \end{bmatrix}, \tag{6.264}$$

where $\overline{y}_k$ and $\overline{z}_k$ are the coordinates of the midpoints of the wall segments, and α_k is the angle between η and the y coordinates at which η is tangent to the wall segment (Fig. 6.60). The values of these parameters for each flange and web are shown in Figure 6.66. With these values $[R_k]$ are

$$[R_1] = \begin{bmatrix} 1 & -0.035 & 0 & 0 \\ 0 & 1 & 0 & 0 \\ 0 & 0 & 1 & 0 \\ 0 & 0 & 0 & 1 \end{bmatrix} \qquad [R_2] = \begin{bmatrix} 1 & 0 & 0.025 & 0 \\ 0 & 0 & -1 & 0 \\ 0 & 1 & 0 & 0 \\ 0 & 0 & 0 & 1 \end{bmatrix}$$

$$[R_3] = \begin{bmatrix} 1 & 0.035 & 0 & 0 \\ 0 & -1 & 0 & 0 \\ 0 & 0 & -1 & 0 \\ 0 & 0 & 0 & 1 \end{bmatrix} \qquad [R_4] = \begin{bmatrix} 1 & 0 & -0.025 & 0 \\ 0 & 0 & 1 & 0 \\ 0 & -1 & 0 & 0 \\ 0 & 0 & 0 & 1 \end{bmatrix}.$$

The $[\widetilde{A}]$ matrix for each web and each flange is

$$\begin{bmatrix} \widetilde{A}_{11} & \widetilde{A}_{12} & \widetilde{A}_{13} \\ \widetilde{A}_{12} & \widetilde{A}_{22} & \widetilde{A}_{23} \\ \widetilde{A}_{13} & \widetilde{A}_{23} & \widetilde{A}_{33} \end{bmatrix}_k = \begin{bmatrix} \alpha_{11} & \beta_{11} & \beta_{16} \\ \beta_{11} & \delta_{11} & \delta_{16} \\ \beta_{16} & \delta_{16} & \delta_{66} \end{bmatrix}_k^{-1}. \tag{6.265}$$

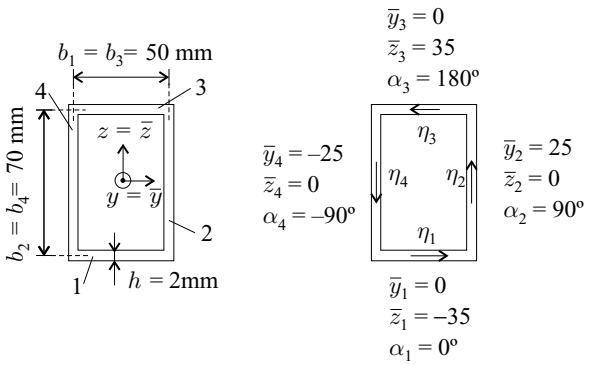

Figure 6.66: Parameters of the walls of the beam in Example 6.5.

With the elements of the compliance matrix in Eq. (3.56), $\widetilde{A}_{11}$ for the flanges ($k = 1, 3$) and for the webs ($k = 2, 4$) are

$$(\widetilde{A}_{11})_1 = (\widetilde{A}_{11})_2 = (\widetilde{A}_{11})_3 = (\widetilde{A}_{11})_4 = 1.615 \times 10^8. \tag{6.266}$$

The distances between the midplanes of the corresponding wall segments are $b_1 = b_3 = 0.050$ m, $b_2 = b_4 = 0.070$ m (Fig. 6.66). The elements of $[\omega_k]$ are

$$[\omega_1] = [\omega_3] = \begin{bmatrix} 0.2688 & 341.4 & 0 & 110.6 \\ 341.4 & 806\,350 & 0 & 214\,130 \\ 0 & 0 & 594 & 0 \\ 110.6 & 214\,130 & 0 & 974\,290 \end{bmatrix} 10^{-6}$$

$$[\omega_2] = [\omega_4] = \begin{bmatrix} 0.1920 & 243.8 & 0 & 78.98 \\ 243.8 & 575\,970 & 0 & 152\,950 \\ 0 & 0 & 216.62 & 0 \\ 78.98 & 152\,950 & 0 & 695\,920 \end{bmatrix} \times 10^{-6}.$$

The $[I]$, $[L]$, and $[F]$ matrices are

$$\begin{aligned} [I] &= \begin{bmatrix} -107.82 & 0 & 0 & 0.080\,61 \\ -24.10 & 0 & 0 & 0.187\,36 \end{bmatrix} \times 10^{-3} \\ [L] &= \begin{bmatrix} 0.107\,8 & 0 & 0 & 0.006\,919 \\ 24.10 & 0 & 0 & -0.187\,36 \end{bmatrix} \times 10^{3} \\ [F] &= \begin{bmatrix} 0.013\,39 & -6.474 \\ -6.474 & 22\,150 \end{bmatrix} \times 10^{-6}. \end{aligned} \tag{6.267}$$

The stiffness matrix of the beam is

$$\begin{aligned} [\overline{P}] &= ([R_1]^T[\omega_1]^{-1}[R_1] + [R_2]^T[\omega_2]^{-1}[R_2] + [R_3]^T[\omega_3]^{-1}[R_3] + [L]^T[F]^{-1}[L]) \\ &= \begin{bmatrix} 39.93 & 0 & 0 & 0.067\,53 \\ 0 & 0.029\,49 & 0 & 0 \\ 0 & 0 & 0.017\,98 & 0 \\ 0.067\,53 & 0 & 0 & 0.004\,105 \end{bmatrix} \times 10^6, \end{aligned} \tag{6.268}$$

where $\overline{P}_{11}$ is in N; $\overline{P}_{22}$, $\overline{P}_{33}$, and $\overline{P}_{44}$ are in $\mathrm{N}\cdot\mathrm{m}^2$; and $\overline{P}_{14}$ is in $\mathrm{N}\cdot\mathrm{m}$. The compliance matrix is

$$[\overline{W}] = [\overline{P}]^{-1} = \begin{bmatrix} 0.025\,76 & 0 & 0 & -0.423\,7 \\ 0 & 33.91 & 0 & 0 \\ 0 & 0 & 55.63 & 0 \\ -0.423\,7 & 0 & 0 & 250.56 \end{bmatrix} \times 10^{-6}, \tag{6.269}$$

where $\overline{W}_{11}$ is in $\frac{1}{\mathrm{N}}$; $\overline{W}_{22}$, $\overline{W}_{33}$, and $\overline{W}_{44}$ are in $\frac{1}{\mathrm{N}\cdot\mathrm{m}^2}$; $\overline{W}_{14}$ is in $\frac{1}{\mathrm{N}\cdot\mathrm{m}}$.

The location of the centroid is given by Eq. (6.262). With the preceding elements of the compliance matrix, we have

$$\begin{Bmatrix} z_\mathrm{c} \\ y_\mathrm{c} \end{Bmatrix} = -\begin{bmatrix} \overline{W}_{22} & \overline{W}_{23} \\ \overline{W}_{23} & \overline{W}_{33} \end{bmatrix}^{-1} \begin{bmatrix} \overline{W}_{12} \\ \overline{W}_{13} \end{bmatrix} = \begin{Bmatrix} 0 \\ 0 \end{Bmatrix}. \tag{6.270}$$

The forces acting at the centroid are

$$\begin{Bmatrix} \widehat{N} \\ \widehat{M}_y \\ \widehat{M}_z \\ \widehat{T} \end{Bmatrix} = \begin{Bmatrix} 24\,000 \\ 0 \\ 0 \\ 0 \end{Bmatrix}. \tag{6.271}$$

The strains, which are uniform along the cantilever, are (Eq. 6.249)

$$\begin{Bmatrix} \epsilon_x^\mathrm{o} \\ \frac{1}{\rho_y} \\ \frac{1}{\rho_z} \\ \vartheta \end{Bmatrix} = 10^{-7} \times \begin{bmatrix} 0.2576 & 0 & 0 & -0.0042 \\ 0 & 0.0004 & 0 & 0 \\ 0 & 0 & 0.0006 & 0 \\ -0.0042 & 0 & 0 & 0.0025 \end{bmatrix} \begin{Bmatrix} 24\,000 \\ 0 \\ 0 \\ 0 \end{Bmatrix}$$

$$= \begin{Bmatrix} 0.6182 \times 10^{-3} \\ 0 \\ 0 \\ -0.010\,17 \end{Bmatrix}. \tag{6.272}$$

The unit of ϑ is $1/\mathrm{m}$. The axial displacement and the twist of the free end are

$$\begin{aligned} u &= \epsilon_x^\mathrm{o} \times L = 0.6182 \times 10^{-3} \times 1 = 0.000\,618\ \mathrm{m} = 0.618\ \mathrm{mm} \\ \psi &= \vartheta \times L = -0.010\,17 \times 1 = -0.010\,17\ \mathrm{rad} = -0.58^\circ. \end{aligned} \tag{6.273}$$

In comparison, u and ψ calculated by the finite element method are

$$u = 0.616\ \mathrm{mm} \qquad \psi = -0.57^\circ. \tag{6.274}$$

6.7 Transversely Loaded Thin-Walled Beams

We consider a transversely loaded beam (Fig. 6.67). The applied transverse load, with components p_y and p_z, produces bending moments $\widehat{M}_y$, $\widehat{M}_z$, a torque $\widehat{T}$, and transverse shear forces $\widehat{V}_y$, $\widehat{V}_z$. The bending moments $\widehat{M}_y$, $\widehat{M}_z$ give rise to an axial

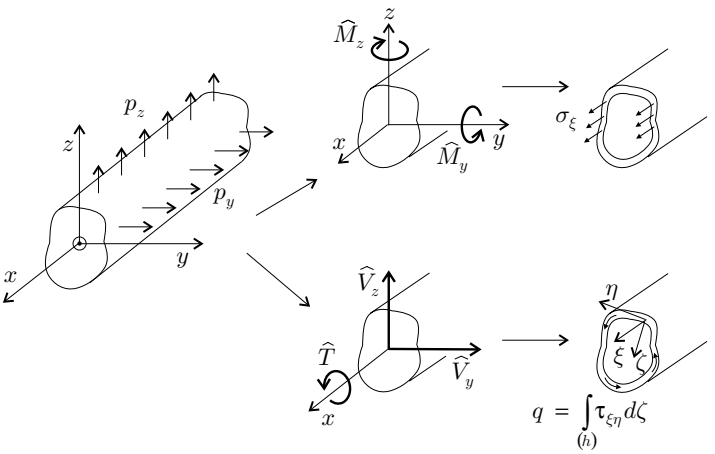

Figure 6.67: Internal forces and stresses acting on the cross section of a transversely loaded thin-walled beam. The ξ–η–ζ coordinate system is shown in Figure 6.60.

stress σ_ξ, and the internal forces $\widehat{V}_y$, $\widehat{V}_z$, and $\widehat{T}$ give rise to shear stress $\tau_{\xi\eta}$ in the wall. It is customary to represent the shear stress by the shear flow q defined as (Eq. 6.189),

$$q \equiv \int_{(h)} \tau_{\xi\eta} d\zeta = N_{\xi\eta}, \tag{6.275}$$

where h is the thickness of the wall.

The load p_z applied along a line A–A may be replaced by an equivalent load system consisting of a load p_z applied along line B–B and a torque load $t = -p_z d$, where d is the horizontal distance between points A and B (Fig. 6.68). The load p_z results in a shear flow q^V while the torque load introduces a shear flow q^T. The total shear flow is

$$q = q^T + q^V. \tag{6.276}$$

Both shear flows q^T and q^V as well as the axial stress σ_ξ cause twisting of the beam, represented by the rate of twist ϑ as follows:

$$\vartheta \Longrightarrow \begin{matrix}\text{due to}\\ \sigma_\xi\end{matrix} + \begin{matrix}\text{due to}\\ q^T\end{matrix} + \begin{matrix}\text{due to}\\ q^V\end{matrix} \qquad \begin{matrix}p_z \text{ along an arbitrary}\\ \text{line } A\text{–}A.\end{matrix}$$

There is a special location of the line B–B referred to as the shear center.[14] When the load is applied at this location (i.e., at the shear center), the shear flow q^V does not cause twisting of the beam, and the rate of twist depends only on σ_ξ and q^T:

$$\vartheta \Longrightarrow \begin{matrix}\text{due to}\\ \sigma_\xi\end{matrix} + \begin{matrix}\text{due to}\\ q^T\end{matrix} \qquad \begin{matrix}p_z \text{ at the}\\ \text{shear center.}\end{matrix}$$

[14] E. H. Mansfield and A. J. Sobey, The Fiber Composite Helicopter Blade – Part 1: Stiffness Properties – Part 2: Prospects for Aeroelastic Tailoring. *Aeronautical Quarterly*, Vol. 30, 413–449, 1979.

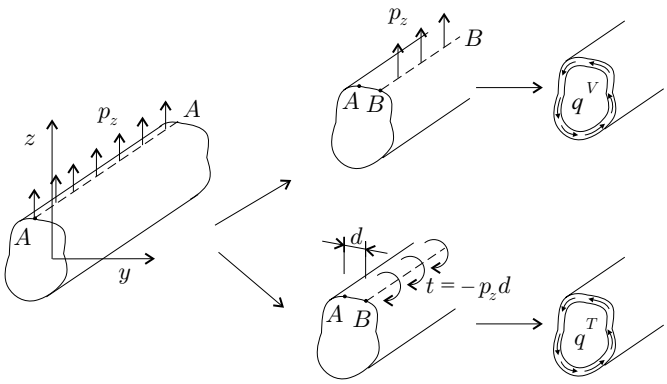

Figure 6.68: Shear flow in a transversely loaded thin-walled beam.

For a beam with arbitrary layup the axial stress σ_ξ introduces a twist even when the load is applied at the shear center. However, σ_ξ does not introduce a twist in orthotropic beams. Therefore, when the beam is orthotropic *and* the load acts at the shear center, the rate of twist depends only on the shear flow due to the torque:

$$\vartheta \Longrightarrow \text{due to } q^T \qquad \begin{matrix} \text{orthotropic} \\ p_z \text{ at the shear center.} \end{matrix}$$

In summary, when the transverse load acts at the shear center, an orthotropic beam does not twist, whereas a beam with arbitrary layup does twist.

The transverse load p_z causes transverse shear forces $\widehat{V}_y$, $\widehat{V}_z$, bending moments $\widehat{M}_y$, $\widehat{M}_z$, and torque $\widehat{T}$ (Fig. 6.67). The displacements caused by the shear forces $\widehat{V}_y$, $\widehat{V}_z$ are neglected. The displacements due to the bending moments $\widehat{M}_y$ and $\widehat{M}_z$ and the torque $\widehat{T}$ are determined by the analyses presented in Sections 6.3–6.6.

The normal stresses are determined by the analyses presented in Sections 6.3.4, 6.4, and 6.6.2.

The shear stresses in the wall induced by the bending moments $\widehat{M}_y$ and $\widehat{M}_z$ and the torque $\widehat{T}$ are determined by the analyses presented in Sections 6.5 and 6.6. The shear stresses in the wall due to the shear forces $\widehat{V}_y$, $\widehat{V}_z$ are discussed next. The total stresses are obtained by superimposing the stresses caused by bending, torsion, and shear.

6.7.1 Beams with Orthotropic Layup or with Symmetrical Cross Section

We consider beams that have either orthotropic layup (page 207) or have symmetrical cross section with the loads applied in the symmetry plane (Fig. 6.4).

In the following we calculate the shear flow in open- and closed-section beams when the shear forces $\widehat{V}_z$ and $\widehat{V}_y$ act at the shear center (Fig. 6.69).

Open-section beams. There is no load applied in the axial direction. Equilibrium of an element in the axial $\xi \equiv x$ direction gives (Fig. 6.70)

$$\frac{\partial q^{\text{op}}}{\partial \eta} + \frac{\partial N_\xi}{\partial \xi} = 0, \tag{6.277}$$

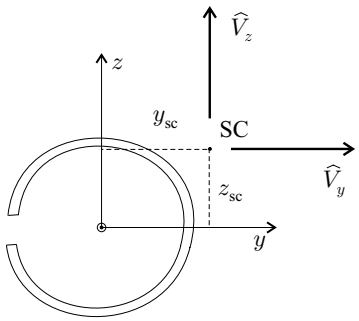

Figure 6.69: Beam subjected to shear forces at the shear center.

where q^{op} is the shear flow and N_ξ is the axial force (per unit length) at an arbitrarily chosen reference surface. Integration of this expression yields

$$q^{\text{op}}(s_1) = -\int_0^{s_1} \frac{\partial N_\xi}{\partial \xi} d\eta, \tag{6.278}$$

where η is the coordinate along the wall and s_1 is the distance from the free edge to the point of interest.

For an orthotropic wall segment (unsymmetrical layup) N_ξ is obtained by combining Eqs. (6.118), (6.111), and (6.112) as follows:

$$\begin{aligned} N_\xi = {} & \frac{\widehat{EI}_{zz}\widehat{M}_y - \widehat{EI}_{yz}\widehat{M}_z}{\widehat{EI}_{yy}\widehat{EI}_{zz} - (\widehat{EI}_{yz})^2}\left(z\frac{\delta_{11}}{D} - \cos\alpha\frac{\beta_{11}}{D}\right) \\ & + \frac{-\widehat{EI}_{yz}\widehat{M}_y + \widehat{EI}_{yy}\widehat{M}_z}{\widehat{EI}_{yy}\widehat{EI}_{zz} - (\widehat{EI}_{yz})^2}\left(y\frac{\delta_{11}}{D} + \sin\alpha\frac{\beta_{11}}{D}\right) + \frac{\widehat{N}}{\widehat{EA}}\frac{\delta_{11}}{D}. \end{aligned} \tag{6.279}$$

The relationship between the shear forces and the bending moments are (Eq. 6.3)

$$\widehat{V}_z = \frac{\partial \widehat{M}_y}{\partial x} \qquad \widehat{V}_y = \frac{\partial \widehat{M}_z}{\partial x}. \tag{6.280}$$

By combining Eqs. (6.278)–(6.280), and by noting that for a transversely loaded beam the normal force $\widehat{N}$ is zero, we obtain the following expression for the shear flow:

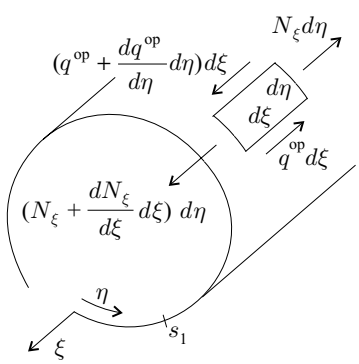

Figure 6.70: Forces on an element of a transversely loaded, thin-walled open-section beam.

orthotropic and unsymmetrical layup, arbitrary cross section:

$$q^{\text{op}}(s_1) = -\frac{\widehat{EI}_{zz}\widehat{V}_z - \widehat{EI}_{yz}\widehat{V}_y}{\widehat{EI}_{yy}\widehat{EI}_{zz} - (\widehat{EI}_{yz})^2}\int_0^{s_1}\left(z\frac{\delta_{11}}{D} - \cos\alpha\frac{\beta_{11}}{D}\right)d\eta$$
$$-\frac{-\widehat{EI}_{yz}\widehat{V}_z + \widehat{EI}_{yy}\widehat{V}_y}{\widehat{EI}_{yy}\widehat{EI}_{zz} - (\widehat{EI}_{yz})^2}\int_0^{s_1}\left(y\frac{\delta_{11}}{D} + \sin\alpha\frac{\beta_{11}}{D}\right)d\eta. \tag{6.281}$$

We emphasize that $\widehat{V}_z$ and $\widehat{V}_y$ act at the shear center and $\widehat{EI}_{yy}$, $\widehat{EI}_{yz}$, $\widehat{EI}_{zz}$, are the bending stiffnesses in the y–z coordinate system attached to the centroid of the cross section.

When the layup of each wall segment is orthotropic and symmetrical, the expression for the shear flow is obtained from Eqs. (6.278), (6.280), (6.111), (6.112), and (6.125)

orthotropic and symmetrical layup, arbitrary cross section:

$$q^{\text{op}}(s_1) = -\frac{\widehat{EI}_{zz}\widehat{V}_z - \widehat{EI}_{yz}\widehat{V}_y}{\widehat{EI}_{yy}\widehat{EI}_{zz} - (\widehat{EI}_{yz})^2}\int_0^{s_1}\left(z\frac{1}{a_{11}}\right)d\eta$$
$$-\frac{-\widehat{EI}_{yz}\widehat{V}_z + \widehat{EI}_{yy}\widehat{V}_y}{\widehat{EI}_{yy}\widehat{EI}_{zz} - (\widehat{EI}_{yz})^2}\int_0^{s_1}\left(y\frac{1}{a_{11}}\right)d\eta. \tag{6.282}$$

When the beam's cross section is symmetrical, the shear center is in the x–z symmetry plane. When the transverse load acts in this symmetry plane, the force is given by Eq. (6.131), (nonorthotropic, unsymmetrical layup). This equation, in combination with Eqs. (6.278), (6.280), and (6.111), yields

arbitrary layup, symmetrical cross section:

$$q^{\text{op}}(s_1) = -\frac{\widehat{V}_z}{\widehat{EI}_{yy}}\int_0^{s_1}\left(z\frac{\overline{\delta}_{11}}{\overline{D}} - \cos\alpha\frac{\overline{\beta}_{11}}{\overline{D}}\right)d\eta. \tag{6.283}$$

For an isotropic beam $1/a_{11} = Eh$ (Eq. 3.43), and the expression for the shear flow (Eq. 6.282) becomes

isotropic beam:

$$q^{\text{op}}(s_1) = -\frac{I_{zz}\widehat{V}_z - I_{yz}\widehat{V}_y}{I_{yy}I_{zz} - (I_{yz})^2}\int_0^{s_1}(zh)\,d\eta - \frac{-I_{yz}\widehat{V}_z + I_{yy}\widehat{V}_y}{I_{yy}I_{zz} - (I_{yz})^2}\int_0^{s_1}(yh)\,d\eta. \tag{6.284}$$

Illustration of the shear flow in an open-section beam is given in Example 6.2 (page 239).

Closed-section beams – single cell. In a single-cell, closed-section beam, the shear flow may be expressed in two parts. The first part is the shear flow (denoted by q^{op}) that would exist if the beam were cut longitudinally and the beam were open. The second is a constant shear flow q^{c} induced by the forces acting along

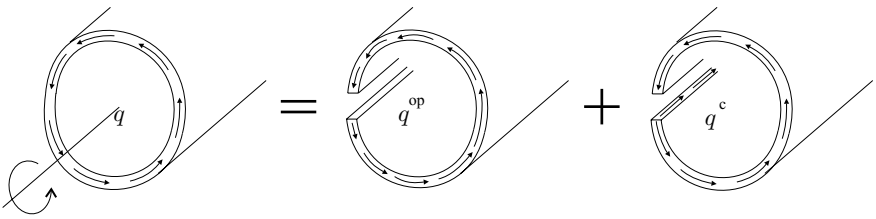

Figure 6.71: Superposition of the open cell and constant shear flows in a transversely loaded, single-cell closed-section beam.

the "cut" edges (Fig. 6.71) (q^{c} depends on the location of the cut). Thus, we write the shear flow in the closed single-cell beam as

$$q = q^{\mathrm{op}} + q^{\mathrm{c}}. \tag{6.285}$$

The shear flow q^{op} is calculated by Eqs. (6.278)–(6.283). The constant shear flow q^{c} is determined as follows. When the shear forces $\widehat{V}_y$ and $\widehat{V}_z$ act at the shear center (which is the case here), the beam does not twist. Hence, from Eq. (6.188) we have

$$\vartheta = \frac{1}{2A}\oint \gamma^{\mathrm{o}}_{\xi\eta} d\eta = 0. \tag{6.286}$$

The shear strain $\gamma^{\mathrm{o}}_{\xi\eta}$ in each wall segment is calculated at the "torque neutral" surface. From Eq. (6.195) we have

$$\gamma^{\mathrm{o}}_{\xi\eta} = \alpha^{\nu}_{66} q. \tag{6.287}$$

From Eqs. (6.285)–(6.287) we obtain

$$\vartheta = \frac{1}{2A}\oint \alpha^{\nu}_{66} q^{\mathrm{op}} d\eta + \frac{1}{2A} q^{\mathrm{c}} \oint \alpha^{\nu}_{66} d\eta = 0. \tag{6.288}$$

From this equation we have

$$q^{\mathrm{c}} = -\frac{\oint \alpha^{\nu}_{66} q^{\mathrm{op}} d\eta}{\oint \alpha^{\nu}_{66} d\eta}. \tag{6.289}$$

Closed-section beams – multicell. To calculate the shear flow in a multicell beam (Fig. 6.72), we "cut" longitudinally each cell, thereby producing an open-section beam. The shear flow q^{op} in this open-section beam is calculated by the analysis given by Eqs. (6.278)–(6.283).

In each cell there is a constant shear flow q^{c}_l induced by the forces acting along the edges of the cut. In a beam with L cells there are L constant shear flows. The shear flow is the sum of the open-section and the constant shear flows. For a wall that belongs to one cell only, q is the sum of the open-cell shear flow and the constant shear flow in the appropriate cell ($q = q^{\mathrm{op}} + q^{\mathrm{c}}_l$). For a wall adjoining two cells, the shear flow is the sum of the constant shear flows of the adjacent cells and the open-section beam shear flow, as illustrated in Fig. 6.72.

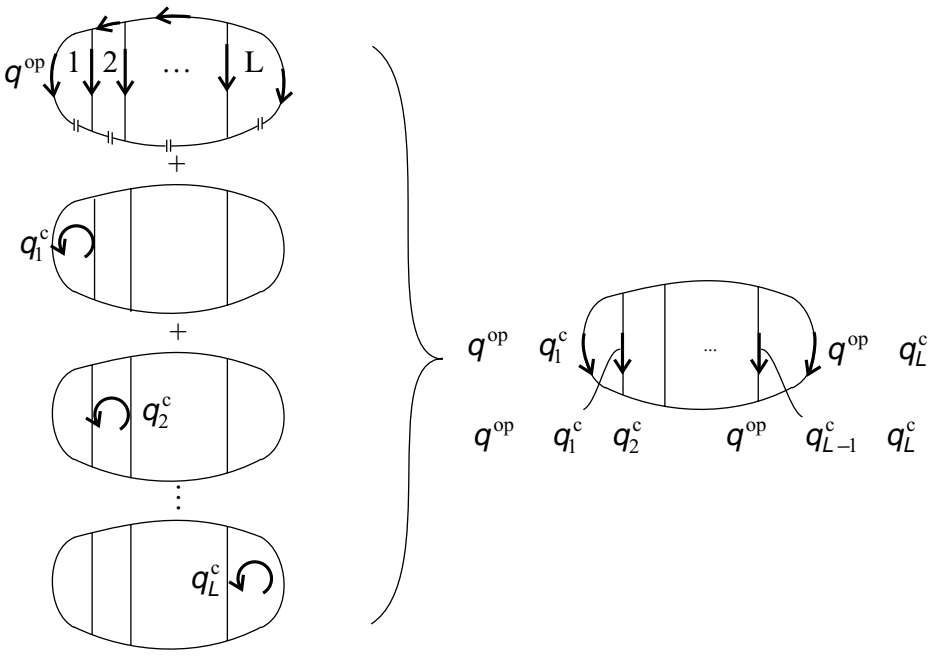

Figure 6.72: Superposition of the open cell and the constant shear flows in a transversely loaded, multicell, closed-section beam.

When the shear forces $\widehat{V}_y$ and $\widehat{V}_z$ act at the shear center (which is the case here), the beam does not twist ($\vartheta = 0$). Hence, for each cell we write (Eq. 6.188)

$$\vartheta = \frac{1}{2A_l} \oint_{\text{cell } l} \gamma^{\text{o}}_{\xi\eta} d\eta = 0 \qquad l = 1, 2, \ldots, L. \tag{6.290}$$

The shear strain $\gamma^{\text{o}}_{\xi\eta}$ at the "torque neutral" surface in each wall segment is (Eq. 6.195)

$$\gamma^{\text{o}}_{\xi\eta} = \alpha^{\nu}_{66} q, \tag{6.291}$$

where q is the shear flow in the wall segment (Eq. 6.285).

By combining Eqs. (6.290) and (6.291), we obtain

$$\frac{1}{2A_l} \oint_{\text{cell } l} \alpha^{\nu}_{66} q d\eta = 0 \qquad l = 1, 2, \ldots, L. \tag{6.292}$$

Equation (6.292) represents L equations, which can be solved for the L unknowns: $q_1^{\text{c}}, q_2^{\text{c}}, \ldots, q_L^{\text{c}}$.

The stresses in the walls are calculated the same way as for a single-cell beam.

6.7.2 Beams with Arbitrary Layup

In this section we determine the shear flows (caused by the shear forces $\widehat{V}_z$ and $\widehat{V}_y$ acting at the shear center) in beams consisting of wall segments with arbitrary layup. No load is applied in the axial direction. Equilibrium in the ξ direction gives

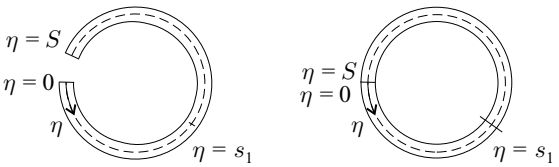

Figure 6.73: Coordinate η along the circumference of an open- and a closed-section beam.

(Eq. 6.277, see Fig. 6.70)

$$\frac{\partial q}{\partial \eta} + \frac{\partial N_\xi}{\partial \xi} = 0. \tag{6.293}$$

To determine the shear flow q, the derivative of the axial force (per unit length) $\partial N_\xi / \partial \xi$ must be known.

Open-section beams. In an open-section beam the shear flow is (Eq. 6.278)

$$q^{\text{op}}(s_1) = -\int_0^{s_1} \frac{\partial N_\xi}{\partial \xi} d\eta, \tag{6.294}$$

where η is the coordinate along the circumference (Fig. 6.73, left). The term $\partial N_\xi / \partial \xi$ is evaluated as follows. By differentiating both sides of Eq. (6.256) with respect to ξ, we have

$$\begin{Bmatrix} \frac{\partial N_\xi}{\partial \xi} \\ \frac{\partial M_\xi}{\partial \xi} \\ \frac{\partial M_{\xi\eta}}{\partial \xi} \end{Bmatrix}_k = [\widetilde{\mu}_k]^{-1} [R_\eta] [R_k] [\overline{W}] \begin{Bmatrix} \frac{\partial \widehat{N}_{\overline{x}}}{\partial \xi} \\ \frac{\partial \widehat{M}_{\overline{y}}}{\partial \xi} \\ \frac{\partial \widehat{M}_{\overline{z}}}{\partial \xi} \\ \frac{\partial \widehat{T}_{\overline{x}}}{\partial \xi} \end{Bmatrix}. \tag{6.295}$$

There is no applied load in the axial direction ($\widehat{N}_{\overline{x}} = 0$), and $\partial \widehat{N}_{\overline{x}} / \partial \xi$ is zero. In addition, (see Eq. 6.247) we have

$$\widehat{M}_{\overline{y}} = \widehat{M}_y \qquad \widehat{M}_{\overline{z}} = \widehat{M}_z. \tag{6.296}$$

The shear forces are (Eq. 6.3, $\xi \equiv x$)

$$\widehat{V}_z = \frac{\partial \widehat{M}_{\overline{y}}}{\partial \xi} \qquad \widehat{V}_y = \frac{\partial \widehat{M}_{\overline{z}}}{\partial \xi}. \tag{6.297}$$

The transverse load acts at the shear center. Hence, the torque load t is zero, and we have (see Eq. 6.3)

$$\frac{\partial \widehat{T}}{\partial \xi} = -t = 0. \tag{6.298}$$

Substitution of Eqs. (6.297), (6.298) and $\partial \widehat{N}_{\overline{x}} / \partial \xi = 0$ into Eq. (6.295) gives

$$\begin{Bmatrix} \frac{\partial N_\xi}{\partial \xi} \\ \frac{\partial M_\xi}{\partial \xi} \\ \frac{\partial M_{\xi\eta}}{\partial \xi} \end{Bmatrix}_k = [\widetilde{\mu}_k]^{-1} [R_\eta] [R_k] [\overline{W}] \begin{Bmatrix} 0 \\ \widehat{V}_z \\ \widehat{V}_y \\ 0 \end{Bmatrix}. \tag{6.299}$$

We are interested only in $\partial N_\xi/\partial\xi$ given by this equation since this is used in Eq. (6.294) to determine the shear flow.

Closed-section beams. In a closed-section beam the shear flow is obtained by integration of Eq. (6.293),

$$q = \underbrace{-\int_0^{s_1} \frac{\partial N_\xi}{\partial \xi} d\eta}_{q^{\mathrm{op}}} + q^{\mathrm{c}}, \tag{6.300}$$

where q^{op} is defined as

$$q^{\mathrm{op}} = -\int_0^{s_1} \frac{\partial N_\xi}{\partial \xi} d\eta, \tag{6.301}$$

η is the coordinate along the circumference (Fig. 6.73, right) and q^{c} is a constant shear flow. The term $\partial N_\xi/\partial\xi$ is obtained by differentiating both sides of Eq. (6.259) as follows:

$$\left\{ \begin{array}{c} \frac{\partial N_\xi}{\partial \xi} \\ \frac{\partial M_\xi}{\partial \xi} \\ \frac{\partial M_{\xi\eta}}{\partial \xi} \end{array} \right\}_k = [\widetilde{\mu}_k]^{-1} \left([R_\eta][R_k] - [\widetilde{\nu}_k][F]^{-1}[L] \right) [\overline{W}] \left\{ \begin{array}{c} \frac{\partial \widehat{N}_{\overline{x}}}{\partial \xi} \\ \frac{\partial \widehat{M}_{\overline{y}}}{\partial \xi} \\ \frac{\partial \widehat{M}_{\overline{z}}}{\partial \xi} \\ \frac{\partial \widehat{T}_{\overline{x}}}{\partial \xi} \end{array} \right\}. \tag{6.302}$$

Since there is no applied load in the axial direction, $\partial \widehat{N}_{\overline{x}}/\partial\xi$ is zero. Furthermore, the transverse load acts at the shear center. Hence, the torque load t is zero and, consequently, $\partial \widehat{T}/\partial\xi$ is zero (see Eq. 6.3). When Eq. (6.297) is used, the preceding equation (Eq. 6.302) results in

$$\left\{ \begin{array}{c} \frac{\partial N_\xi}{\partial \xi} \\ \frac{\partial M_\xi}{\partial \xi} \\ \frac{\partial M_{\xi\eta}}{\partial \xi} \end{array} \right\}_k = [\widetilde{\mu}_k]^{-1} \left([R_\eta][R_k] - [\widetilde{\nu}_k][F]^{-1}[L] \right) [\overline{W}] \left\{ \begin{array}{c} 0 \\ \widehat{V}_z \\ \widehat{V}_y \\ 0 \end{array} \right\}, \tag{6.303}$$

where $\widehat{V}_y$ and $\widehat{V}_z$ are the shear forces (Fig. 6.2). The term $\partial N_\xi/\partial\xi$ given by this expression is used to calculate q^{op} (Eq. 6.301).

The constant shear flow is denoted by q^{c} . We note that the rate of twist ϑ in the x–y–z coordinate system is the same as the rate of twist $\overline{\vartheta}$ in the $\overline{x}$–$\overline{y}$–$\overline{z}$ coordinate system. Thus, from Eq. (6.187) we have

$$-2A\overline{\vartheta} + \oint \gamma^{\mathrm{o}}_{\xi\eta} d\eta = 0. \tag{6.304}$$

Equation (6.151) gives

$$\oint \kappa_\eta d\eta = 0. \tag{6.305}$$

By introducing Eq. (6.254) into these equations, and by noting that $N_{\xi\eta} = q$, and $N_\eta = 0$, we obtain

$$0 = \begin{Bmatrix} -2A\overline{\vartheta} \\ 0 \end{Bmatrix} + \oint \begin{bmatrix} \alpha_{16} & \beta_{16} & \beta_{66} \\ \beta_{12} & \delta_{12} & \delta_{26} \end{bmatrix} \begin{Bmatrix} N_\xi \\ M_\xi \\ M_{\xi\eta} \end{Bmatrix} d\eta + \oint \begin{bmatrix} \alpha_{66} & \beta_{26} \\ \beta_{26} & \delta_{22} \end{bmatrix} \begin{Bmatrix} q \\ M_\eta \end{Bmatrix} d\eta, \tag{6.306}$$

where $q = q^{\text{op}} + q^{\text{c}}$. The terms N_ξ, M_ξ, and $M_{\xi\eta}$ are evaluated by Eq. (6.259), and q^{op} by Eqs. (6.301) and (6.303). To determine M_η and q^{c}, we observe that these result from the bending moments $\widehat{M}_{\overline{z}}$, $\widehat{M}_{\overline{y}}$ and the shear forces $\widehat{V}_y$, $\widehat{V}_z$. Thus, we write

$$\begin{aligned} M_\eta &= M'_\eta + M''_\eta \\ q &= \underbrace{q^{\text{c}\prime}}_{\substack{\text{due to} \\ \widehat{M}_{\overline{z}},\, \widehat{M}_{\overline{y}}}} + \underbrace{q^{\text{op}} + q^{\text{c}\prime\prime}}_{\substack{\text{due to} \\ \widehat{V}_y,\, \widehat{V}_z}}, \end{aligned} \tag{6.307}$$

where M'_η and $q^{\text{c}\prime}$ are calculated by Eq. (6.258).

The terms $\widehat{V}_y$ and $\widehat{V}_z$ introduce only M''_η, q^{op}, and $q^{\text{c}\prime\prime}$. Thus, when these shear forces are considered, we have $M_\eta = M''_\eta$, $q = q^{\text{op}} + q^{\text{c}} = q^{\text{op}} + q^{\text{c}\prime\prime}$, and $N_\xi = M_\xi = M_{\xi\eta} = 0$. The shear forces act at the shear center and hence the cross section does not twist ($\overline{\vartheta} = 0$). Accordingly, (Eq. 6.306) becomes

$$0 = \oint \begin{Bmatrix} \alpha_{66} \\ \beta_{26} \end{Bmatrix} q^{\text{op}} d\eta + \oint \begin{bmatrix} \alpha_{66} & \beta_{26} \\ \beta_{26} & \delta_{22} \end{bmatrix} d\eta \begin{Bmatrix} q^{\text{c}\prime\prime} \\ M''_\eta \end{Bmatrix}. \tag{6.308}$$

These equations are to be solved for $q^{\text{c}\prime\prime}$ and M''_η as follows:

$$\begin{Bmatrix} q^{\text{c}\prime\prime} \\ M''_\eta \end{Bmatrix} = -\left\{ \oint \begin{bmatrix} \alpha_{66} & \beta_{26} \\ \beta_{26} & \delta_{22} \end{bmatrix} d\eta \right\}^{-1} \oint \begin{Bmatrix} \alpha_{66} \\ \beta_{26} \end{Bmatrix} q^{\text{op}} d\eta. \tag{6.309}$$

6.7.3 Shear Center

By definition, shear forces acting at the shear center do not cause twist. We designate the location of the shear center by the distances z_{sc} and y_{sc} from the centroid (Fig. 6.74). To determine these distances, we apply a force $\widehat{V}_y$ acting at the shear center and calculate the corresponding shear flow q. The torque of the external force about the centroid is equal to the torque produced by the internal shear flow (Fig. 6.75) as follows:

$$-\widehat{V}_y z_{\text{sc}} = \int_{(S)} qp\, d\eta. \tag{6.310}$$

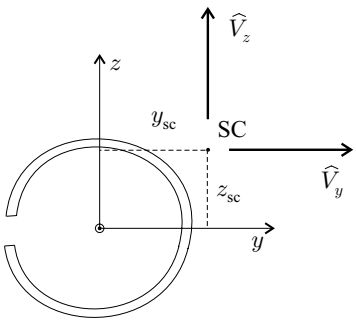

Figure 6.74: Shear center.

Hence, the z coordinate of the shear center is

$$z_{sc} = -\frac{\int_{(S)} qpd\eta}{\widehat{V}_y}, \tag{6.311}$$

where q is the shear flow due to $\widehat{V}_y$.

The distance y_{sc} is determined by applying a force $\widehat{V}_z$ at the shear center (Fig. 6.74). By an argument similar to that leading to the preceding equation, we have

$$y_{sc} = \frac{\int_{(S)} qpd\eta}{\widehat{V}_z}, \tag{6.312}$$

where q is the shear flow due to $\widehat{V}_z$.

For beams with arbitrary layup, the shear flow is determined by the equations given in Section 6.7.2. For orthotropic beams the shear flows are determined by the equations given in Section 6.7.1.

Approximate calculation of the shear center. Approximate expressions for the location of the shear center of open-section orthotropic beams can be obtained as follows. The major contributor to the shear flow is the normal axial stress N_ξ caused by bending. In a thin-walled composite segment N_ξ may be approximated by Eq. (6.243) and in an isotropic beam by Eq. (6.241). By comparing these equations we see that the composite beam's tensile stiffness $1/\alpha_{11}^o$ corresponds to the isotropic beam's tensile stiffness Eh. Thus, the location of the shear center of an open-section orthotropic beam may be approximated by replacing Eh by $1/\alpha_{11}^o$ in the expression[15] for the location of the shear center of the corresponding isotropic beam. The coordinates of shear centers of frequently used cross sections are given in Table A.5.

6.6 Example. *An $L = 0.6$-m-long C-section beam, with the cross section shown in Figure 6.76, is made of graphite epoxy. The material properties are given in Table 3.6 (page 81). The layup is $[\pm 45_2^f/0_{12}/\pm 45_2^f]$. The beam is built-in at both ends. The beam is subjected to a uniformly distributed load ($p = -1\,500$ N/m) acting along*

[15] S. P. Timoshenko and J. Gere, *Theory of Elastic Stability.* 2nd edition. McGraw-Hill, New York, 1961, p. 530.

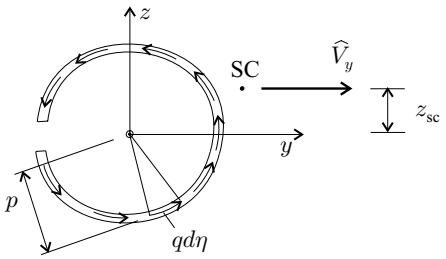

Figure 6.75: The shear force $\widehat{V}_y$ and the corresponding shear flow.

the centerline of the flange (Fig. 6.77). By neglecting the effects of axial restraint, find the position of the shear center and calculate the maximum deflection, the maximum twist, and the ply stresses and strains.

Solution. From Table A.1 the tensile stiffness and the location of the centroid are

$$\begin{aligned} \widehat{EA} &= \frac{2b_{\mathrm{f}}}{(a_{11})_{\mathrm{f}}} + \frac{b_{\mathrm{w}}}{(a_{11})_{\mathrm{w}}} = 30.87 \times 10^6 \text{ N} \\ y_{\mathrm{c}} &= \frac{1}{\widehat{EA}} \left(\frac{2b_{\mathrm{f}}}{(a_{11})_{\mathrm{f}}} \frac{b_{\mathrm{f}}}{2} + \frac{b_{\mathrm{w}}}{(a_{11})_{\mathrm{w}}} d_{\mathrm{f}} \right) = 0.0340 \text{ m}, \end{aligned} \tag{6.313}$$

where a_{11} for both the web and the flange is $(a_{11})_{\mathrm{w}} = (a_{11})_{\mathrm{f}} = 5.18 \times 10^{-9}$ m/N (Table 3.8, page 85). The dimensions $b_{\mathrm{f}} = 0.05$ m, $b_{\mathrm{w}} = 0.06$ m, $d_{\mathrm{f}} = 0.049$ m, and $d = 0.062$ m are shown in Fig.6.76. The bending stiffnesses are (Table A.1)

$$\begin{aligned} \widehat{EI}_{yy} &= \frac{b_{\mathrm{f}}}{(a_{11})_{\mathrm{f}}} \frac{d^2}{2} + \frac{2b_{\mathrm{f}}}{(d_{11})_{\mathrm{f}}} + \frac{b_{\mathrm{w}}^3}{12(a_{11})_{\mathrm{w}}} \\ \widehat{EI}_{zz} &= \frac{b_{\mathrm{w}}}{(a_{11})_{\mathrm{w}}} (d_{\mathrm{f}} - y_{\mathrm{c}})^2 + \frac{b_{\mathrm{w}}}{(d_{11})_{\mathrm{w}}} + \frac{2}{(a_{11})_{\mathrm{f}}} \left(\frac{y_{\mathrm{c}}^3}{3} + \frac{(b_{\mathrm{f}} - y_{\mathrm{c}})^3}{3} \right), \end{aligned} \tag{6.314}$$

where d_{11} for both the web and the flange is $(d_{11})_{\mathrm{w}} = (d_{11})_{\mathrm{f}} = 33.10 \times 10^{-3} \frac{1}{\mathrm{N \cdot m}}$ (Table 3.8, page 85). Equation (6.314) yields

$$\widehat{EI}_{yy} = 22\,015 \text{ N} \cdot \text{m}^2 \qquad \widehat{EI}_{zz} = 8\,188 \text{ N} \cdot \text{m}^2. \tag{6.315}$$

The torsional stiffness and the location of the shear center are given in Table A.5. For symmetrical layup (which is the case here), δ is replaced by d

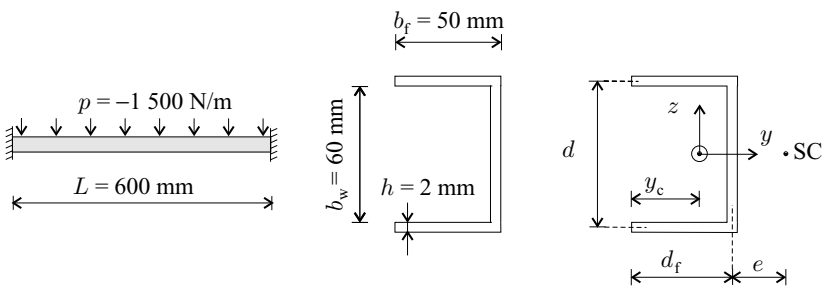

Figure 6.76: The beam in Example 6.6.

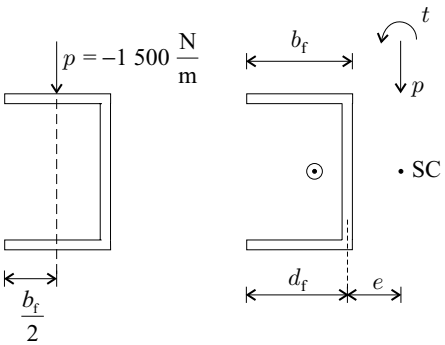

Figure 6.77: Loading on the C-section beam in Example 6.6 (left) and loading with respect to the shear center (right).

and α by a, and we write

$$\widehat{GI}_\mathrm{t} = 4\left(\frac{2b_\mathrm{f}}{(d_{66})_\mathrm{f}} + \frac{b_\mathrm{w}}{(d_{66})_\mathrm{w}}\right) = 13.19\ \mathrm{N}\cdot\mathrm{m}^2 \tag{6.316}$$

$$e = \frac{\frac{3b_\mathrm{f}^2}{(a_{11})_\mathrm{f}}}{\frac{6b_\mathrm{f}}{(a_{11})_\mathrm{f}} + \frac{d}{(a_{11})_\mathrm{w}}} = 0.0207\ \mathrm{m}, \tag{6.317}$$

where for both the web and the flange d_{66} is $(d_{66})_\mathrm{w} = (d_{66})_\mathrm{f} = 48.51 \times 10^{-3}\frac{1}{\mathrm{N}\cdot\mathrm{m}}$ (Table 3.8, page 85).

The loads with respect to the shear center are (Fig. 6.77, $d_\mathrm{f} + e - \frac{b_\mathrm{f}}{2} = 0.0447\,\mathrm{m}$)

$$\begin{aligned} p &= -1\ 500\ \frac{\mathrm{N}}{\mathrm{m}} && \text{(distributed load)} \\ t &= -p \times \left(d_\mathrm{f} + e - \frac{b_\mathrm{f}}{2}\right) = 67.08\ \frac{\mathrm{N}\cdot\mathrm{m}}{\mathrm{m}} && \text{(distributed torque).} \end{aligned} \tag{6.318}$$

The corresponding bending moment $\widehat{M}_y$, shear force $\widehat{V}_z$, and torque $\widehat{T}$ diagrams are given in Figure 6.78. The maximum values are

$$\begin{aligned} \widehat{M}_y^{\max} &= -\frac{pL^2}{12} = 45\ \mathrm{N}\cdot\mathrm{m} \\ \widehat{V}_z^{\max} &= \frac{pL}{2} = -450\ \mathrm{N} \\ \widehat{T}^{\max} &= \frac{tL}{2} = 20.12\ \mathrm{N}\cdot\mathrm{m}. \end{aligned} \tag{6.319}$$

The maximum deflection is (Table 7.3, page 332)

$$\widetilde{w} = \frac{1}{384}\frac{pL^4}{\widehat{EI}_{yy}} = -0.023 \times 10^{-3}\ \mathrm{m} = -0.0230\ \mathrm{mm}. \tag{6.320}$$

The maximum twist is at $x = L/2$ and is

$$\psi = \int_0^{L/2} \vartheta\, dx = \int_0^{L/2} \frac{\widehat{T}}{\widehat{GI}_\mathrm{t}} dx, \tag{6.321}$$

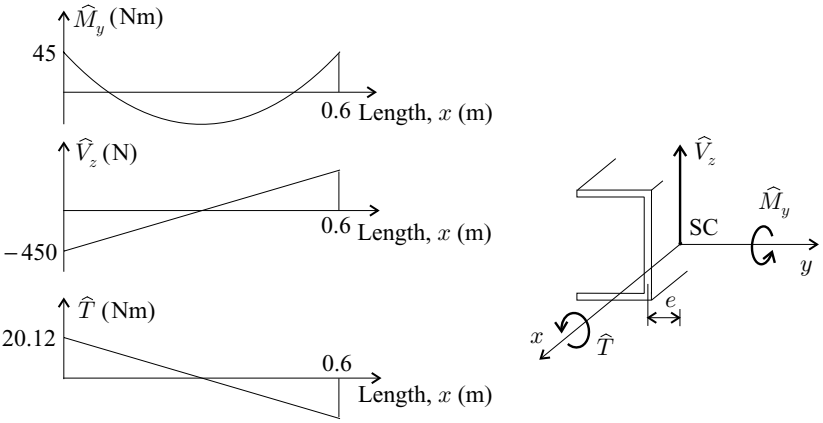

Figure 6.78: Bending moment $\widehat{M}_y$, shear force $\widehat{V}_z$, and torque $\widehat{T}$ diagrams for the beam in Example. 6.6.

where $\widehat{T}$ varies linearly with x (Fig. 6.78). Thus, the preceding integral yields

$$\psi = \frac{\widehat{T}^{\max} L}{4\widehat{G}\widehat{I}_{\mathrm{t}}} = 0.2288 \text{ rad} = 13.1^{\circ}. \tag{6.322}$$

When restrained warping is taken into account, ψ is 0.217° (Example 6.7, Eq. 6.324). This demonstrates that restrained warping must be considered when calculating the rotation of open-section beams.

6.7 Example. *An $L = 0.6$-m-long C-section beam, with the cross section shown in Figure 6.79, is made of graphite epoxy. The material properties are given in Table 3.6 (page 81). The layup is $[\pm 45_2^{\mathrm{f}}/0_{12}/\pm 45_2^{\mathrm{f}}]$. The beam is built-in at both ends. The beam is subjected to a uniformly distributed load ($p = -1\,500$ N/m) acting along the centerline of the flange. By taking axial restraint into account, calculate the maximum deflection and the maximum twist.*

Solution. The bending moment $\widehat{M}_y$, shear force $\widehat{V}_z$, torque $\widehat{T}$, and the maximum deflection are identical to those given in Example 6.6. The twist is calculated as follows. The warping stiffness is given in Table A.5 (page 457). We replace α by a,

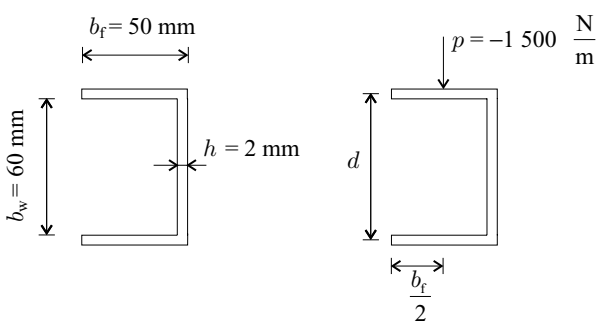

Figure 6.79: The cross section of the beam in Example 6.7 and the loading on the beam.

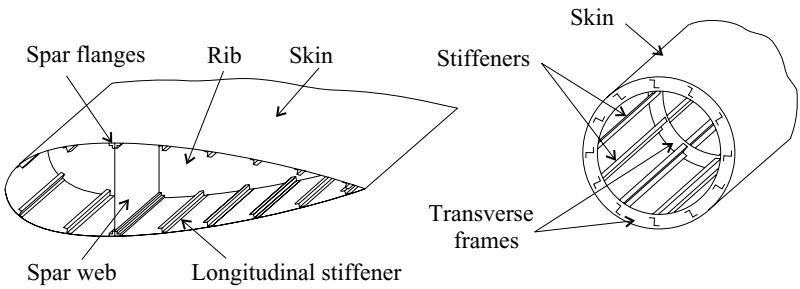

Figure 6.80: Illustration of stiffened structures.

and write

$$\widehat{EI}_\omega = \frac{b_f^3 d^2 \frac{1}{(a_{11})_f}}{12} \frac{\frac{3b_f}{(a_{11})_f} + \frac{2d}{(a_{11})_w}}{\frac{6b_f}{(a_{11})_f} + \frac{d}{(a_{11})_w}} = 5.847 \text{ N} \cdot \text{m}^4, \tag{6.323}$$

where the dimensions $b_f = 0.05$ m and $d = 0.062$ m are shown in Figure 6.79, and a_{11} for both the web and the flange is $(a_{11})_w = (a_{11})_f = 5.18 \times 10^{-9} \frac{\text{m}}{\text{N}}$ (Table 3.8, page 85).

The maximum twist is at $x = L/2$ and is[16]

$$\psi = \frac{tL}{2\widehat{EI}_\omega \beta^3} \left[\frac{\beta L}{4} - \tanh\left(\frac{\beta L}{4}\right) \right] = 0.003\,79 \text{ rad} = 0.217^\circ. \tag{6.324}$$

where t is the distributed torque load ($t = 67.08 \ \frac{\text{N} \cdot \text{m}}{\text{m}}$, Eq. 6.318), and β is

$$\beta = \sqrt{\frac{\widehat{GI}_t}{\widehat{EI}_\omega}} = 1.502, \tag{6.325}$$

where $\widehat{GI}_t = 13.19 \text{ N} \cdot \text{m}^2$ is given by Eq. (6.316). If we disregard restrained warping, the maximum twist is $\psi = 13.1^\circ$ (Eq. 6.322). By comparing this value with the value given above in Eq. (6.324), we see that restrained warping significantly reduces the twist.

6.8 Stiffened Thin-Walled Beams

Thin-walled structures are often reinforced with longitudinal stiffeners and transverse frames. Illustrations of such reinforced (semimonocoque) structures are airplane wings and fuselages (Fig. 6.80). In many applications such structures may be treated as reinforced thin-walled beams. Then, to simplify the analysis, the beam is idealized by representing the stiffeners as concentrated areas, sometimes called flanges or booms (Fig. 6.81). It is assumed that the flange carries all the bending load, and the web between the flanges carries the shear load. In the following we analyze stiffened beams in which the web is orthotropic.

[16] W. C. Young and R. G. Budynas, *Roark's Formulas for Stresses and Strains*. 7th edition. McGraw-Hill, New York, 2002, p. 425.

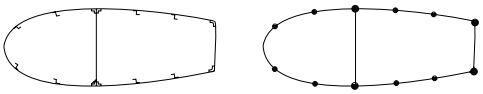

Figure 6.81: An actual and the idealized stiffened thin-walled beam.

The tensile stiffness of the beam is

$$\widehat{EA} = \sum_{m=1}^{M} \widehat{EA}_{\mathrm{m}}, \tag{6.326}$$

where $\widehat{EA}_{\mathrm{m}}$ is the tensile stiffness of the mth flange, and M is the total number of flanges (Fig. 6.82). The coordinates of the centroid are

$$y_{\mathrm{c}} = \frac{\sum_{m=1}^{M} \overline{y}_{\mathrm{m}} \widehat{EA}_{\mathrm{m}}}{\widehat{EA}} \qquad z_{\mathrm{c}} = \frac{\sum_{m=1}^{M} \overline{z}_{\mathrm{m}} \widehat{EA}_{\mathrm{m}}}{\widehat{EA}}, \tag{6.327}$$

where $\overline{z}_{\mathrm{m}}$ and $\overline{y}_{\mathrm{m}}$ are the coordinates of the mth flange in the $\overline{y}$–$\overline{z}$ arbitrarily chosen coordinate system.

The bending stiffnesses are

$$\widehat{EI}_{zz} = \sum_{m=1}^{M} y_{\mathrm{m}}^2 \widehat{EA}_{\mathrm{m}} \tag{6.328}$$

$$\widehat{EI}_{yy} = \sum_{m=1}^{M} z_{\mathrm{m}}^2 \widehat{EA}_{\mathrm{m}} \tag{6.329}$$

$$\widehat{EI}_{yz} = \sum_{m=1}^{M} y_{\mathrm{m}} z_{\mathrm{m}} \widehat{EA}_{\mathrm{m}}, \tag{6.330}$$

where z_{m} and y_{m} are coordinates of the mth flange in the coordinate system attached to the centroid. The displacements and the radii of curvatures of semimonocoque beams can be obtained by replacing EA and EI by the preceding replacement stiffnesses in the expressions describing the deflections of the corresponding isotropic beam.

The normal force carried by the mth flange is

$$\widehat{N}_{x\mathrm{m}} = \left(\frac{1}{\rho_y} z_{\mathrm{m}} + \frac{1}{\rho_z} y_{\mathrm{m}} + \epsilon_x^{\mathrm{o}} \right) \widehat{EA}_{\mathrm{m}}, \tag{6.331}$$

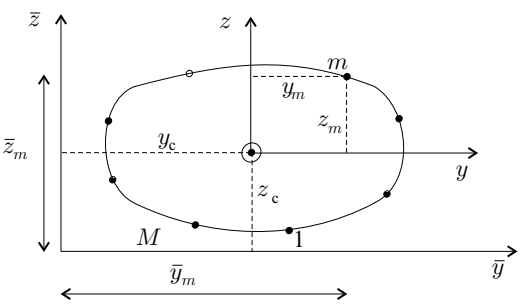

Figure 6.82: Stiffened thin-walled beam.

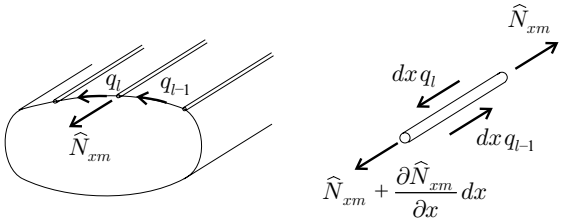

Figure 6.83: Equilibrium of a flange of a stiffened thin-walled beam.

where ρ_y, ρ_z are the radii of curvatures of the axis passing through the centroid and ϵ_x° is the elongation of the longitudinal axis through the centroid (Eqs. 6.17 and 6.19).

The shear flows in reinforced (semimonocoque) and unreinforced (monocoque) beams are different. In reinforced walls the shear flow is calculated on the basis of the preceding stated approximation, namely, that the flanges carry all the bending load and the walls the shear load. Force balance in the direction of the flange results in (Fig. 6.83)

$$q_l - q_{l-1} = -\frac{\partial \widehat{N}_{x\mathrm{m}}}{\partial x}, \tag{6.332}$$

where q_l and q_{l-1} are the shear flows in two adjacent walls, and $\widehat{N}_{x\mathrm{m}}$ is the axial force in the mth flange. By utilizing the expression given for $\widehat{N}_{x\mathrm{m}}$ in Eq. (6.331) and employing Eqs. (6.17) and (6.19), we obtain the change in shear flow induced by a flange as follows:

$$\begin{aligned} q_l - q_{l-1} = &-\frac{\widehat{EI}_{zz}\widehat{V}_z - \widehat{EI}_{yz}\widehat{V}_y}{\widehat{EI}_{yy}\widehat{EI}_{zz} - (\widehat{EI}_{yz})^2} z_{\mathrm{m}} \widehat{EA}_{\mathrm{m}} \\ &-\frac{-\widehat{EI}_{yz}\widehat{V}_z + \widehat{EI}_{yy}\widehat{V}_y}{\widehat{EI}_{yy}\widehat{EI}_{zz} - (\widehat{EI}_{yz})^2} y_{\mathrm{m}} \widehat{EA}_{\mathrm{m}}. \end{aligned} \tag{6.333}$$

Torsion. In the absence of axial constraint there are no axial forces either in open- or in closed-section semimonocoque beams subjected to pure torque. Therefore, the presence of booms does not affect the shear flow, and the analyses given in Section 6.5 for the torsion of unreinforced (monocoque) thin-walled beams apply to reinforced (semimonocoque) thin-walled beams.

6.9 Buckling of Beams

In this section we address the buckling loads of orthotropic composite beams. The buckling loads of such beams are calculated from the equilibrium equations (which include the changes in geometry during buckling) and the strain–displacement and the force–strain relationships. The first two of these are identical for isotropic and orthotropic beams. However, the force–strain relationships of isotropic and orthotropic beams are different. The force–strain relationships for an isotropic beam are obtained by combining Eqs. (6.4) and (6.239)

isotropic:

$$\begin{Bmatrix} \widehat{N} \\ \widehat{M}_y \\ \widehat{M}_z \\ \widehat{T}_{\mathrm{sv}} \\ \widehat{T}_{\omega} \end{Bmatrix} = \begin{bmatrix} EA & 0 & 0 & 0 & 0 \\ 0 & EI_{yy} & EI_{yz} & 0 & 0 \\ 0 & EI_{yz} & EI_{zz} & 0 & 0 \\ 0 & 0 & 0 & GI_{\mathrm{t}} & 0 \\ 0 & 0 & 0 & 0 & EI_{\omega} \end{bmatrix} \begin{Bmatrix} \epsilon_x^{\mathrm{o}} \\ \frac{1}{\rho_y} \\ \frac{1}{\rho_z} \\ \vartheta \\ -\frac{\partial^2 \vartheta}{\partial x^2} \end{Bmatrix}. \tag{6.334}$$

We express the force–strain relationships of orthotropic beams as (Eqs. 6.7, 6.8, and 6.240)

orthotropic:

$$\begin{Bmatrix} \widehat{N} \\ \widehat{M}_y \\ \widehat{M}_z \\ \widehat{T}_{\mathrm{sv}} \\ \widehat{T}_{\omega} \end{Bmatrix} = \begin{bmatrix} \widehat{EA} & 0 & 0 & 0 & 0 \\ 0 & \widehat{EI}_{yy} & \widehat{EI}_{yz} & 0 & 0 \\ 0 & \widehat{EI}_{yz} & \widehat{EI}_{zz} & 0 & 0 \\ 0 & 0 & 0 & \widehat{GI}_{\mathrm{t}} & 0 \\ 0 & 0 & 0 & 0 & \widehat{EI}_{\omega} \end{bmatrix} \begin{Bmatrix} \epsilon_x^{\mathrm{o}} \\ \frac{1}{\rho_y} \\ \frac{1}{\rho_z} \\ \vartheta \\ -\frac{\partial^2 \vartheta}{\partial x^2} \end{Bmatrix}. \tag{6.335}$$

The equations governing the buckling loads of isotropic and orthotropic beams differ only in their stiffness matrices. Therefore, the buckling load of an orthotropic beam can be obtained by replacing the isotropic stiffnesses with the replacement stiffnesses in the expression of the buckling load of the corresponding isotropic beam as follows:

$$\begin{array}{rl} \text{Isotropic beams} & \text{Orthotropic beams} \\ EA & \Longrightarrow \widehat{EA} \\ EI_{yy},\, EI_{zz},\, EI_{yz} & \Longrightarrow \widehat{EI}_{yy},\, \widehat{EI}_{zz},\, \widehat{EI}_{yz} \\ GI_{\mathrm{t}},\, EI_{\omega} & \Longrightarrow \widehat{GI}_{\mathrm{t}},\, \widehat{EI}_{\omega}. \end{array} \tag{6.336}$$

The stiffnesses of selected orthotropic beams are given in Tables A.1–A.5. The warping stiffness $\widehat{EI}_{\omega}$ is given only for open-section beams because, generally, it can be neglected for closed-section beams.

As examples, in the following we present the buckling loads of beams subjected to axial loads, bending moments, and transverse loads.

6.9.1 Beams Subjected to Axial Load (Flexural–Torsional Buckling)

We now consider orthotropic beams subjected to an axial load. Under this load the beam may undergo flexural and torsional buckling.

Doubly symmetrical cross section. We consider orthotropic beams with cross sections symmetrical with respect to both the y- and the z-axes ($\widehat{EI}_{yz} = 0$). When the cross section of the beam has two axes of symmetry (doubly symmetrical cross section), it may buckle (a) in one of the planes of symmetry, (b) in the other plane of symmetry, and (c) torsionally (Fig. 6.84).

Buckling loads of doubly symmetrical cross-section isotropic beams are given by Timoshenko and Gere.[17] By exchanging the isotropic stiffnesses in the

[17] S. P. Timoshenko and J. Gere, *Theory of Elastic Stability.* 2nd edition. McGraw-Hill, New York, 1961, pp. 49 and 229.

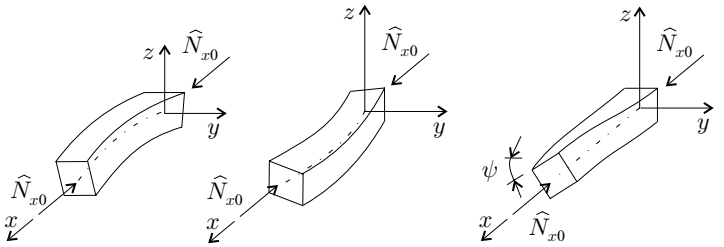

Figure 6.84: Illustrations of buckling in the x–z and x–y planes and of torsional buckling.

Timoshenko and Gere expressions with the replacement stiffnesses (see Eq. 6.336), the buckling loads of orthotropic beams are

$$\begin{aligned}
\widehat{N}^{\mathrm{B}}_{\mathrm{cr}y} &= \frac{\pi^2 \widehat{EI}_{yy}}{(kL)^2} && \text{buckling in the } x\text{–}z \text{ plane} \\
\widehat{N}^{\mathrm{B}}_{\mathrm{cr}z} &= \frac{\pi^2 \widehat{EI}_{zz}}{(kL)^2} && \text{buckling in the } x\text{–}y \text{ plane} \\
\widehat{N}^{\mathrm{B}}_{\mathrm{cr}\psi} &= \widehat{N}^{\mathrm{B}}_{\mathrm{cr}\omega} + \frac{1}{i_\omega^2}\widehat{GI}_{\mathrm{t}} && \text{torsional buckling,}
\end{aligned} \tag{6.337}$$

where $\widehat{N}^{\mathrm{B}}_{\mathrm{cr}\omega}$ is

$$\widehat{N}^{\mathrm{B}}_{\mathrm{cr}\omega} = \frac{1}{i_\omega^2}\frac{\pi^2 \widehat{EI}_\omega}{(kL)^2}, \tag{6.338}$$

L is the length of the beam, i_ω is the polar radius of gyration of the cross section about the shear center, which, for an isotropic beam,[18] is

$$i_\omega^2 = z_{\mathrm{sc}}^2 + y_{\mathrm{sc}}^2 + \frac{I_{zz} + I_{yy}}{A}, \tag{6.339}$$

where y_{sc} and z_{sc} are the coordinates of the shear center with respect to the centroid. For an orthotropic composite beam we define i_ω as

$$i_\omega^2 = z_{\mathrm{sc}}^2 + y_{\mathrm{sc}}^2 + \frac{\widehat{EI}_{zz} + \widehat{EI}_{yy}}{\widehat{EA}}. \tag{6.340}$$

The effective length factor k is given in Table 6.11 for different end conditions.

For long beams ($\widehat{GI}_{\mathrm{t}} \gg \widehat{EI}_\omega/L^2$) the torsional buckling load simplifies to

$$\widehat{N}^{\mathrm{B}}_{\mathrm{cr}\psi} = \frac{1}{i_\omega^2}\widehat{GI}_{\mathrm{t}} \qquad \begin{matrix}\text{torsional buckling} \\ \text{long beam.}\end{matrix} \tag{6.341}$$

For short beams ($\widehat{GI}_{\mathrm{t}} \ll \widehat{EI}_\omega/L^2$) the torsional buckling load is

$$\widehat{N}^{\mathrm{B}}_{\mathrm{cr}\psi} = \widehat{N}^{\mathrm{B}}_{\mathrm{cr}\omega} = \frac{1}{i_\omega^2}\frac{\pi^2 \widehat{EI}_\omega}{(kL)^2} \qquad \begin{matrix}\text{torsional buckling} \\ \text{short beam.}\end{matrix} \tag{6.342}$$

[18] Ibid., p. 233.

Table 6.11. The factor k in Eqs. (6.337) and (6.338). The simple supports in cases (a) and (b) restrain the rotation about the x-axis, but the cross section is free to warp and free to rotate about the y- and z-axes

Geometry, loading		k
(a)	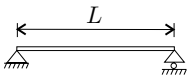	$k = 1$
(b)		$k = 0.7$
(c)		$k = 0.5$
(d)		$k = 2$

Symmetrical cross section. We consider orthotropic beams with cross sections symmetrical with respect to the z-axis ($\widehat{EI}_{yz} = 0$). When the cross section of the beam has one axis of symmetry, it may undergo (a) buckling in the plane of symmetry (x–z plane), or (b) combined flexural–torsional buckling. The buckling load corresponding to buckling in the x–z plane is[19]

$$\widehat{N}_{\mathrm{cr1}} = \widehat{N}^{\mathrm{B}}_{\mathrm{cr}y} \qquad \text{buckling in the } x\text{–}z \text{ plane.} \tag{6.343}$$

The buckling loads $\widehat{N}_{\mathrm{cr2}}$ and $\widehat{N}_{\mathrm{cr3}}$, corresponding to flexural–torsional buckling, are the roots of the following equation:

$$\left| \begin{bmatrix} \widehat{N}^{\mathrm{B}}_{\mathrm{cr}z} & \\ & \widehat{N}^{\mathrm{B}}_{\mathrm{cr}\psi} i_\omega^2 \end{bmatrix} - \widehat{N}_{\mathrm{cr}} \begin{bmatrix} 1 & z_{\mathrm{sc}} \\ z_{\mathrm{sc}} & i_\omega^2 \end{bmatrix} \right| = 0, \tag{6.344}$$

where $|\quad|$ denotes the determinant. This equation can be written in the form

$$\widehat{N}^2_{\mathrm{cr}}\left(i_\omega^2 - z_{\mathrm{sc}}^2\right) - \widehat{N}_{\mathrm{cr}}\left(\widehat{N}^{\mathrm{B}}_{\mathrm{cr}z} + \widehat{N}^{\mathrm{B}}_{\mathrm{cr}\psi}\right) i_\omega^2 + \widehat{N}^{\mathrm{B}}_{\mathrm{cr}z} \widehat{N}^{\mathrm{B}}_{\mathrm{cr}\psi} i_\omega^2 = 0, \tag{6.345}$$

where $\widehat{N}^{\mathrm{B}}_{\mathrm{cr}y}$, $\widehat{N}^{\mathrm{B}}_{\mathrm{cr}z}$, and $\widehat{N}^{\mathrm{B}}_{\mathrm{cr}\psi}$ are given by Eq. (6.337), and the effective length factor k is given in Table 6.11.

Equation (6.343) yields the value of $\widehat{N}_{\mathrm{cr1}}$, and Eq. (6.345) yields two values of $\widehat{N}_{\mathrm{cr}}$ denoted by $\widehat{N}_{\mathrm{cr2}}$ and $\widehat{N}_{\mathrm{cr3}}$. The buckling load of interest is the lowest of these three values. We note that the $\widehat{N}_{\mathrm{cr2}}$ and $\widehat{N}_{\mathrm{cr3}}$ values resulting from Eq. (6.345) are approximate when one end of the beam is fixed and the other end is simply supported (case b in Table 6.11).

[19] Ibid., p. 235.

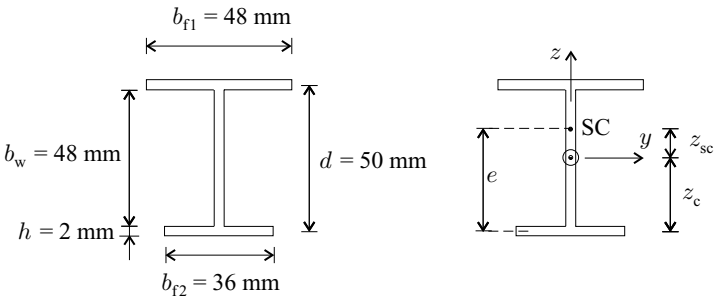

Figure 6.85: The cross section of the beam in Example 6.8 and the loading on the beam.

Unsymmetrical cross sections. When the cross section is unsymmetrical, an orthotropic beam undergoes combined flexural–torsional buckling, and the buckling loads $\widehat{N}_{cr}$ are given by the solution of the following (third-order) equation[20]:

$$\left| \begin{bmatrix} \widehat{N}^{B}_{crz} & 0 & 0 \\ 0 & \widehat{N}^{B}_{cry} & 0 \\ 0 & 0 & \widehat{N}^{B}_{cr\psi} i_\omega^2 \end{bmatrix} - \widehat{N}_{cr} \begin{bmatrix} 1 & 0 & z_{sc} \\ 0 & 1 & -y_{sc} \\ z_{sc} & -y_{sc} & i_\omega^2 \end{bmatrix} \right| = 0. \qquad (6.346)$$

In the preceding equation the coordinate directions y and z must be in the principal directions (page 208) such that $\widehat{EI}_{yz}$ is zero ($\widehat{EI}_{yz} = 0$); $|\ \ |$ denotes the determinant. The terms $\widehat{N}^{B}_{cry}$, $\widehat{N}^{B}_{crz}$, and $\widehat{N}^{B}_{cr\psi}$ are given by Eq. (6.337), and the constant k is given in Table 6.11. The solution of Eq. (6.346) results in three values of $\widehat{N}_{cr}$, of which the lowest value is of interest. The resulting $\widehat{N}_{cr}$ is approximate when one end of the beam is fixed and the other end is simply supported (case b in Table 6.11).

6.8 Example. *An $L = 0.5$-m-long I-section beam, with the cross section shown in Figure 6.85, is made of graphite epoxy unidirectional plies. The material properties are given in Table 3.6 (page 81). The layup is* $[0_{20}]$. *The beam is simply supported at each end. Determine the buckling load when the beam is subjected to an axial load.*

Solution. The compliance matrices for the flange and the web are the same, and their relevant elements are (Table 3.8, page 85)

$$a_{11} = 3.38 \times 10^{-9} \frac{\text{m}}{\text{N}}$$
$$d_{11} = 10.14 \times 10^{-3} \frac{1}{\text{N} \cdot \text{m}} \qquad d_{66} = 329.67 \times 10^{-3} \frac{1}{\text{N} \cdot \text{m}}.$$

The dimensions of the cross section are $b_{f1} = 0.048\,\text{m}$, $b_{f2} = 0.036\,\text{m}$, $b_w = 0.048\,\text{m}$, $d = 0.050\,\text{m}$, $h = 0.002\,\text{m}$ (Fig. 6.85).

The tensile stiffness, the location of the centroid, and the bending stiffnesses are given in Table A.2. For symmetrical layup $(\delta_{11})_f$ and $(\delta_{11})_w$ are replaced by d_{11}

[20] Ibid., p. 233.

and $(\alpha_{11})_f$ and $(\alpha_{11})_w$ by a_{11}, and from Table A.2 we have

$$\begin{aligned}
\widehat{EA} &= \frac{b_{f1}}{a_{11}} + \frac{b_{f2}}{a_{11}} + \frac{b_w}{a_{11}} = 39.07 \times 10^6 \text{ N} \\
z_c &= \frac{1}{\widehat{EA}}\left(\frac{b_{f1}}{a_{11}}d + \frac{b_w}{a_{11}}\frac{d}{2}\right) = 0.027\,27 \text{ m} \\
\widehat{EI}_{zz} &= \frac{b_w}{d_{11}} + \frac{1}{a_{11}}\frac{b_{f1}^3}{12} + \frac{1}{a_{11}}\frac{b_{f2}^3}{12} = 3\,884 \text{ N}\cdot\text{m}^2 \\
\widehat{EI}_{yy} &= \frac{b_{f1}}{a_{11}}(d - z_c)^2 + \frac{b_{f2}}{a_{11}}z_c^2 + \frac{b_{f1}}{d_{11}} \\
&\quad + \frac{b_{f2}}{d_{11}} + \frac{1}{a_{11}}\left(\frac{b_{w1}^3 + b_{w2}^3}{3}\right) = 18\,074 \text{ N}\cdot\text{m}^2,
\end{aligned} \tag{6.347}$$

where b_{w1} and b_{w2} are calculated with the preceding value of z_c (see Table A.2) as follows:

$$b_{w1} = z_c - \frac{h}{2} = 0.026\,27 \text{ m} \qquad b_{w2} = b_w - b_{w1} = 0.021\,73 \text{ m}.$$

The torsional stiffness, the location of the shear center, and the warping stiffness are given in Table A.5. For symmetrical layup $(\delta_{66})_f$ and $(\delta_{66})_w$ are replaced by d_{66} and $(\alpha_{11})_f$ and $(\alpha_{11})_w$ by a_{11} (Table 3.8, page 85), and we write

$$\begin{aligned}
\widehat{GI}_t &= 4\left(\frac{b_{f1}}{d_{66}} + \frac{b_{f2}}{d_{66}} + \frac{d}{d_{66}}\right) = 1.602 \text{ N}\cdot\text{m}^2 \\
e &= d\frac{\frac{b_{f1}^3}{a_{11}}}{\frac{b_{f1}^3}{a_{11}} + \frac{b_{f2}^3}{a_{11}}} = 0.035\,17 \text{ m} \\
\widehat{EI}_\omega &= \frac{\frac{b_{f2}^3}{a_{11}}}{12}ed = 2.024 \text{ N}\cdot\text{m}^4.
\end{aligned} \tag{6.348}$$

The cross section is symmetrical with respect to the z-axis, and the coordinates of the shear center with respect to the centroid are (Fig. 6.85)

$$y_{sc} = 0 \qquad z_{sc} = e - z_c = 0.000\,789 \text{ m}. \tag{6.349}$$

The polar radius of gyration about the shear center i_ω is (Eq. 6.340)

$$i_\omega = \sqrt{z_{sc}^2 + y_{sc}^2 + \frac{\widehat{EI}_{zz} + \widehat{EI}_{yy}}{\widehat{EA}}} = 0.024\,99 \text{ m}. \tag{6.350}$$

For a simply supported beam ($k = 1$, Table 6.11, page 293), Eq. (6.337) gives

$$\begin{aligned}
\widehat{N}_{cry}^B &= \frac{\pi^2 \widehat{EI}_{yy}}{L^2} = 713.55 \text{ kN} && x\text{–}z \text{ plane} \\
\widehat{N}_{crz}^B &= \frac{\pi^2 \widehat{EI}_{zz}}{L^2} = 153.32 \text{ kN} && x\text{–}y \text{ plane} \\
\widehat{N}_{cr\psi}^B &= \widehat{N}_{cr\omega}^B + \frac{1}{i_\omega^2}\widehat{GI}_t = 130.53 \text{ kN} && \text{torsion},
\end{aligned} \tag{6.351}$$

where (Eq. 6.338)

$$\widehat{N}_{cr\omega}^B = \frac{1}{i_\omega^2}\frac{\pi^2 \widehat{EI}_\omega}{(kL)^2} = 127.96 \text{ kN}. \tag{6.352}$$

The buckling load $\widehat{N}_{\mathrm{cr1}}$ is (Eq. 6.343),

$$\widehat{N}_{\mathrm{cr1}} = \widehat{N}^{\mathrm{B}}_{\mathrm{cr}y} = 713.55\ \mathrm{kN} \qquad \text{buckling in the } x\text{–}z \text{ plane,} \tag{6.353}$$

and $\widehat{N}_{\mathrm{cr2}}$ and $\widehat{N}_{\mathrm{cr3}}$ are the roots of Eq. (6.345) as follows:

$$\widehat{N}^2_{\mathrm{cr}} \left(i^2_\omega - z^2_{\mathrm{sc}}\right) - \widehat{N}_{\mathrm{cr}} \left(\widehat{N}^{\mathrm{B}}_{\mathrm{cr}z} + \widehat{N}^{\mathrm{B}}_{\mathrm{cr}\psi}\right) i^2_\omega + \widehat{N}^{\mathrm{B}}_{\mathrm{cr}z} \widehat{N}^{\mathrm{B}}_{\mathrm{cr}\psi} i^2_\omega = 0. \tag{6.354}$$

Solution of this equation yields the flexural–torsional buckling loads

$$\widehat{N}_{\mathrm{cr2}} = 208.88\ \mathrm{kN} \qquad \widehat{N}_{\mathrm{cr3}} = 106.43\ \mathrm{kN}. \tag{6.355}$$

6.9.2 Lateral–Torsional Buckling of Orthotropic Beams with Symmetrical Cross Section

We consider orthotropic beams. The cross section of the beam is symmetrical with respect to the z-axis ($\widehat{EI}_{yz} = 0$). The beam is simply supported at each end. At the simple support the beam is restrained from rotating about the x-axis, but the cross section is free to rotate about the y- and z-axes and is free to warp.

The beam is subjected to two equal and opposite bending moments at the two ends of the beam (Fig. 6.86, top), a uniformly distributed load p in the plane of symmetry (Fig. 6.86, middle), or a concentrated force P in the plane of symmetry at the midspan of the beam (Fig. 6.86, bottom). The distance between the shear center and the point where the load acts is denoted by Δ.

At certain applied loads the beam buckles laterally while the cross sections of the beam rotate (Fig. 6.87). This phenomenon is called lateral buckling, or lateral–torsional buckling.

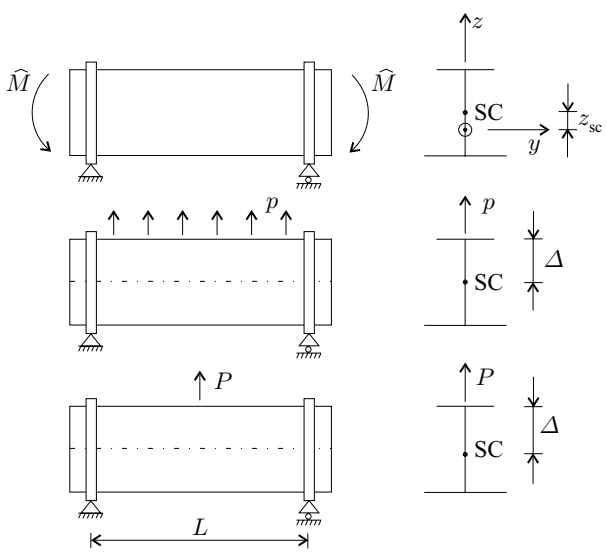

Figure 6.86: Lateral buckling of beams subjected to two equal and opposite bending moments at the two ends of the beam (top), a uniformly distributed load p in the plane of symmetry (middle), and a concentrated force P in the plane of symmetry at the midspan of the beam (bottom). The distance between the shear center and the point where the load acts is denoted by Δ.

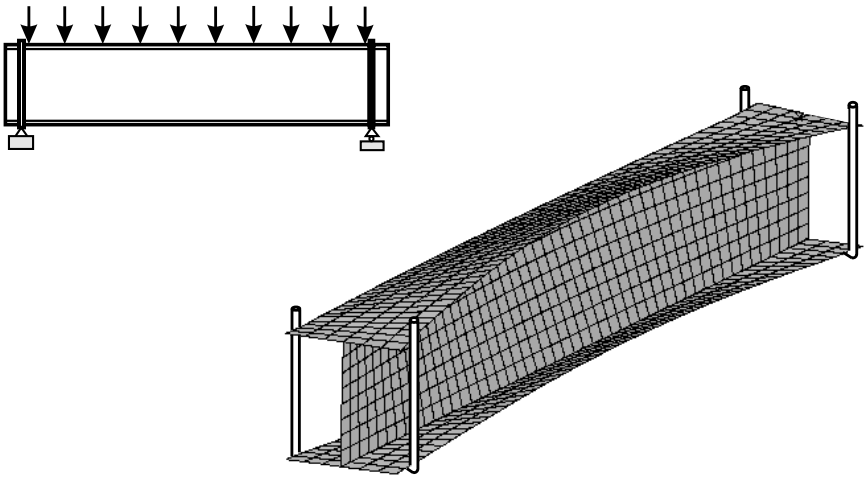

Figure 6.87: Illustration of lateral buckling of a simply supported beam.

Allen and Bulson[21] presented the following formula for the buckling load of an isotropic beam:

$$\widehat{Q}_{\mathrm{cr}} = G_1 \frac{\pi^2}{L^2} \widehat{EI}_{zz} \left[G_2 \Delta + G_3 \frac{\beta_1}{2} \pm \sqrt{\left(G_2 \Delta + G_3 \frac{\beta_1}{2} \right)^2 + \frac{\widehat{EI}_\omega}{\widehat{EI}_{zz}} \left(1 + \frac{\widehat{GI}_{\mathrm{t}}}{\widehat{EI}_\omega} \frac{L^2}{\pi^2} \right)} \right], \tag{6.356}$$

where $\widehat{Q}_{\mathrm{cr}}$ is the critical value of the bending moment and is related to the applied loads, as shown in Table 6.12. The positive sign before the square root results in a positive load (which acts upward), whereas the negative sign results in a negative load (which acts downward); G_1–G_3 are constants. We recall Eqs. (6.337) and (6.338), which relate $\widehat{N}^{\mathrm{B}}_{\mathrm{cr}z}$ and $\widehat{N}^{\mathrm{B}}_{\mathrm{cr}\psi}$ to the stiffnesses

$$\widehat{N}^{\mathrm{B}}_{\mathrm{cr}z} = \frac{\pi^2 \widehat{EI}_{zz}}{(kL)^2} \tag{6.357}$$

$$\widehat{N}^{\mathrm{B}}_{\mathrm{cr}\psi} = \widehat{N}^{\mathrm{B}}_{\mathrm{cr}\omega} + \frac{1}{i_\omega^2} \widehat{GI}_{\mathrm{t}} = \frac{1}{i_\omega^2} \frac{\pi^2 \widehat{EI}_\omega}{(kL)^2} + \frac{1}{i_\omega^2} \widehat{GI}_{\mathrm{t}}, \tag{6.358}$$

where $k = 1$ for a simply supported beam. By combining and rearranging Eqs. (6.356)–(6.358), we obtain

$$\widehat{Q}_{\mathrm{cr}} = F_1 \widehat{N}^{\mathrm{B}}_{\mathrm{cr}z} \left(F_2 \Delta + F_3 \beta_1 \pm \sqrt{(F_2 \Delta + F_3 \beta_1)^2 + \frac{\widehat{N}^{\mathrm{B}}_{\mathrm{cr}\psi} i_\omega^2}{\widehat{N}^{\mathrm{B}}_{\mathrm{cr}z}}} \right), \tag{6.359}$$

where F_1, F_2, F_3 are constants (their values are also listed in Table 6.12), and β_1 is a parameter that depends on the shape of the cross section[22]

$$\beta_1 = J_1 + J_2 - 2z_{\mathrm{sc}}. \tag{6.360}$$

[21] H. G. Allen and P. S. Bulson, *Background to Buckling.* McGraw-Hill, London, 1980, p. 492.
[22] Ibid., p. 495.

Table 6.12. The buckling loads and the corresponding constants in Eq. (6.359).

		F_1	F_2	F_3
(a) Moment	$\widehat{M}_{\text{cr}} = \widehat{Q}_{\text{cr}}$	1	0	0.5
(b) Distributed load	$p_{\text{cr}} = \frac{8\widehat{Q}_{\text{cr}}}{L^2}$	1.13	0.45	0.267
(c) Concentrated force	$P_{\text{cr}} = \frac{4\widehat{Q}_{\text{cr}}}{L}$	1.35	0.55	0.212

For a beam made of isotropic material J_1 and J_2 are

$$J_1 = \frac{1}{I_{yy}} \int_{(A)} z^3 dA \qquad J_2 = \frac{1}{I_{yy}} \int_{(A)} zy^2 dA. \tag{6.361}$$

For a thin-walled, open-section isotropic beam, J_1 and J_2 may be written as

$$\begin{aligned} J_1 &= \frac{1}{EI_{yy}} \int_{(S)} (Eh)\, z^3 d\eta \\ J_2 &= \frac{1}{EI_{yy}} \int_{(S)} (Eh)\, zy^2 d\eta \end{aligned} \qquad \text{isotropic,} \tag{6.362}$$

where h is the thickness of the wall and η is the coordinate along the circumference. For an orthotropic beam Eh is replaced by $1/\alpha_{11}^{\varrho}$ (Eqs. 6.243 and 6.241), and EI is replaced by $\widehat{EI}$ (α_{11}^{ϱ} is evaluated at the "neutral" plane; see Eq. 6.105). This gives

$$\begin{aligned} J_1 &= \frac{1}{\widehat{EI}_{yy}} \int_{(S)} \frac{1}{\alpha_{11}^{\varrho}} z^3 d\eta \\ J_2 &= \frac{1}{\widehat{EI}_{yy}} \int_{(S)} \frac{1}{\alpha_{11}^{\varrho}} zy^2 d\eta \end{aligned} \qquad \text{orthotropic.} \tag{6.363}$$

For orthotropic I-beams whose cross-section is symmetrical with respect the midplane of the web the preceding integrals give

$$\begin{aligned} J_1 &= \frac{1}{\widehat{EI}_{yy}} \left(\frac{1}{(\alpha_{11}^{\varrho})_{\text{f1}}} b_{\text{f1}} (d - z_{\text{c}})^3 - \frac{1}{(\alpha_{11}^{\varrho})_{\text{f2}}} b_{\text{f2}} z_{\text{c}}^3 + \frac{1}{(a_{11})_{\text{w}}} \frac{b_{\text{w1}}^4 - b_{\text{w2}}^4}{4} \right) \\ J_2 &= \frac{1}{\widehat{EI}_{yy}} \left(\frac{1}{(\alpha_{11}^{\varrho})_{\text{f1}}} \frac{b_{\text{f1}}^3}{12} (d - z_{\text{c}}) - \frac{1}{(\alpha_{11}^{\varrho})_{\text{f2}}} \frac{b_{\text{f2}}^3}{12} z_{\text{c}} \right). \end{aligned} \tag{6.364}$$

The dimensions are defined in Table A.2 (page 455).

For doubly symmetrical isotropic and orthotropic beams, β_1 is zero.

Equation (6.359) is accurate for beams subjected to concentrated bending moments (Fig. 6.86, top). For simply supported beams subjected to a distributed load or to a concentrated force at the midspan, Eq. (6.359) gives the buckling load within about 5 percent.

6.9 Example. *An $L = 0.5$-m-long I-section beam, with the cross section shown in Figure 6.85, is made of graphite epoxy unidirectional plies. The material properties are given in Table 3.6 (page 81). The layup is* $[0_{20}]$. *The beam is simply supported at*

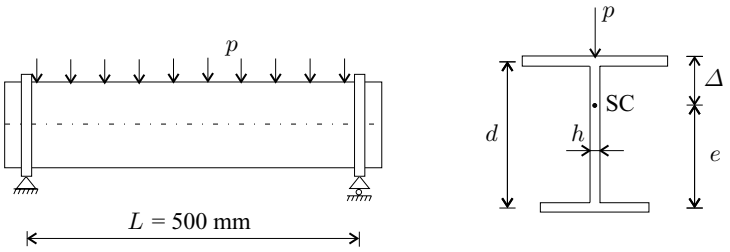

Figure 6.88: The beam in Example. 6.9.

each end. Determine the buckling load when the beam is subjected to a distributed load along the top flange (Fig. 6.88).

Solution. For a transversely loaded beam the buckling load is (Table 6.12)

$$p_{\mathrm{cr}} = \frac{8\widehat{Q}_{\mathrm{cr}}}{L^2}, \tag{6.365}$$

where $\widehat{Q}_{\mathrm{cr}}$ is given by Eq.(6.359) as

$$\widehat{Q}_{\mathrm{cr}} = F_1 \widehat{N}^{\mathrm{B}}_{\mathrm{cr}z} \left(F_2\Delta + F_3\beta_1 - \sqrt{(F_2\Delta + F_3\beta_1)^2 + \frac{\widehat{N}^{\mathrm{B}}_{\mathrm{cr}\psi} i_\omega^2}{\widehat{N}^{\mathrm{B}}_{\mathrm{cr}z}}} \right). \tag{6.366}$$

The sign before the square root is negative because the load is downward. From Eq. (6.364) with α^{ϱ}_{11} replaced by a_{11}, we have

$$\begin{aligned} J_1 &= \frac{1}{\widehat{EI}_{yy}} \left(\frac{1}{a_{11}} b_{\mathrm{f1}} (d - z_{\mathrm{c}})^3 - \frac{1}{a_{11}} b_{\mathrm{f2}} z_{\mathrm{c}}^3 + \frac{1}{a_{11}} \frac{b_{\mathrm{w1}}^4 - b_{\mathrm{w2}}^4}{4} \right) \\ J_2 &= \frac{1}{\widehat{EI}_{yy}} \left(\frac{1}{a_{11}} \frac{b_{\mathrm{f1}}^3}{12} (d - z_{\mathrm{c}}) - \frac{1}{a_{11}} \frac{b_{\mathrm{f2}}^3}{12} z_{\mathrm{c}} \right). \end{aligned} \tag{6.367}$$

The parameters of interest in this problem are (see Example 6.8, page 294)

$$\begin{array}{lll} a_{11} = 3.38 \times 10^{-9}\ \dfrac{\mathrm{m}}{\mathrm{N}} & \widehat{EI}_{yy} = 18\,074\ \mathrm{N \cdot m^2} & h = 0.002\ \mathrm{m} \\ b_{\mathrm{f1}} = 0.048\ \mathrm{m} & b_{\mathrm{f2}} = 0.036\ \mathrm{m} & d = 0.050\ \mathrm{m} \\ b_{\mathrm{w2}} = 0.021\ 73\ \mathrm{m} & b_{\mathrm{w1}} = 0.026\ 27\ \mathrm{m} & z_{\mathrm{c}} = 0.027\ 27\ \mathrm{m} \\ z_{\mathrm{sc}} = 0.000\ 789\ \mathrm{m} & e = 0.035\ 17\ \mathrm{m} & i_\omega = 0.024\ 99\ \mathrm{m} \\ \widehat{N}^{\mathrm{B}}_{\mathrm{cr}z} = 153.32\ \mathrm{kN} & \widehat{N}^{\mathrm{B}}_{\mathrm{cr}y} = 713.55\ \mathrm{kN} & \widehat{N}^{\mathrm{B}}_{\mathrm{cr}\psi} = 130.53\ \mathrm{kN}. \end{array}$$

With the preceding parameters we obtain

$$J_1 = -0.003\ 770\ \mathrm{m} \qquad J_2 = 0.001\ 694\ \mathrm{m}, \tag{6.368}$$

and β_1 is (Eq. 6.360)

$$\beta_1 = J_1 + J_2 - 2z_{sc} = -0.017\ 86\ \text{m}. \tag{6.369}$$

The beam is loaded on the top flange; hence, we have

$$\Delta = d - e + h/2 = 0.015\ 84\ \text{m}. \tag{6.370}$$

The value of $\widehat{Q}_{cr}$ is calculated with the preceding parameters and with $F_1 = 1.13$, $F_2 = 0.45$, $F_3 = 0.267$ (Table 6.12, page 298). The result is

$$\widehat{Q}_{cr} = -3\ 607\ \text{N} \cdot \text{m}. \tag{6.371}$$

Equations (6.365) and (6.371) give

$$p_{cr} = \frac{8\widehat{Q}_{cr}}{L^2} = -115\ 407\ \frac{\text{N}}{\text{m}}. \tag{6.372}$$

6.9.3 Local Buckling

In this section we consider local buckling of orthotropic thin-walled beams that arise due to axial compressive stresses introduced by axial forces and bending moments.

Local buckling analyses of beams are generally performed by modeling the wall segments as long plates and by assuming that edges common to two or more plates remain straight. Then the buckling load may be determined either by assuming that every wall segment buckles simultaneously while the continuity conditions at each intersection are satisfied,[23,24] or by considering the wall segments as individual plates rotationally restrained by the adjacent wall segments.[25–27] Here, we derive explicit expressions for the local buckling loads based on the latter method.

The procedure for calculating the load at which local buckling occurs is illustrated via the example of an axially loaded thin-walled, closed-section rectangular beam (Fig. 6.89). First, each wall segment is considered to be simply supported (Fig. 6.89, a) and the load $(N_{x,\,cr})^{ss}$ for each wall segment is calculated using the expression given in the first row of Table 4.11 (page 136). The axial strain at which the wall segment buckles is calculated by $(N_{x,\,cr})^{ss}a_{11}$ (Eq. 3.31), where a_{11} is the 11 element of the compliance matrix of the wall segment. The segment with the lowest

[23] D. J. Lee, The Local Buckling Coefficient for Orthotropic Structural Sections. *Aeronautical Journal,* Vol. 82, 313–320, 1978.

[24] A. Zureick and B. Shih, Local Buckling of Fiber-Reinforced Polymeric Structural Members Under Linearly-Varying Edge Loading – Part 1. Theoretical Formulation. *Composite Structures*, Vol. 41, 79–86, 1998.

[25] P. Qiao, J. F. Davalos, and J. Wang, Local Buckling of Composite FRP Shapes by Discrete Plate Analysis. *Journal of Structural Engineering*, Vol. 127, 245–255, 2001.

[26] E. J. Barbero and I. Raftoyiannis, Local Buckling of FRP Beams and Columns. *Journal of Materials in Civil Engineering*, Vol. 5, 339–355, 1993.

[27] J. P. H. Webber, P. T. Holt, and D. A. Lee, Instability of Carbon Fibre Reinforced Flanges of I Section Beams and Columns. *Composite Structures,* Vol. 4, 245–265, 1985.

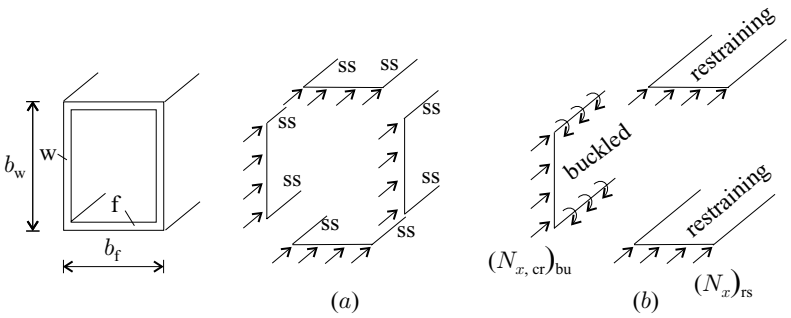

Figure 6.89: Local buckling of an axially loaded box beam.

critical strain is considered further because the wall segment (web or flange) in which the axial strain is the lowest is most susceptible to buckling. We calculate the buckling load of this segment by treating it as a plate rotationally restrained by the adjoining wall segment or segments (Fig. 6.89, b). The buckling load is calculated by the expression given in the fourth row of Table 4.11 (page 136).

The spring constant $\widetilde{k}$ depends on the adjacent (restraining) wall segment. To determine the spring constant, we recall Eq. (4.149)

$$\widetilde{k} = \frac{M_y}{\frac{\partial w}{\partial y}}, \tag{6.373}$$

where $\partial w/\partial y$ is the rotation of the edge.

A conservative estimate of $\widetilde{k}$ is obtained[28] when the deformed shape is cylindrical ("long-plate" approximation). For a long plate ($\kappa_x = \kappa_{xy} = 0$), the moment is (Eq. 4.3)

$$M_y = (D_{22})_{rs}\,\kappa_y, \tag{6.374}$$

where the subscript rs refers to the restraining segment (Fig. 6.90). The term $\kappa_y = -\partial^2 w^o/\partial y^2$ (Eq. 4.2), and we write

$$\int_0^{L_{rs}/2} (-\kappa_y)\,dy = \underbrace{\left.\frac{\partial w}{\partial y}\right|_{\text{at } L_{rs}/2}}_{0} - \left.\frac{\partial w}{\partial y}\right|_{\text{at } 0}, \tag{6.375}$$

where $\partial w/\partial y$ is zero at $L_{rs}/2$ (Fig. 6.90), and we have

$$\kappa_y \frac{L_{rs}}{2} = \left.\frac{\partial w}{\partial y}\right|_{\text{at } 0}. \tag{6.376}$$

Equations (6.373), (6.374), and (6.376) give

$$\widetilde{k} = \frac{2\,(D_{22})_{rs}}{L_{rs}}. \tag{6.377}$$

[28] F. Bleich, *Buckling of Metal Structures*. McGraw-Hill, New York, 1952, p. 339.

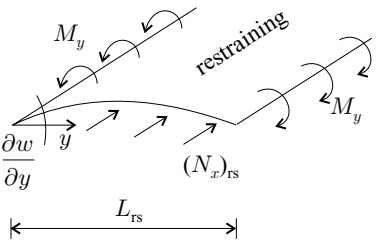

Figure 6.90: The restraining wall segment of the box beam.

The preceding expression is valid when no axial load acts. The effect of axial loading is taken into account by an amplification factor r defined as[29,30]

$$r = \frac{1}{1 - \frac{(N_x)_{\text{rs}}}{(N_{x,\,\text{cr}})^{\text{ss}}_{\text{rs}}}}, \tag{6.378}$$

where $(N_x)_{\text{rs}}$ is the applied axial load (Fig. 6.90) and $(N_{x,\,\text{cr}})^{\text{ss}}_{\text{rs}}$ is the buckling load of the simply supported restraining wall segment; r is unity when the axial load is zero and is infinity when the axial load is equal to the buckling load. Taking this amplification factor into account, the spring constant is

$$\widetilde{k} = \frac{2(D_{22})_{\text{rs}}}{L_{\text{rs}}}\,\frac{1}{r}. \tag{6.379}$$

The axial strains of the restraining and the buckled wall segments are the same, and, consequently, $(N_x)_{\text{rs}}$ is (Fig. 6.89, b)

$$(N_x)_{\text{rs}} = (N_{x,\,\text{cr}})_{\text{bu}}\frac{(a_{11})_{\text{bu}}}{(a_{11})_{\text{rs}}}, \tag{6.380}$$

where the subscript bu refers to the wall segment that buckles and $(N_{x,\,\text{cr}})_{\text{bu}}$ is the buckling load of the rotationally restrained buckled wall segment. The value of $(N_{x,\,\text{cr}})_{\text{bu}}$ is not known a priori. We may approximate $(N_{x,\,\text{cr}})_{\text{bu}}$ by the buckling load $(N_{x,\,\text{cr}})^{\text{ss}}_{\text{bu}}$ of a simply supported wall. With this approximation, r becomes

$$r = \frac{1}{1 - \frac{(N_{x,\,\text{cr}})^{\text{ss}}_{\text{bu}}(a_{11})_{\text{bu}}}{(N_{x,\,\text{cr}})^{\text{ss}}_{\text{rs}}(a_{11})_{\text{rs}}}}. \tag{6.381}$$

If the webs and the flanges were simply supported, their buckling loads would be (Table 4.11, first row, page 136)

$$\begin{aligned}(N_{x,\,\text{cr}})^{\text{ss}}_{\text{f}} &= \frac{\pi^2}{b_{\text{f}}^2}\left[2\sqrt{(D_{11})_{\text{f}}(D_{22})_{\text{f}}} + 2((D_{12})_{\text{f}} + 2(D_{66})_{\text{f}})\right]\\ (N_{x,\,\text{cr}})^{\text{ss}}_{\text{w}} &= \frac{\pi^2}{b_{\text{w}}^2}\left[2\sqrt{(D_{11})_{\text{w}}(D_{22})_{\text{w}}} + 2((D_{12})_{\text{w}} + 2(D_{66})_{\text{w}})\right].\end{aligned} \tag{6.382}$$

[29] Ibid., pp. 331–339.

[30] S. P. Timoshenko and J. Gere, *Theory of Elastic Stability.* 2nd edition. McGraw-Hill, New York, 1961, pp. 15 and 424.

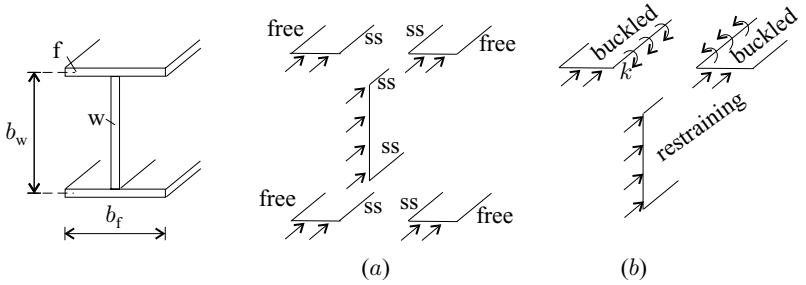

Figure 6.91: Local buckling of an axially loaded I-beam.

The flanges buckle first when $(N_{x,\,\mathrm{cr}})_{\mathrm{f}}^{\mathrm{ss}}(a_{11})_{\mathrm{f}} < (N_{x,\,\mathrm{cr}})_{\mathrm{w}}^{\mathrm{ss}}\,(a_{11})_{\mathrm{w}}$. In this case the web restrains the rotation of the flange, and the spring constant is

$$\widetilde{k} = \frac{2(D_{22})_{\mathrm{w}}}{b_{\mathrm{w}}}\left(1 - \frac{(N_{x,\,\mathrm{cr}})_{\mathrm{f}}^{\mathrm{ss}}(a_{11})_{\mathrm{f}}}{(N_{x,\,\mathrm{cr}})_{\mathrm{w}}^{\mathrm{ss}}(a_{11})_{\mathrm{w}}}\right). \tag{6.383}$$

The buckling load of the flange is then calculated with this spring constant by the expression in the fourth row of Table 4.11 (page 136).

The webs buckle first when $(N_{x,\,\mathrm{cr}})_{\mathrm{f}}^{\mathrm{ss}}(a_{11})_{\mathrm{f}} > (N_{x,\,\mathrm{cr}})_{\mathrm{w}}^{\mathrm{ss}}(a_{11})_{\mathrm{w}}$. In this case the flange restrains the rotation of the web, and the spring constant is

$$\widetilde{k} = \frac{2(D_{22})_{\mathrm{f}}}{b_{\mathrm{f}}}\left(1 - \frac{(N_{x,\,\mathrm{cr}})_{\mathrm{w}}^{\mathrm{ss}}(a_{11})_{\mathrm{w}}}{(N_{x,\,\mathrm{cr}})_{\mathrm{f}}^{\mathrm{ss}}(a_{11})_{\mathrm{f}}}\right). \tag{6.384}$$

The buckling load of the web is then calculated with this spring constant by the expression in the fourth row of Table 4.11.

I-beams. We now apply the preceeding procedure to I-beams (Fig. 6.91).

If the web and the flanges were simply supported, their buckling loads would be (Tables 4.9, and 4.11, first row, pages 125 and 136)

$$\begin{aligned}(N_{x,\,\mathrm{cr}})_{\mathrm{f}}^{\mathrm{ss}} &= \frac{12(D_{66})_{\mathrm{f}}}{(b_{\mathrm{f}}/2)^2}\\ (N_{x,\,\mathrm{cr}})_{\mathrm{w}}^{\mathrm{ss}} &= \frac{\pi^2}{b_{\mathrm{w}}^2}(2\sqrt{(D_{11})_{\mathrm{w}}(D_{22})_{\mathrm{w}}} + 2((D_{12})_{\mathrm{w}} + 2(D_{66})_{\mathrm{w}})).\end{aligned} \tag{6.385}$$

The flanges buckle first when $(N_{x,\,\mathrm{cr}})_{\mathrm{f}}^{\mathrm{ss}}(a_{11})_{\mathrm{f}} < (N_{x,\,\mathrm{cr}})_{\mathrm{w}}^{\mathrm{ss}}(a_{11})_{\mathrm{w}}$. In this case the web restrains the rotation of the flanges, and the spring constant is

$$\widetilde{k} = \frac{(D_{22})_{\mathrm{w}}}{b_{\mathrm{w}}}\left(1 - \frac{(N_{x,\,\mathrm{cr}})_{\mathrm{f}}^{\mathrm{ss}}\,(a_{11})_{\mathrm{f}}}{(N_{x,\,\mathrm{cr}})_{\mathrm{w}}^{\mathrm{ss}}(a_{11})_{\mathrm{w}}}\right). \tag{6.386}$$

The factor 2 is omitted because the web restrains two "half" flanges. The buckling load of the flanges is calculated with this spring constant by the expression in the sixth row of Table 4.11.

The web buckles first when $(N_{x,\,\mathrm{cr}})_{\mathrm{f}}^{\mathrm{ss}}(a_{11})_{\mathrm{f}} > (N_{x,\,\mathrm{cr}})_{\mathrm{w}}^{\mathrm{ss}}(a_{11})_{\mathrm{w}}$. In this case, as a conservative estimate, we take $\widetilde{k}$ to be zero ($\widetilde{k} = 0$). The buckling load is then calculated by the expression in the first row of Table 4.11. This expression is developed by replacing the rotationally restrained wall segments by simply supported

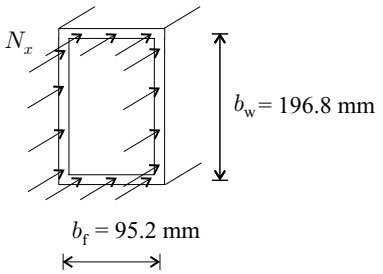

Figure 6.92: The cross section of the beam in Example 6.10.

wall segments. Expressions that do not include this simplification but take the rotational restraint into account are given by Kollár.[31]

6.10 Example. *The box-section beam shown in Figure 6.92 is subjected to axial compression. Determine the load that results in local buckling. The beam is orthotropic, and the bending stiffnesses of both the flange and the web are* $D_{11} = 444\ N\cdot m$, $D_{22} = 461\ N\cdot m$, $D_{12} = 103\ N\cdot m$, $D_{66} = 107\ N\cdot m$.

Solution. The widths of the flange and the web are $b_f = 0.0952$ m and $b_w = 0.1968$ m. With these values the buckling loads (with the flange and the web considered as simply supported plates) are (Eq. 6.382)

$$\begin{aligned}(N_{x,\,\mathrm{cr}})_f^{ss} &= \frac{\pi^2}{b_f^2}[2\sqrt{D_{11}D_{22}} + 2(D_{12} + 2D_{66})] = 1\,674\,\frac{\mathrm{kN}}{\mathrm{m}}\\ (N_{x,\,\mathrm{cr}})_w^{ss} &= \frac{\pi^2}{b_w^2}[2\sqrt{D_{11}D_{22}} + 2(D_{12} + 2D_{66})] = 392\,\frac{\mathrm{kN}}{\mathrm{m}}.\end{aligned} \tag{6.387}$$

The layups of the web and the flange are identical, $(a_{11})_f = (a_{11})_w$. Consequently, $(N_{x,\,\mathrm{cr}})_f^{ss}\,(a_{11})_f > (N_{x,\,\mathrm{cr}})_w^{ss}(a_{11})_w$, and the web buckles first. The web is restrained by the flanges (Fig. 6.92, right). The spring constant is (Eq. 6.383)

$$\widetilde{k} = \frac{2(D_{22})_f}{b_f}\left(1 - \frac{(N_{x,\,\mathrm{cr}})_w^{ss}(a_{11})_w}{(N_{x,\,\mathrm{cr}})_f^{ss}(a_{11})_f}\right) = 7\,414\ \mathrm{N} \tag{6.388}$$

The parameter of restraint is (Table 4.11, page 136)

$$\zeta = \frac{(D_{22})_w}{\widetilde{k}b_w} = 0.316. \tag{6.389}$$

The buckling load of the web is calculated by the expression in Table 4.11 (page 136, fourth row) as follows:

$$(N_{x,\,\mathrm{cr}})_w = \frac{\pi^2}{b_w^2}\left[2\sqrt{1 + 4.139\xi}\sqrt{(D_{11})_w(D_{22})_w} + (2 + 0.62\xi^2)((D_{12})_w + 2\,(D_{66})_w)\right],$$

where

$$\xi = \frac{1}{1 + 10\zeta} = 0.240. \tag{6.390}$$

[31] L. P. Kollár, Local Buckling of Composite (FRP) Beams. *Journal of Structural Engineering*, 2003.

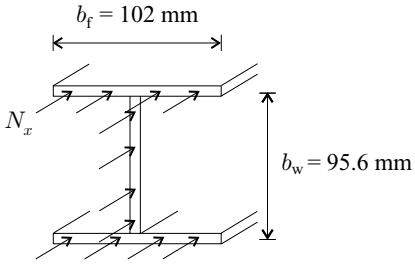

Figure 6.93: The cross section of the beam in Example. 6.11

With this value the buckling load of the web is

$$(N_{x,\,\mathrm{cr}})_w = 490\ \frac{\mathrm{kN}}{\mathrm{m}}. \tag{6.391}$$

This buckling load agrees closely with the result of a finite element analysis ($N_{x,\,\mathrm{cr}} = 501$ kN/m) and with the buckling load calculated by the numerical solution of the equations given by Lee[32] ($N_{x,\,\mathrm{cr}} = 519$ kN/m).

6.11 Example. *The I-section beam shown in Figure 6.93 is subjected to axial compression. Determine the load that results in local buckling. The beam is orthotropic and the bending stiffnesses of both the flange and the web are* $D_{11} = 698\,N\cdot m$, $D_{22} = 326\,N\cdot m$, $D_{12} = 127\,N\cdot m$, $D_{66} = 103\,N\cdot m$.

Solution. The width of the flange and the web are $b_f = 0.102$ m and $b_w = 0.0956$ m. When the flange is simply supported along one edge and free at the other edge and the web is simply supported at both edges, the buckling loads are (Eq. 6.385)

$$\begin{aligned}(N_{x,\,\mathrm{cr}})_f^{ss} &= \frac{12\,(D_{66})_f}{(b_f/2)^2} = 475\ \frac{\mathrm{kN}}{\mathrm{m}}\\ (N_{x,\,\mathrm{cr}})_w^{ss} &= \frac{\pi^2}{b_w^2}[2\sqrt{D_{11}D_{22}} + 2\,(D_{12}+2D_{66})] = 1\,750\ \frac{\mathrm{kN}}{\mathrm{m}}.\end{aligned} \tag{6.392}$$

The layups of the web and the flange are identical, $(a_{11})_f = (a_{11})_w$. Consequently, $(N_{x,\,\mathrm{cr}})_f^{ss}\,(a_{11})_f < (N_{x,\,\mathrm{cr}})_w^{ss}(a_{11})_w$, and the flange buckles first. The flange is restrained by the web (Fig. 6.93, right). The spring constant is (Eq. 6.386)

$$\widetilde{k} = \frac{(D_{22})_w}{b_w}\left(1 - \frac{(N_{x,\mathrm{cr}})_f^{ss}\,(a_{11})_f}{(N_{x,\,\mathrm{cr}})_w^{ss}\,(a_{11})_w}\right) = 2\,484\ \mathrm{N}. \tag{6.393}$$

The parameters ν, K, ζ, and η are (Table 4.11, page 136)

$$\nu = \frac{D_{12}}{2D_{66}+D_{12}} = 0.381 \qquad K = \frac{2D_{66}+D_{12}}{\sqrt{D_{11}D_{22}}} = 0.698 \tag{6.394}$$

$$\zeta = \frac{(D_{22})_w}{\widetilde{k}\,(b_f/2)} = 2.57 \qquad \eta = \frac{1}{\sqrt{1+(7.22-3.55\,\nu)\,\zeta}} = 0.249. \tag{6.395}$$

[32] D. J. Lee, The Local Buckling Coefficient for Orthotropic Structural Sections. *Aeronautical Journal,* Vol. 82, 313–320, 1978.

The buckling load of the flange is calculated by the expression in Table 4.11 (page 136, sixth row, $K < 1$) as follows:

$$(N_{x,\,\mathrm{cr}})_{\mathrm{f}} = \frac{\sqrt{(D_{11})_{\mathrm{f}}\,(D_{22})_{\mathrm{f}}}}{(b_{\mathrm{f}}/2)^2}\left\{K[\eta 15.1\sqrt{1-\nu} + (1-\eta)\,6\,(1-\nu)] + \frac{7\,(1-K)}{\sqrt{1+4.12\,\zeta}}\right\}$$
$$= 850 \text{ kN/m}. \tag{6.396}$$

This buckling load agrees closely with the result of the finite element analysis of Qiao et al.[33] ($N_{x,\,\mathrm{cr}} = 824$ kN/m), with the buckling load calculated by the numerical solution of the equations given by Lee[34] ($N_{x,\,\mathrm{cr}} = 916$ kN/m), and with the data of Tomblin and Barbero,[35] who tested beams of different lengths. The buckling loads measured by Tomblin and Barbero are $P_{\mathrm{cr}} = 247, 224$, and 222 kN, which yield $N_{x,\,\mathrm{cr}} = 841, 763$, and 759 kN/m.

6.10 Free Vibration of Beams (Flexural–Torsional Vibration)

In this section we present the natural frequencies of orthotropic beams. These frequencies are determined from the equilibrium, strain–displacement, and force–strain relationships. The first two of these equations are identical for isotropic and orthotropic beams, whereas the force–strain relationships differ, the differences being in the stiffness matrices (see Eqs. 6.334 and 6.335). Therefore, as in the case of buckling loads, the natural frequencies of an orthotropic beam can be obtained by replacing the isotropic stiffnesses with the replacement stiffnesses (Eq. 6.336) in the expression of the corresponding isotropic beam.

In the next sections we present the circular frequencies ω of orthotropic beams with doubly symmetrical, symmetrical, and unsymmetrical cross sections. The natural frequencies and the period of vibration are related to ω as follows:

$$f = \frac{\omega}{2\pi} \qquad T = \frac{2\pi}{\omega}. \tag{6.397}$$

6.10.1 Doubly Symmetrical Cross Sections

The beam is orthotropic and its cross section has two axes of symmetry y and z. The mass is also symmetrical with respect to these axes, and, accordingly, the center of mass coincides with the origin of the y–z coordinate system.

A beam with two cross-sectional planes of symmetry may undergo flexural vibration in either of the two planes of symmetry and torsional vibration (Fig. 6.94).

[33] P. Qiao, J. F. Davalos, and J. Wang, Local Buckling of Composite FRP Shapes by Discrete Plate Analysis. *Journal of Structural Engineering*, Vol. 127, 245–255, 2001.

[34] D. J. Lee, The Local Buckling Coefficient for Orthotropic Structural Sections. *Aeronautical Journal,* Vol. 82, 313–320, 1978.

[35] J. Tomblin and E. J. Barbero, Local Buckling Experiments on FRP Columns. *Thin-Walled Structures*, Vol. 18, 97–116, 1994.

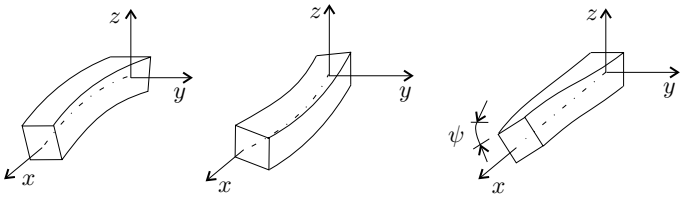

Figure 6.94: Illustration of vibration in the x–z and x–y planes and of torsional vibration.

Expressions for the circular frequencies corresponding to the flexural vibration of an isotropic beam are given by Weaver et al.[36] By replacing EI by $\widehat{EI}$ the circular frequencies of orthotropic beams are

$$\left(\omega^{\mathrm{B}}_{yi}\right)^2 = \frac{\widehat{EI}_{yy}}{\rho}\frac{\mu^4_{Bi}}{L^4} \qquad \text{vibration in the } x\text{–}z \text{ plane} \tag{6.398}$$

$$\left(\omega^{\mathrm{B}}_{zi}\right)^2 = \frac{\widehat{EI}_{zz}}{\rho}\frac{\mu^4_{Bi}}{L^4} \qquad \text{vibration in the } x\text{–}y \text{ plane.} \tag{6.399}$$

where L is the length of the beam, ρ is the mass per unit length, and μ_{Bi} for different end supports are given in Table 6.13. The subscript $i = 1, 2, \ldots$ indicates the first, second, and so forth, modes.

Expressions for the torsional circular frequencies $\omega^{\mathrm{B}}_{\psi i}$ of isotropic beams are also given by Weaver et al. With the replacement stiffnesses, the circular frequencies of long ($\widehat{GI}_{\mathrm{t}} \gg \widehat{EI}_{\omega}/L^2$) and short ($\widehat{GI}_{\mathrm{t}} \ll \widehat{EI}_{\omega}/L^2$) orthotropic beams are

$$\left(\omega^{\mathrm{B}}_{\psi i}\right)^2 = \frac{\widehat{GI}_{\mathrm{t}}}{\Theta}\frac{\mu^2_{Gi}}{L^2} \qquad \begin{array}{c}\text{torsional vibration}\\ \text{long beam}\end{array} \tag{6.400}$$

$$\left(\omega^{\mathrm{B}}_{\psi i}\right)^2 = \frac{\widehat{EI}_{\omega}}{\Theta}\frac{\mu^4_{Bi}}{L^4} \qquad \begin{array}{c}\text{torsional vibration}\\ \text{short beam.}\end{array} \tag{6.401}$$

where Θ is the polar moment of mass per unit length about the shear center[37],

$$\Theta = \int_{(A)} \rho_{\mathrm{comp}}(y^2 + z^2)\,dA, \tag{6.402}$$

ρ_{comp} is mass per unit volume, A is the area of the cross section, and μ_{Bi} and μ_{Gi} are given in Table 6.13 for different end supports.

We approximate the torsional circular frequencies of a beam of arbitrary length by

$$\left(\omega^{\mathrm{B}}_{\psi i}\right)^2 = \left(\omega^{\mathrm{B}}_{\psi i}\right)^2\Big|_{\mathrm{short}} + \left(\omega^{\mathrm{B}}_{\psi i}\right)^2\Big|_{\mathrm{long}} \qquad \text{torsional vibration.} \tag{6.403}$$

[36] W. Weaver, S. P. Timoshenko, and D. H. Young, *Vibration Problems in Engineering.* 5th edition. John Wiley & Sons, New York, 1990, pp. 422–432.

[37] Ibid., p. 476.

Table 6.13. The constants μ_{Bi} and μ_{Gi} in Eqs. (6.398), (6.399), (6.401), (6.406). The simple supports in cases (a) and (b) restrain the rotation about the *x*-axis, but the cross section is free to warp and free to rotate about the *y*- and *z*-axes.

Geometry	μ_B	μ_G
(a) 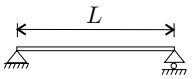	$\mu_{Bi} = i\pi$	$\mu_{Gi} = i\pi$
(b) 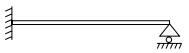	$\mu_{B1} = 3.927$ $\mu_{B2} = 7.069$ $\mu_{Bi} \approx (i + 0.25)\,\pi$	$\mu_{Gi} = i\pi$
(c) 	$\mu_{B1} = 4.730$ $\mu_{B2} = 7.853$ $\mu_{Bi} \approx (i + 0.5)\,\pi$	$\mu_{Gi} = i\pi$
(d) 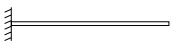	$\mu_{B1} = 1.875$ $\mu_{B2} = 4.694$ $\mu_{Bi} \approx (i - 0.5)\,\pi$	$\mu_{Gi} = (i - 0.5)\,\pi$
(e)	$\mu_{B1} = 4.730$ $\mu_{B2} = 7.853$ $\mu_{B3} = 10.996$ $\mu_{Bi} \approx (i + 0.5)\,\pi$	$\mu_{G1} = 6.283$ $\mu_{G2} = 8.987$ $\mu_{G3} = 12.566$ $\mu_{Gi} \approx (i + 1)\,\pi$

By using Eqs. (6.400) and (6.401), we have

$$\left(\omega^{\mathrm{B}}_{\psi i}\right)^2 = \frac{\widehat{EI}_\omega}{\Theta}\frac{\mu^4_{Bi}}{L^4} + \frac{\widehat{GI}_{\mathrm{t}}}{\Theta}\frac{\mu^2_{Gi}}{L^2}. \tag{6.404}$$

We introduce the definition

$$\omega^{\mathrm{B}}_{\omega i} = \sqrt{\frac{\widehat{EI}_\omega}{\Theta}\frac{\mu^4_{Bi}}{L^4}}. \tag{6.405}$$

With this definition the circular frequency is

$$\left(\omega^{\mathrm{B}}_{\psi i}\right)^2 = \left(\omega^{\mathrm{B}}_{\omega i}\right)^2 + \frac{\widehat{GI}_{\mathrm{t}}}{\Theta}\frac{\mu^2_{Gi}}{L^2} \qquad \begin{matrix}\text{torsional}\\ \text{vibration.}\end{matrix} \tag{6.406}$$

Equation (6.406) is exact for simply supported beams (case (a) in Table 6.13). For beams with the types of supports shown as cases (b), (c), and (e), the equation underestimates the circular frequencies (and overestimates the period of vibration) by less than 6 percent. For cantilever beams (case d), Eq. (6.406) may underestimate the circular frequencies (and overestimate the period of vibration) by up to 14 percent.

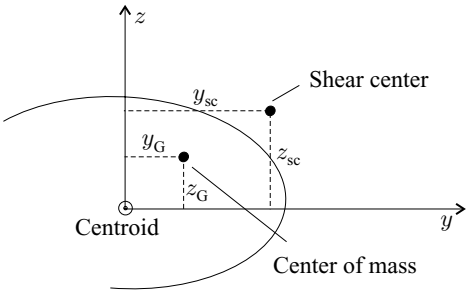

Figure 6.95: Coordinates of the center of mass and the shear center.

6.10.2 Beams with Symmetrical Cross Sections

We consider orthotropic beams with cross sections symmetrical with respect to the z-axis ($\widehat{EI}_{yz} = 0$). The mass is also symmetrical with respect to the z-axis, and, accordingly, the center of mass is on the z-axis. When the cross section of the beam has one axis of symmetry, it may undergo flexural vibration in the x–z plane as well as flexural–torsional vibration.

For such a beam there are three sets of circular frequencies. The first of these is[38]

$$\omega_1 = \omega_{yi}^{\mathrm{B}} \qquad \text{vibration in the } x\text{–}z \text{ plane.} \tag{6.407}$$

The second and third sets of circular frequencies, ω_2 and ω_3, corresponding to the flexural–torsional vibration, are the two roots of the following equation:

$$\left| \begin{bmatrix} \left(\omega_{zi}^{\mathrm{B}}\right)^2 & 0 \\ 0 & \left(\omega_{\psi i}^{\mathrm{B}}\right)^2 \frac{\Theta}{\rho} \end{bmatrix} - \omega^2 \begin{bmatrix} 1 & -(z_G - z_{\mathrm{sc}}) \\ -(z_G - z_{\mathrm{sc}}) & \frac{\Theta}{\rho} \end{bmatrix} \right| = 0, \tag{6.408}$$

where $|\quad|$ denotes the determinant, ρ is the mass per unit length, z_{sc} is the coordinate of the shear center, z_G is the coordinate of the center of mass (Fig. 6.95), and Θ is the polar moment of mass per unit length about the shear center

$$\Theta = \int_A \rho_{\mathrm{comp}} \left[y^2 + (z - z_{\mathrm{sc}})^2 \right] dA. \tag{6.409}$$

In these equations ω_{yi}^{B}, ω_{zi}^{B}, and $\omega_{\psi i}^{\mathrm{B}}$ are given by Eqs. (6.398), (6.399), and (6.406). Solution of Eq. (6.408) provides the exact values of ω_2 and ω_3 only for simply supported beams (case (a) in Table 6.13).

6.10.3 Beams with Unsymmetrical Cross Sections

The cross section of the beam is unsymmetrical and the layup is orthotropic. The beam undergoes combined flexural–torsional vibration, which is analogous to flexural–torsional buckling. Therefore, we extend Eq. (6.408) and write it in the

[38] Ibid., p. 477.

following form, which is analogous to Eq. (6.346):

$$\left| \begin{bmatrix} \left(\omega_{zi}^{\mathrm{B}}\right)^2 & 0 & 0 \\ 0 & \left(\omega_{yi}^{\mathrm{B}}\right)^2 & 0 \\ 0 & 0 & \left(\omega_{\psi i}^{\mathrm{B}}\right)^2 \frac{\Theta}{\rho} \end{bmatrix} - \omega^2 \begin{bmatrix} 1 & 0 & -(z_G - z_{\mathrm{sc}}) \\ 0 & 1 & (y_G - y_{\mathrm{sc}}) \\ -(z_G - z_{\mathrm{sc}}) & (y_G - y_{\mathrm{sc}}) & \frac{\Theta}{\rho} \end{bmatrix} \right| = 0, \tag{6.410}$$

where ω is the circular frequency, y_{sc} and z_{sc} are the coordinates of the shear center, ρ is the mass per unit length, y_G and z_G are the coordinates of the center of mass (Fig. 6.95), and Θ is the polar moment of mass per unit length about the shear center,

$$\Theta = \int_A \rho_{\mathrm{comp}} \left[(y - y_{\mathrm{sc}})^2 + (z - z_{\mathrm{sc}})^2 \right] dA, \tag{6.411}$$

where ω_{yi}^{B}, ω_{zi}^{B} and $\omega_{\psi i}^{\mathrm{B}}$ are given by Eqs. (6.398), (6.399), and (6.406). Equation (6.410) yields three sets of ω; the values are only exact for simply supported beams (case (a) in Table 6.13).

6.12 Example. *An $L = 0.5$-m-long I-section beam, with the cross section shown in Figure 6.96, is made of graphite epoxy unidirectional plies. The material properties are given in Table 3.6 (page 81). The density of the composite is 1.6 g/cm^3. The layup is $[0_{20}]$. The beam is simply supported at each end. Calculate the natural frequencies of the beam.*

Solution. The mass per unit length is

$$\rho = \rho_{\mathrm{comp}} A = 1600 \, \frac{\mathrm{kg}}{\mathrm{m}^3} \times 0.264 \times 10^{-3} \, \mathrm{m}^2 = 0.4224 \, \frac{\mathrm{kg}}{\mathrm{m}}, \tag{6.412}$$

where A is the area of the cross section $A = h(b_{\mathrm{f1}} + b_{\mathrm{f2}} + b_{\mathrm{w}}) = 0.264 \times 10^{-3} \, \mathrm{m}^2$ (Fig. 6.96). The location of the center of mass coincides with the centroid of the cross section

$$z_G = 0. \tag{6.413}$$

The polar moment of mass per unit length about the shear center is (Eq. 6.402)

$$\begin{aligned} \Theta &= \int_{(A)} \rho_{\mathrm{comp}} \left[y^2 + (z - z_{\mathrm{sc}})^2 \right] dA = \rho_{\mathrm{comp}} \left[I_{\mathrm{p}} + (z_G - z_{\mathrm{sc}})^2 A \right] \\ &= 263.7 \times 10^{-6} \, \mathrm{kg \cdot m}, \end{aligned} \tag{6.414}$$

where $z_{\mathrm{sc}} = 0.000\,789$ m (Eq. 6.349) and $I_{\mathrm{p}} = I_{zz} + I_{yy}$ is the polar moment of inertia ($I_{zz} = 26.24 \times 10^{-9} \, \mathrm{m}^4$, $I_{yy} = 122.12 \times 10^{-9} \, \mathrm{m}^4$).

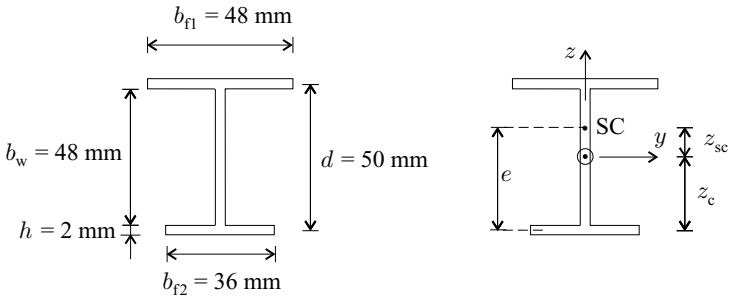

Figure 6.96: The cross section of the beam in Example 6.12.

With the preceding values of ρ and Θ, and with the parameters $\mu_{B1} = \mu_{G1} = \pi$ (Table 6.13, page 308), Eqs. (6.398), (6.399), (6.405), and (6.406) give

$$\omega_{y1}^{\mathrm{B}} = \sqrt{\frac{\widehat{EI}_{yy}}{\rho}\frac{\mu_{B1}^4}{L^4}} = 8\,166\,\frac{1}{\mathrm{s}}$$

$$\omega_{z1}^{\mathrm{B}} = \sqrt{\frac{\widehat{EI}_{zz}}{\rho}\frac{\mu_{B1}^4}{L^4}} = 3\,785\,\frac{1}{\mathrm{s}} \tag{6.415}$$

$$\omega_{\omega 1}^{\mathrm{B}} = \sqrt{\frac{\widehat{EI}_{\omega}}{\Theta}\frac{\mu_{B1}^4}{L^4}} = 3\,458\,\frac{1}{\mathrm{s}}$$

$$\omega_{\psi 1}^{\mathrm{B}} = \sqrt{\left(\omega_{\omega 1}^{\mathrm{B}}\right)^2 + \frac{\widehat{GI}_{\mathrm{t}}}{\Theta}\frac{\mu_{G1}^2}{L^2}} = 3\,493\,\frac{1}{\mathrm{s}}. \tag{6.416}$$

The circular frequency ω_1 is (Eq. 6.407)

$$\omega_1 = \omega_{y1}^{\mathrm{B}} = 8\,166\,\frac{1}{\mathrm{s}}, \tag{6.417}$$

and ω_2 and ω_3 are the roots of Eq. (6.408) as follows:

$$\left|\begin{bmatrix}\left(\omega_{z1}^{\mathrm{B}}\right)^2 & 0\\ 0 & \left(\omega_{\psi 1}^{\mathrm{B}}\right)^2\frac{\Theta}{\rho}\end{bmatrix} - \omega^2\begin{bmatrix}1 & (z_G - z_{\mathrm{sc}})\\ (z_G - z_{\mathrm{sc}}) & \frac{\Theta}{\rho}\end{bmatrix}\right| = 0 \tag{6.418}$$

$$\omega_2 = 6\,024\,\frac{1}{\mathrm{s}} \qquad \omega_3 = 2\,838\,\frac{1}{\mathrm{s}}. \tag{6.419}$$

The natural frequencies are $f = \omega/2\pi$

$$f_1 = 1\,300\ \mathrm{Hz} \qquad f_2 = 959\ \mathrm{Hz} \qquad f_3 = 452\ \mathrm{Hz}. \tag{6.420}$$

6.11 Summary

In Table 6.14 we summarize the various beam problems considered in this chapter and the relevant section numbers.

Attention is called again to the important fact that the displacements, buckling loads, and natural frequencies of an orthotropic or symmetrical cross-section beam can be determined by simply replacing the isotropic stiffnesses with the appropriate replacement stiffnesses in the expressions for the corresponding isotropic beam. It is for this reason that, in this chapter, emphasis is given to the development of replacement stiffnesses.

For beams with arbitrary layup there is no direct analogy with isotropic beams. Therefore, each problem must be treated individually.

Table 6.14. Section numbers for solid cross section and for thin-walled unreinforced (monocoque) beams. Stiffened thin-walled (semimonocoque) beams are discussed in Section 6.8.

		Monocoque	
	Solid	**Thin-walled open-section**	**Thin-walled closed-section**
End loads ($\widehat{N}$, $\widehat{M}_y$, $\widehat{M}_z$, $\widehat{T}$)			
Orthotropic layup			
Axial and bending ($\widehat{EA}$, $\widehat{EI}$)	6.2	6.3	6.4
Torsion			
no restrained warping ($\widehat{GI}_t$)	6.5.1	6.5.2	6.5.3, 6.5.4
with restrained warping ($\widehat{EI}_\omega$)	–	6.5.5	–
Arbitrary layup			
Axial, bending, and torsion			
no restrained warping	6.2, 6.5.1	6.6.1, 6.6.2	6.6.1, 6.6.2
with restrained warping	–	6.6.4	–
Transverse loads			
Orthotropic layup		6.7.1, 6.7.3	
Arbitrary layup		6.7.2, 6.7.3	
Buckling			
Axially loaded (orthotropic layup or symmetrical cross section)		6.9.1	
Lateral buckling (symmetrical cross section)		6.9.2	
Local buckling		6.9.3	
Free vibration (orthotropic layup or symmetrical cross section)		6.10	